DISSERTATION

submitted to the

Combined Faculty of Natural Sciences and Mathematics

of Ruperto Carola University of Heidelberg, Germany

for the degree of

Doctor of Natural Sciences

Presented by

M.Pharm M.Sc Evangelia Giannakouri

Born in: Athens, Greece

Oral-examination: 30.03.2020

Bone marrow Angiopoietin/Tie signaling in the control of hematopoietic stem cells

Referees:

PD. Dr. Karin Müller-Decker

Prof. Dr. Hellmut G. Augustin

Die vorliegende Arbeit wurde in der Abteilung „Vaskuläre Onkologie und Metastasierung“ am Deutschen Krebsforschungszentrum (DKFZ) in Heidelberg zwischen Oktober 2015 und Dezember 2019 durchgeführt.

Στον Κύριο Παπαγιάννη

ACKNOWLEDGMENTS

My endeavor to complete my PhD has been an exciting, stimulating, illuminating and from time to time nerve-wrecking experience. I have definitely evolved as a scientist and as a person and for these past four long years I have many people to be thankful for.

*First, I would like to thank **Prof. Hellmut G. Augustin** for giving me the opportunity to work on my project and for his guidance and supervision. It was a pleasure being part of your research team and work alongside incredible scientists.*

*I also would like to thank my Thesis Advisory Committee members, **Prof Tsvee Lapidot** and **PD. Dr. Karin Müller-Decker** for their invaluable advice and encouragement. I am very thankful to the Helmholtz International Graduate School for Cancer Research, for the financial support and for providing a unique international research atmosphere at the DKFZ. I am proud to have been part of it.*

*Special thanks go to the **A190** crew for their great scientific input, continuous encouragement and lively discussion over science or other matters. I am grateful for your help and I will cherish all memories. Lise, Claudia, Beate, Kshitij, Martin T, Anja R, Tina, Silvia, Courtney, Mahak, Ashik ,Corinne, Jingjing, Nico, Laura, Moritz, Katha, Aida, Stephi K, Ki, Martin A, Donato Paula, Dimitri, Denise, Anja, G, Stephanie P, Stephanie G, Till, Miki, Xiaowen, Catalina, Shubhada, Stefan Jessy, Stella, Carleen, Claudine, Doro, Eva B, Maria, Daniela, Maike, Barbara, Petra, Lorena thank you for being so wonderful. Ranging from "helping hands" to "drinks and parties" to "crazy bachelorettes and scientific trip"' – this lab family has been unique from the beginning. A very special "THANK YOU" goes to **Benny** for his immense help and incredible work ethic. My PhD would have been a lot harder and dull without your assistance. **Anja** and **Mahak,** I am very grateful for the meticulous corrections of my thesis and **Stephis G** and **P** for their kind help with translations.*

*I thank the **"Helmholtz International Graduate School for Cancer Research"** for giving me the opportunity to work within such an inspirational institution. I thank the **FACS** and **Light Microscopy Core Facilities** for their assistance, the good and bad memories and their banter.*

Similar to hematopoietic stem cells, my own "niche" was essential for "maintenance" and "quiescent" peace of mind. Family and good friends outside the lab have either actively or unknowingly contributed to helping me in keeping things in perspective.

*Thank you, **Eva Tsipi** and **Alex Gouvatsos** for never drifting apart from me. I love and admire you both and I am honored to have you by my side. June is going to be lit. **Silvia, Kosti, Eleni, Elena, Sotiri, Ilona**, **Maria**, **Grigori**, **Gianni, Pari** you are all very loud and hilarious so thank you for spicing up our life in Heidelberg – each and every one in your own special way. I would also like to thank **Rocco** and his pizza. He was always there for me when I got a result… and when I didn't (except Tuesdays).*

*I would not be where I am now as a person and as a scientist without my parents. Eleni and Kostas I am very grateful and very proud of you both. Thank you for giving me sturdy roots and even more for giving me wings. I am thankful to **Natalia** for teaching me how to be an older sister. We have grown a lot and we still learn a ton from each other. My love and gratitude is unconditional and eternal.*

Acknowledgments

*Last but not least, I would like to take this opportunity to thank **Mr. V** for absolutely everything. If my defense goes well, I dedicate this thesis to you. If not, I will dedicate it to everyone you have sent off to Serres.*

***Tristan** and **Erimis** you simply are perfect, you deserve all the ham in the world. Never change.*

TABLE OF CONTENTS

Table of Contents

LIST OF FIGURES

LIST OF TABLES

SUMMARY

Hematopoietic stem cells (HSC) primarily reside in the bone marrow (BM) and possess the ability of self-renewal and differentiation to any progenitor or mature blood cell through hematopoiesis. Adult HSCs are found in specialized bone marrow niches that are essential for the regulation of quiescence, mobilization and differentiation of HSCs. Multiple studies have attempted to shed light on the complex signaling pathways between stromal and hematopoietic cells of the niche at steady state, inflammation and disease. Endothelial cells (EC) and perivascular stromal niches are known to illicit paracrine signals for the control of HSC maintenance and function. Curative transplantation approaches dwell on the effective activation and mobilization of hematopoietic stem and progenitor cells (HSPC) to the blood circulation. Current pharmaceutical approaches involve the use of mobilizing agent granulocyte-colony stimulating factor (G-CSF). The Angiopoietin/Tie (Ang/Tie) signaling pathway is essential for embryonic blood and lymphatic vessel development and maturation as well as vessel homeostasis in the adult. Few studies attempted to investigate Ang/Tie signaling in the BM stem cell niche. Angiopoietin-1 (Ang1) has been studied in the context of HSC maintenance and quiescence in the BM. It has also been shown that Ang1/Tie2 signaling is important for vascular recovery following BM irradiation. Besides the well-established role of Ang/Tie signaling in EC, Tie2 receptor is also known for its expression in HSPC. These findings led to the hypothesis that Ang/Tie signaling might impact HSPC in the bone marrow niche.

The present study investigated Angiopoietin-2 (Ang2) *in vivo* in the context of HSPC activation, egress and mobilization to the periphery. For this purpose, both genetic approaches as well as pharmaceutical inhibition of Ang2 were employed. Although Ang2 did effect HSPC egress at steady state, $Ang2^{KO}$ mice demonstrated a delayed and reduced HSPC mobilization to the periphery upon G-CSF stimulation. Further dissection of the phenotype revealed that the absence of Ang2 hindered the prompt activation of HSPC rather than the process of mobilization. The bone marrow vasculature and its function seemed unaffected by Ang2 at steady state and upon G-CSF mobilization. Further assessment of Ang2 function on HSPC was carried out in the context of hematopoietic reconstitution upon lethal irradiation. The reduced capability of immune cell reconstitution in $Ang2^{KO}$ mice confirmed the ligand's importance in replenishing the BM. The next focus of the thesis was elucidating the roles of Tie1 receptor on ECs in the BM *in vivo*. The investigation of HSPC egress and G-CSF-induced mobilization revealed fewer HSPCs in the periphery. Functional assays on blood vessels revealed that subtle changes in the vasculature are responsible for the reduced ability of HSPC mobilization in $Tie1^{iECKO}$ mice. Finally, since Tie1 receptor is not only expressed in ECs but also in HSPCs, this study involved the investigation of the receptor's role in progenitor colony formation *in vitro* and BM reconstitution *in vivo*. Colony forming unit (CFU) assays revealed that *Tie1* deletion on HSPC ($Tie1^{KO}$) reduced the cells' ability to form differentiated colonies. Serial and competitive

transplantations in mice confirmed the reduced ability of *Tie1*-deleted HSPC to repopulate the myeloid BM compartment of lethally irradiated mice.

The present thesis sheds lights on the interactions of blood vessels and HSPCs from an ''Ang/Tie-centric'' perspective. The experiments have unraveled the contribution of the context-dependent partial agonist Ang2, and the orphan receptor Tie1 in HSPC egress, mobilization and bone marrow reconstitution. These new discoveries are important in elucidating Ang/Tie signaling in the BM and potentially contribute to HSPC mobilization research for the treatment of hematological malignancies.

ZUSAMMENFASSUNG

Hämatopoietische Stammzellen (HSC) sind primär im Knochenmark angesiedelt und besitzen die Fähigkeiten der Selbst-Erneuerung und der Differenzierung in jede Zelle der Hämatopoese. Adulte HSC befinden sich in spezialisierten Knochenmark-Nischen, die ihren Ruhezustand, ihre Mobilisierung und ihre Differenzierung essentiell regulieren. Mehrere Studien untersuchten die komplexen Signalwege zwischen Stromazellen und hämatopoietischen Zellen in physiologischem, entzündetem und erkranktem Kontext. Erhalt und Funktion von HSC werden durch Endothelzellen (EC) und perivaskuläre Stroma-Nischen mit parakrinen Signalen kontrolliert. Verschiedene Transplantations-ansätze basieren auf der Aktivierung von hämatoipoetischen Stamm- und Vorläufer-Zellen (HSPC) und ihre Mobilisierung in die Zirkulation, welches hauptsächlich durch die pharmakologische Verwendung des HSPC-mobilisierenden Granulozyten-Kolonie-stimulierenden Faktors (G-CSF) hervorgerufen wird. Das Angiopoietin/Tie (Ang/Tie) Signalsystem ist essentiell für ein funktionsfähiges Gefäßsystem, da es eine wichtige Rolle bei der embryonalen Entwicklung und beim Reifesprozess von Blut- und Lymph-Gefäßen sowie bei der adulten Gefäß-Homöostase spielt. Nur wenige Studien haben die Ang/Tie Signalwege in der Stammzell-Nische des Knochenmarks untersucht. Dennoch bestätigen Experimente die Wichtigkeit von Angiopoietin-1 (Ang1) beim Erhalt und beim Ruhezustand der HSC im Knochenmark. Neben der bekannten Funktion von Ang1/Tie2 in EC wurde Tie2 auch in HSC nachgewiesen. Weiterhin ist das Ang1/Tie2 Signalsystem für vaskuläre Regeneration nach Knochenmarksbestrahlungen verantwortlich. Aufgrund dieser Informationen wurde die Hypothese formuliert, dass das Ang/Tie Signalsystem einen Einfluss auf HSPC in der Knochenmark-Nische haben.

In der vorliegenden Arbeit wurde die Rolle von Angiopoietin-2 (Ang2) bei der Aktivierung und der Mobilisierung in die Peripherie von HSPC in vivo studiert. Dafür wurden genetische als auch pharmakologische Ansätze zur Hemmung von Ang2 etabliert. Obwohl Ang2 keinen Effekt auf die Mobilisierung von HSPC im physiologischen Kontext hatte, wurde bei Ang2 Knock-out (Ang2KO) Mäusen eine verspätete und verminderte HSPC Mobilisierung in die Zirkulation nach G-CSF Stimulierung festgestellt. Weitere Untersuchungen des Phänotyps ergaben, dass der Verlust von Ang2 eher die direkte Aktivierung von HSPC als den Prozess der Mobilisierung verhinderte. Die Knockemarksgefäße und ihre Funktionen blieben sowohl im physiologischen Kontext als auch nach G-CSF Stimulierung unbeeinflusst. Nach letaler Bestrahlung bestätigte eine verminderte Immunzell-Regeneration in Ang2KO Mäusen die Rolle von Ang2 bei hämatopoietischer Regeneration von HSPC. Weiterhin wurde in der vorliegenden Studie die Rolle des Tie1 Rezeptors in ECs im Knochenmark in vivo erforscht. Untersuchungen der physiologischen sowie der G-CSF-induzierten Mobilisierung von HSPC in Tie1 Endothelzell-spezifischen Knock-out (Tie1iECKO) Mäusen wiesen auf weniger HSPC in der Peripherie hin. Durch feine Änderungen der Gefäßstruktur reduzierte sich die HSPC Mobilisierung in Tie1iECKO Mäusen. Da der Tie1 Rezeptor nicht nur in ECs sondern auch in HSPC exprimiert ist, wurde die Funktion von Tie1 bei der Formation von Kolonien in vitro und Knochenmark-Rekonstruktion in vivo untersucht. Colony Formation Assays zeigten, dass Tie1 Knock-out in HSPC (Tie1KO) die

Formation von differenzierten Kolonien reduzierte. Serielle und kompetitive Transplantationen in Mäusen bestätigten, dass Tie1KO die Ansiedlung von HSPC im Knochenmark nach letaler Bestrahlung reduziert.

Die vorliegende Promotion analysiert die Interaktion von Blutgefäßen und HSPC mit dem Ang/Tie Signalsystem in Schwerpunkt. Die Einflüsse des kontextabhängigen, partiellen Agonisten Ang2 und dem Rezeptor Tie1 auf die Mobilisierung von HSPC und auch auf Knochenmark-Regeneration wurden detailliert untersucht. Die gewonnenen Erkenntnisse über die Funktion von Ang/Tie Signalwegen im Knochenmark könnten für die Entwicklung von HSPC Mobilisierungstherapien bei hämatologische genutzt werden.

1. INTRODUCTION

1.1 THE VASCULAR SYSTEM

Vertebrate body architecture consists of two highly branched, tree-like tubular networks: the blood and lymphatic vessels. Endothelial cells are the building blocks for both networks which are essential for efficient and concurrent transport of gas, liquids, nutrients, waster products, signaling molecules, cells and heat. The blood vascular system consists of the heart that pumps O_2-rich blood into the efferent arteries, smaller arterioles and capillary beds. Small-diameter capillaries are where the gas exchange takes place before deoxygenated CO_2-rich blood and metabolic waste products are carried via afferent venules and veins to the lung circuit for replenishment (1, 2). On the other hand, the functions of the lymphatic vasculature involve immune surveillance and collection and draining of protein-rich fluid back to blood vessels. Upon inflammatory stimuli, immune cells such as lymphocytes and antigen-presenting dendritic cells travel via lymphatic vessels towards lymphoid organs (3).

Blood vessels can be generated via two ways: vasculogenesis and angiogenesis. At early stages of embryonic development, cells from the mesoderm differentiate into hemangioblasts and then migrate forming aggregates to give rise to primitive vessels as part of vasculogenesis (4). Angiogenesis on the other hand, is the process through which the expansion of existing vascular networks takes place. Angiogenesis can be divided into a series of processes such as EC sprouting, migration, proliferation, vessel anastomosis and pruning (2, 5, 6). Endothelial, perivascular and smooth muscle cells are essential in order to orchestrate such processes with extensive coordination to ensure vessel integrity via vascular remodeling, stabilization and maturation (1, 7).

1.1.1 Bone angiogenesis

Bone vasculature is formed almost exclusively by endochondral angiogenesis instead of vasculogenesis. At mouse embryonic day (E) 13,5 to 14,5, already existing blood vessels invade the cartilage template and angiogenesis takes place until reaching the plateau at early adulthood (8). Initially, the primary ossification center (POC) is determined by onsite chondrocytes which stop proliferating, become hypertrophic and secrete pro-angiogenic factors in order to stimulate angiogenesis. Consequently, blood vessels invade the POC and form a vascular network while simultaneous ossification processes are also taking place (9). Finally, vessels penetrate the epiphyseal chondrocytes at both distal ends of the long bones and initiate the formation of the secondary ossification center (SOC). Notably, flat bones develop via intramembranous ossification without the need for an intermediate chondrocyte template (10).

Bone vascularization has been shown to be the result of various molecular factors that derive from both blood vessels and bone suggesting that the processes of bone angiogenesis and osteogenesis are coupled. One of the vital regulators of angiogenesis, VEGFA, is expressed by hypertrophic chondrocytes and signals via the VEGFR2 receptor triggering cell migration, proliferation and survival

in ECs (11). Hypoxia further activates a chain of intracellular signaling pathways via hypoxia inducible factor (HIF). All metabolic gene regulations in chondrocytes are orchestrated by hypoxia since these cells function in hypoxic conditions with anaerobic metabolism (12). Matrix remodeling and mineralization are carried out by matrix metalloproteases secreted by chondrocytes (e.g. COL2) and osteoblasts (e.g. COL1) (13, 14). Finally, Fibroblast growth factors (FGFs) signal through four tyrosine kinase receptors (FGFR1-4) and initiate cell survival, proliferation and differentiation. During osteogenesis, FGFR1-2 are expressed in endothelial cells (15) whereas their ligands are secreted by chondrocytes and osteoprogenitors (16).

1.1.2 Structure of bone vasculature

Early dye-based studies as well as more recent and technologically advanced methods have contributed to the understanding of complex organization and functionality of bone vasculature (17, 18). Such methods include specific antibodies, transgenic fluorescent reporters, confocal and two-photon microscopy and three-dimensional (3D) reconstruction of imaging data. Long bones are calcified, contain the marrow and are highly vascularized except in the growth plate and articular cartilage. The BM has been characterized as an organ in which its microvasculature is termed "sinusoidal" due to the fact that endothelial cells lack connective tissue covering and are in direct contact with the parenchymal cells. The diaphysis is the central core of the bone extending to the metaphysis and the epiphysis. Bone vasculature follows a hierarchical order with afferent arteries feeding into the capillary network which is drained into a large vein at the center of the diaphysis (19, 20). In the attempt to classify blood capillaries based on marker expression and functional characteristics, two classes of H and L capillaries were identified (21). H capillaries are located in the metaphysis and are structured as interconnected tubular columns close to the endosteum. These vessels highly express the junction protein, CD31 and the sialoglycoprotein, endomucin ($CD31^{hi}$ $EMCN^{hi}$). Moreover, they are surrounded by perivascular osterix-expressing osteoprogenitor cells. L vessels on the other hand, are located in dense branched organizations in the diaphysis and correspond to previously mentioned sinusoidal vasculature (22, 23). In terms of marker expression, L vessels express CD31 and endomucin yet in lower levels than H vessels ($CD31^{lo}$ $EMCN^{lo}$). L type vessels are also distinct for being surrounded by densely packed HSCs and for extending to the large central vein. Arterial blood is supplied to the bone via H vessels in the metaphysis and endosteum before entering the L sinusoidal network at the interface between metaphysis and diaphysis and finally reaching the large central vein. Consequently, spatially distinct metabolic states can be identified in the BM depending on the vasculature. The diaphysis is highly hypoxic due to the presence of sinusoidal L vessels and vast number of HSC. On the other hand, the metaphysis is rich with arterial vessels and therefore it is oxygenated in the adult mice (20, 24, 25).

As previously mentioned, bone vasculature is characterized by several types of mural cells. In the diaphysis there are two types of perivascular cells surrounding L type sinusoids, namely leptin receptor $(LEPR)^{+}$ cells (26) and CXCL12-abundant reticular (CAR) cells (27). Besides undertaking

important roles in HSC maintenance, LEPR$^+$ cells also express PDGFRα yet are negative for distinct pericyte markers such as PDGFRβ and NG2. In the metaphysis, as in soft tissues, arteries are surrounded by αSMA$^+$ cells which also express NG2 (28). Interestingly, periarteriolar NG2$^+$/nestin-GFP^{high} cells may differentiate to various mesenchymal lineages such as bone, cartilage and adipocytes (29, 30).

1.1.3 Angiopoietin/Tie system

The Angiopoietin/Tie (Ang/Tie) signaling pathway regulates blood and lymphatic vascular development via sprouting angiogenesis, vessel remodeling, endothelial maturation. It plays essential roles in vessel permeability, inflammation and cancer development and metastasis (31). Tie1 and Tie2 receptors form the Tie receptor family and are most predominantly expressed in the endothelium (32, 33), yet not exclusively. Studies have identified the presence of Tie receptors in top hierarchical HSCs, and Tie2 on monocytes and macrophages (34-38). Tie2 acts as a receptor for the Angiopoietin (Ang) family of ligand proteins (Ang1, Ang2 and Ang4) whereas Tie1 is a receptor that is activated via Ang-Tie2 signaling (39, 40).

The "Tie" acronym stands for "*Tyrosine kinase with Ig and EGF homology domains*" (32). Tie receptors are single transmembrane molecules possessing an extracellular ligand-binding domain and a split intracellular Tyr kinase domain. Their structure share a high degree of homology with 76% and 33% similarity in their intracellular and extracellular domains respectively (41). Both receptors are composed of three EGF-like modules flanked by three immunoglobulin (Ig)-like domains and three fibronectin type III repeats adjacent to the transmembrane (32, 33). The cytoplasmic region possesses kinase domains as well as phosphorylation and protein interaction sites (42) (Fig. 1). The angiopoietins consist of an N-terminal region responsible for their multimerization, a coiled-coil domain that dimerizes and a C-terminal fibrinogen-like domain that comprises of the Tie2-binding region (43, 44). Electron microscopy images have shown that ligands Ang1 and Ang2 are able to form dimeric, trimeric, tetrameric and pentameric multimers. More specifically, Ang1 predominantly forms tetrameric or higher order assemblies (45) whereas Ang2 exists mostly as dimer. The ligand-receptor binding is affected by the Angiopoietin oligomerization status. Ang1 for instance, can bind both ligand-binding sites of Tie2 homodimers due to its multimeric structure. On the other hand, due to the dimeric conformation of Ang2, the bridging of Tie2 extracellular homodimers is not achieved limiting the dimerization and activation of Tie2 (46). Ang2 has therefore been characterized as Ang1/Tie2 antagonist or as a partial agonist of the receptor (Fig. 1) (47, 48).

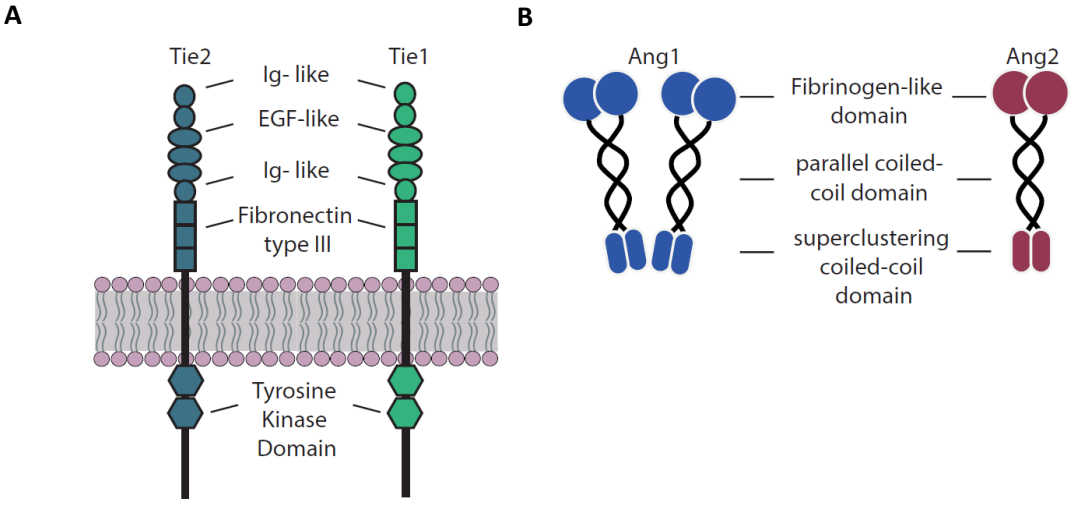

Figure 1: Structure of Tie receptors and Angiopoietin ligands

A) Tie receptors are highly homologous transmembrane receptor Tyrosine kinases. The extracellular domain consists of three immunoglobulin-like (Ig) domains flanking three EGF-like modules and three fibronectin type III repeats. The intracellular domain is made up of a split tyrosine kinase module. **B)** Angiopoietins are secreted glycoproteins that consist of an N-terminal coiled-coil domain and a C-terminal fibrinogen-like domain. The parallel coiled-coil and superclustering coiled-coil domain assist Ang ligand oligomerization. Ang1 exists most commonly in tetramers, wheras Ang2 exists in dimers.

Embryonic lethality occurs in Tie2 and Tie1 deficient mice at E10.5 and E13.5 respectively. The former develop vessel remodeling defects in the plexus of the yolk sac, the brain and lethal heart defects, whereas the latter show loss of structural integrity of vascular endothelial cells which results in lethal edema and hemorrhage (49). Besides fewer numbers of EC and pericytes as well as poor vessel organization, the absence of Tie2 leads to EC apoptosis which leads to lethal hemorrhage (50-52). In the case of Tie1 embryonic deficiency, developmental angiogenesis is not disturbed and hematopoiesis occurs naturally as opposed to Tie2-deficient mice (53). It is now well accepted that Tie1 and Tie2 are important for maintaining the integrity of mature vessels, yet do not play an important role in early angiogenic sprouting (54).

Ang1 deficiency in embryonic development leads to lethality at E11-E12.5 (50) with similar, yet less severe defects as in Tie2 deficiency. The heart of these embryos develops slower with less complex ventricular endocardium. Anatomically, the endocardium is collapsed and is not attached to the myocardial wall. Endothelial cell lining in the atria is collapsed and the trabeculae are not developed. Moreover, vascular defects including a smaller and immature primary capillary plexus and lack of proper pericyte coverage contribute to embryonic lethality. Ang1 myocardial overexpression studies have identified that the agonist dramatically affects early embryonic mouse development yet does not affect vessel structure and heart development in adulthood (55). In the case of Ang2 deficiency, perinatal lethality is strain-dependent. Although 129/J background mice die 14 days after birth (56), C57BL/6 background mice cope better with only 10% postnatal lethality (57). These mice may develop

severe chylous ascites postnatally and their large vessels are poorly organized with deficient smooth muscle cell coverage (58). Moreover, intestinal lymphatic vasculature appears disorganized and irregular (56). Overexpression of Ang2 has similar effects to Ang1 and Tie2 deficient mice supporting the idea that Ang1 acts agonistically on Tie2 whereas Ang2 behaves as an antagonist of the system. Interestingly, Ang2 has been shown to exert different effects depending on presence or absence of other cytokines. Notably, Ang2 and VEGF act synergistically inducing angiogenesis; however, in the absence of VEGF, Ang2 induces EC apoptosis and vessel regression (48, 59, 60).

1.1.4 Angiopoietin-1 mediated Tie2 signaling

At steady state conditions, Ang1 agonistically activates Tie2 signaling in a Tie1 dependent mechanism. This process initiates different signaling pathways that orchestrate cell survival, quiescence, maturation, EC activation, migration and permeability. Ang1 is constitutively released by perivascular cells and binds to Tie2 receptor leading to its dimerization and phosphorylation. The Ang1/Tie2 complex translocates to cell-cell contacts where the formation of trans-endothelial complexes with other Tie1 receptors from adjacent EC. This signals the recruitment of adaptor proteins such as growth factor receptor-bound protein2 (GRB2) and the PI3K regulatory subunit p85 which in turn activate the AKT pathway. AKT signaling promotes EC survival via the induction of Survivin (*BIRC5*) and endothelial nitric oxide synthase (*eNOS*), while suppressing apoptotic signaling such as BCL2-associated agonist of cell death (*BAD*) and caspase 9 (*Casp9*) (61-64). Ang1 binding on Tie2 can repress Ang2 transcription by inducing the phosphorylation, nuclear exclusion and therefore inactivation of the Forkhead transcription factor 1 (FOXO1). Consequently, Ang1/Tie2 signaling drives a negative feedback loop for Ang2 expression (65). On the other hand, AKT inhibition can lead to FOXO1 dephosphorylation which in turn promotes Ang2 secretion and therefore vascular destabilization (66). Moreover, it has also been shown that Tie2 activity is regulated by vascular endothelial protein tyrosine phosphatase (VE-PTP) (67). Ang/Tie signaling is highly responsible for regulation of vascular permeability. Quiescent, “non- leaky” vessels are characterized by tight and adherens junctions. Upon VEGF-mediated permeability, Tie2 induces the sequestration of the non-receptor Tyr kinase Src. This leads to the activation of Rac family small GTPase 1 (Rac1) which then phosphorylates the junctional protein vascular endothelial cadherin (VE-cadherin, *CDH5*). Finally, β-arrestin 2 mediates VE-cadherin internalization, degradation and vascular permeability increase (68, 69). On the other hand, Tie2 signaling leads to small GTPase Ras homolog family member A (RhoA)-dependent sequestration of Src by mammalian diaphanous (mDia) leading to the anti-permeability response of the endothelium (69). Taken together, at resting endothelium Ang1 acts as a vascular protector maintaining vessel integrity and inhibiting permeability. In the case of the activated endothelium where there are no endothelial cell junctions, Ang1 promotes endothelial cell proliferation and migration mediated by the PI3K pathway and FAK phosphorylation (62, 70, 71). Ang1-Tie2 signaling is also involved in reducing inflammation via the recruitment of tumor necrosis

factor α (TNFα)-induced inhibitory protein 3 interacting protein 2 (ABIN2), which inhibits Nuclear factor κB (NFκB) signaling pathway (72, 73).

The role of Ang1/Tie2 signaling in the recruitment of perivascular cells for vascular quiescence and maturation was established early on (31). Although the complete mechanism of this process are yet to be uncovered, studies have so far demonstrated that Ang1 agonistic action on Tie2 initiates the expression of heparin-binding epidermal-like growth factor (HB-EGF) leading to the migration and recruitment of vSMC (74, 75). Moreover, the serotonin pathway is also implicated in Ang1/Tie2-guided recruitment of vSMC to vessels (76). Finally, Platelet-derived growth factor B (PDGFB) is the most well-characterized cytokine released by EC with a pivotal role in pericyte recruitment during neovascularization (77). PDGFB is secreted by sprouting EC during angiogenesis in order to bind to PDGFRB receptor expressed by mural cells. This leads to the proliferation and migration of pericytes contributing to vascular maturation. Notably, there is no molecular evidence for the interaction between Ang1/Tie2 and PDGFB/PDGFRB axis.

1.1.5 Angiopoietin-2 mediated signaling: Agonistic and antagonistic roles

As opposed to Ang1 orchestrating vascular quiescence, Ang2 is required for sprouting angiogenesis, vascular destabilization, remodeling and vessel regression (78). In the event of pro-angiogenic stimuli, Ang2 functions antagonistically against Ang1-mediated Tie2 signaling (48). Ang2-mediated signaling leads to the formation of a Tie2, FAK and $\alpha_v\beta_3$ integrin complex that gets internalized, ubiquitinated and degraded resulting in EC apoptosis (1). Nevertheless, Ang2 has also been reported to act as a Tie2 agonist and it has been studied at both basal as well as inflammatory conditions. At steady state, the agonistic function of Ang2 leads to Tie2 phosphorylation and low FOXO1 activation, a process dependent on the presence of Tie1 receptor. Under inflammatory conditions, Ang2 is released and Tie1 is cleaved thereby preventing Ang2 agonistic activity and resulting in vessel destabilization (79, 80). Besides Tie1, VE-PTP has also been shown to determine the context-dependent actions of Ang2. VE-PTP regulates Ang2 antagonistic activity in blood endothelium and therefore its absence from lymphatic vasculature enables Ang2-Tie2-mediated lymphangiogenesis (81).

Furthermore, in the absence of Tie2, Ang2 can induce pro-angiogenic responses via integrins. The abundant expression of $\alpha_v\beta_3$, $\alpha_v\beta_5$, $\alpha_5\beta_1$ integrins on angiogenic tip cells downregulates Tie2 receptor. Ang2 can therefore bind to integrins leading to FAK phosphorylation on Tyrosin397 resulting in Rac activation and migration ultimately engaging sprouting angiogenesis at the tip cell front (82, 83).

1.1.6 Tie1 signaling

Tie1 was until recently described as an “orphan” receptor. It was discovered in 1992 and its signaling remains poorly understood due to the lack of identified specific ligands. Tie1 receptor on EC has been described as a doublet of 135 and 125 kilo Dalton (kDa) representing the mature glycosylated cell surface receptor and the intracellular non-glycosylated immature receptor, respectively (32). Upon inflammatory stimuli, the cleavage of the mature receptor occurs resulting in the shedding of a 100

kDa soluble fragment that contains the extracellular domain and a 45 kDa fragment containing the transmembrane and intracellular domains which remain within the cell. Tie1 undergoes proteolytic processing of its extracellular domain during stimulation with VEGFA, TNFα, LPS, phorbol-12-myristate-13 acetate (PMA) and other inflammatory cytokines and metalloproteases (84-87). Recent reports emphasized the roles of Tie1 ectodomain shedding in Ang/Tie signaling *in vivo*. Under physiological conditions, full length Tie1 supports the agonistic activity of Ang2 on Tie2. Under inflammatory conditions, however, Ang2 antagonistic actions are favored by the Tie1 ectodomain shedding which leads to reduced Tie2 phosphorylation and expression as well as Ang2 upregulation (79, 80). Tie1 can bind to Tie2 in both its full length and truncated form that exist in pre-formed heterodimers, suggesting that Tie1 endo-domain contributes to the Tie1-Tie2 complex (67, 88). Initially, it was reported that the Tie1-Tie2 hetero-complex is maintained via ectodomain electrostatic interactions which interfere with Tie2 activation and clustering. This early model suggested that upon Ang1 binding to Tie2, the heterodimer would dissociate allowing for Tie2 activation and clustering with other Tie2 receptors. On the other hand, Ang2 binding to Tie2 is not able to dissociate Tie1-Tie2 hetero-complexes and therefore acts as a competitive Tie2 antagonist (67). Tie1 is therefore considered an inhibitory co-receptor for Tie2 signaling which inhibits Ang1/Tie2 mediated AKT and MAPK phosphorylation as shown *in vitro* (89). In an attempt to elucidate Tie1-Tie2 heterodimerization, two recent studies demonstrated that the binding occurs in a β_1 integrin-dependent manner via the formation of β-sheets connecting the membrane-proximal Fibronectin type III domain n3 between receptors (46, 80). Functional *in vivo* studies have been able to elucidate the variety of roles of Tie1 on Tie2 signaling at post-natal retinal vascularization. Endothelial cells expressing Tie1 are able to negatively regulate Tie2 and drive tip cell formation. In contrast, stalk cell formation is orchestrated by the receptors' cooperation to sustain Ang1/Tie2 signaling whereas in quiescent EC there is almost no Tie1 expression (90). As opposed to Tie2, Tie1 is unable to phosphorylate neither other proteins nor itself. The phosphorylation of Tie1 has been shown in several studies via the soluble chimeric form of human COMP (cartilage oligomeric matrix protein)-Ang1 (40, 89, 90). In the absence of Tie2, high concentrations of COMP-Ang1 are sufficient to weakly phosphorylate Tie1. Similarly but to a weaker extend, native Ang1 and Ang4 are also able to illicit Tie1 phosphorylation (40, 90). A chimeric form of Tie1 composed of its original intracellular configuration and the extracellular domain of macrophage colony-stimulating factor1 (CSF-1) has been shown to activate PI3K-AKT survival and inhibit apoptosis pathways (91). This study introduced the notion that Tie1 can potentially transduce signals as Tie2 does. The absence of specific ligands up until very recently rendered Tie1 signaling mechanisms unclarified. A very recent study conducted in the Zhou lab suggests that LECT2 binds to the extracellular Ig3 domain of Tie1 with a K_d affinity of 0.52 μM (92). Binding of LECT2 to Tie1 led to the increase in Tie2/Tie2 homodimers in the expense of Tie1/Tie2 heterodimers. The authors also demonstrated that LECT2 induces Tie1 dephosphorylation, Tie2 phosphorylation, activates MAPK/PPAR/MMP/VE-Cadherin signaling pathway and inhibits EC migration.

1.1.7 Ang/Tie signaling in the bone marrow

The roles of Ang/Tie signaling in the BM have been the focus of interest for few researchers in the past three decades. Early reports had already established that Tie receptors are not exclusively expressed in endothelial cells but also immature hematopoietic stem cells (38, 53). Moreover, Ang1 is also highly expressed in HSCs, and at lower levels in c-Kit$^+$ hematopoietic progenitors, megakaryocytes and leptin receptor$^+$ (LepR$^+$) stromal cells (93).

Literature contains several patient studies on Ang/Tie and blood malignancies with rather contradicting results. Although several studies claim that Tie2 is overexpressed in leukemic blasts of AML patients, the impact of Ang1 and Ang2 is not very clear. Some claim that high plasma Ang2 pretreatment levels benefited overall survival (94, 95), whereas others correlate elevated Ang2 with higher risk for relapse in patients with AML and MM (96, 97). Ang1 has been identified as biomarker for poor prognosis in patients with MDS (98). Regarding tumor metastasis to the bone, Tie2 has been identified as a therapeutic target in harnessing tumor angiogenesis and reducing osteolytic bone metastasis in breast cancer (99). Moreover, Tie2-expressing ECs may be therapeutically targeted in order to increase hematopoietic reconstitution following myelosuppression (100).

In terms of Ang/Tie in relation to HSCs, early reports have emphasized the importance of Tie2 expression on HSCs for maintaining quiescence and evading cell death in the BM. Moreover, such HSCs adhered to osteoblasts and Ang1-mediated Tie2 signaling led to cobblestone formation of HSC *in vitro* and the maintenance of *in vivo* long-term repopulation activity (34). This study was followed by a contradicting report that showed that global and cell-specific Ang1 deletion did not affect hematopoiesis, HSC maintenance and HSC quiescence in normal mouse. On the other hand, Ang1 secreted by HSC/HSCP and LepR$^+$ reduced vascular leakiness, yet slowed down niche recovery after irradiation (93). Furthermore, monotherapy and co-administration of COMP-Ang1 with morphogenetic protein 2 (BMP2) in unstressed mice resulted in enhancement of bone formation and angiogenesis effects (101). *In vitro* studies have also validated that Ang1 is the dominant ligand for Tie2 expressed on long term HSCs in BM (102) and that Tie1 is not essential for the generation of myeloid and lymphoid lineages (53). In addition, *in vivo* fetal liver cell reconstitution assays with Tie1 deletion on HSC further showed that the receptor was not critical for stem cell engraftment and self-renewal (53).

1.2 HEMATOPOIETIC STEM CELLS

Hematopoietic stem cells (HSCs) have the ability to self-renew and differentiate into any progenitor and mature blood cell through a process named "hematopoiesis" (Fig. 2). In adults, these rare cells are hierarchically at the top of hematopoiesis and are predominantly found in the bone marrow (BM) (103). Approximately 4-5x10^{11} hematopoietic cells are generated daily in the adult BM (104). The hematopoietic system is essential for the continuous production of highly specialized cells which carry out important functions such as oxygen transport and immune defense. The unique properties of HSCs are essential in transplantations for the reconstitution of BM after ablation, injury and infection (105-107). On the other hand, properties of self-renewal and differentiation are limited in hierarchically lower committed progenitor cells (103). Fluorescence activated cell sorting (FACS) strategies have allowed the identification of hematopoietic stem cells and progenitors. Notably, the Lineage$^-$ Sca-1$^+$ c-Kit$^+$(LSK) scheme in mice identifies a diverse group of cells such as long-term repopulating cells (LT-HSC), short-term repopulating cells (ST-HSC) and lineage-committed progenitors that lack hematopoietic reconstitution properties (108). LSK cells include both HSCs and multipotent progenitors (MPP) and together they are known as hematopoietic stem and progenitor cells (HSPC).

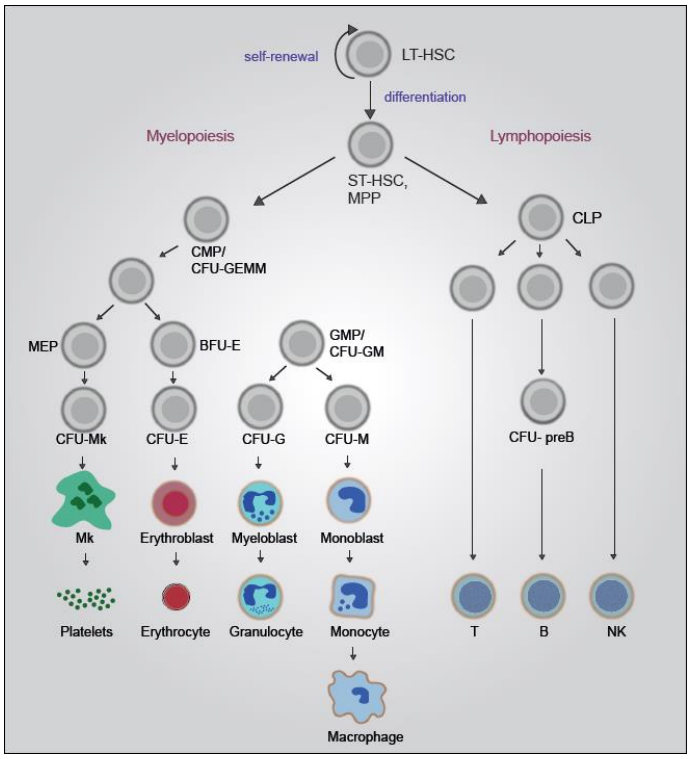

Figure 2: Hematopoiesis

Hematopoiesis is the process by which blood cells including erythrocytes, platelets and white blood cells are generated from hematopoietic stem cells (HSC). HSC undergo lineage restriction followed by differentiation to lineage-committed hematopoietic progenitors via myelopoiesis or lymphopoiesis. Definitions of acronyms can be found under section 7.

1.2.1 The BM niche

The BM is the organ that engulfs several hematopoietic and non-hematopoietic cell types that are connected via a highly vascularized and innervated network within long and axial bones (109). In mice, all bones support hematopoiesis, yet most HSC research involved long bones. In humans on the other hand, the axial skeleton is the major hematopoietic site. This includes the cranium, sternum, ribs, vertebrae and ilium. With age, the hematopoietic (red) marrow in human long bones is replaced by "fatty" yellow marrow and has reduced hematopoietic activity except in the proximal regions of long bones (110).

Ray Schofield developed the niche hypothesis in 1978 (111) in which stem cells are seen in association with other cell types capable of determining their behavior. Around the same time scientists at the University of Manchester and hematologist Michael Dexter showed that primitive hematopoietic cells *ex vivo* could be maintained in the presence of mesenchymal "stromal" cell cultures (112). Only a few years earlier, Brian Lord formulated the hypothesis that bone regulates hematopoiesis based on the observation that primitive cells tended to localize towards the endosteum in long BM cavities (113). Experimental evidence on engineered mouse strains confirmed the notion that bone cells create the HSC niche. A mouse model with an osteoblastic-specific promoter was initially used in order to delete a constitutively active parathyroid hormone receptor (114). Approximately a decade later, another study attempted to delete BMPr1α using a specific promoter for primitive and mature osteolineage cells (115). The results of both studies provided evidence of bone cells regulating mammalian stem cells *in vivo*, however, failed to clarify whether this effect was direct or indirect. As with any interactive system, complicated cross-talk takes place among different cell types in the BM. An imbalance caused by one cell type does not necessarily imply a direct effect on another cell type (116). Current knowledge suggests the existence of numerous specialized niches for hematopoietic stem and progenitor cells comprised of multiple cell types that affect the niche in important as well as redundant ways (Fig. 3).

1.2.1.1 Endothelial cells

Blood vessels in BM are vital for hematopoiesis. During embryogenesis, HSCs arise from the largest artery endothelial cells and remain closely associated with blood vessels throughout development (117). In mice, the idea of a vascular-HSC niche was adopted and supported by imaging of the BM and HSC distribution close to the vasculature (30, 118). Blood vessels in the BM can be categorized by diameter, morphology and basal lamina structure. Arterioles are variable in size, display a continuous basal lamina and are parallel to the long axis. Sinusoids on the other hand are large in diameter, display a fenestrated basal lamina and are positioned perpendicular to the long axis. Transitioning vessels are small in size, possess a continuous basal lamina and are positioned in the outer 20% of marrow volume closest to the bone surface (25, 119).

Endothelial cells (EC) compose the interior of blood vessel lining producing Notch ligands, CXCL12, SCF and pleiothrophin that contribute to regulation of HSC and differentiation of progenitor cells (26, 28,

120-124). Moreover, ECs are essential for secreting factors which promote hematopoietic regeneration after myelosuppressive stress (121-123). Studies in mice using an endothelial cell-specific approach (*Tie2*-Cre or *Cdh5*-Cre) have explored the importance of genes such as *gp130*, *Scf*, *Cxcl12* and *Jag1* regarding HSC maintenance at homeostasis.

Different types of blood vessels have unique molecular identifiers and are associated with distinct perivascular cells. EC-derived Notch signaling within the BM contributes to osteogenesis and generation of type H and arterial vessels as well as their coverage by PDGFRb$^+$ mesenchymal cells (24, 28). Early on, it was believed that hypoxia is an intrinsic characteristic of HSPCs that does not determine their choice of localization (125). However, a more recent study demonstrated that the arteriolar and sinusoidal permeability to blood plasma influences the levels of reactive oxygen species (ROS) in HSCs and therefore their positioning within the BM. In a nutshell, HSPCs localized near arterioles have lower ROS levels and maintain a quiescent phenotype compared to highly active HSPCs with elevated ROS levels near leakier sinusoids (25). Finally, the vascular niche is association with HSC quiescence was the topic of a recent study focusing on age-associated bone metastasis. The study elucidated the bone-specific mechanism where upon irradiation and chemotherapy, H blood vessels undergo remodeling and promote PDGF signaling and therefore the expansion of pericytes. On the other hand, the decline of BM pericytes upon aging is the reason behind loss of quiescence and expansion of cancer cells. Reduced blood flow hindered PDGF-B signaling and therefore pericyte expansion making metastatic cancer cells more susceptible to irradiation and chemotherapy (126).

1.2.1.2 Perivascular cells

The localization of HSC in close proximity to blood vessels suggests the existence of a perivascular niche. The study of perivascular niches in the BM has revealed that these cells are highly enriched in niche signals and mesenchymal stem cell (MSC) activity. Mesenchymal stem and progenitor cells are rare stromal cells (MSPC) with properties such as self-renewal and differentiation into bone, fat and cartilage. Transplantations of such cells into recipient mice resulted in the formation of a heterotopic hematopoietic niche with resident-derived HSC and donor-derived perivascular CD146$^+$ MSPCs (127).

In contrast to the notion that HSCs are located close to sinusoids, most nerve fibers are wrapped around arterioles and therefore HSC niche cells are not directly innervated (25, 29). The sympathetic nervous system (SNS) releases adrenergic signals regulating HSC transfer into the circulation in response to circadian rhythm (128, 129). Nerve fibers and the Schwann cells are not required for the maintenance of HSCs rather than the generation of hematopoiesis after myelosuppressive stress (130, 131). Finally, non-myelated Schwann cells orchestrate the proteolytic activation of TGFb leading to HSC maintenance activation (132).

1.2.1.3 Osteolineage

Historically, osteolineage cells comprised the first population that was associated with HSC regulation since Schofield's niche concept (111). Moreover, early reports suggested that transplanted HSC-enriched populations would preferentially re-locate along bone surface (133). Eradication of

osteoblasts induced acute changes in hematopoiesis such as failure in adequate lymphoid, erythroid and myeloid progenitor numbers (134). Two of the best studied cytokines required for non-cell autonomous HSC maintenance are Cxcl12 and SCF. However, deletion of *Cxcl12* or *Scf* in mouse mature osteoblasts and progenitors did not significantly affect HSC maintenance suggesting that osteolineage cells are not directly involved in this process (26, 116, 120). Other important quiescence regulating cytokines expressed in osteoblasts include osteopontin (OPN), a negative regulators of HSC pool (135, 136), thrombopoietin (THPO) (137, 138) and Angiopoietin-1 (Ang1) (34) although the latter has been questioned by newer studies (93). In conclusion, although osteolineage cells were initially hypothesized to play direct roles in HSC maintenance, it is now know that their roles focus on the maintenance of committed hematopoietic progenitors in the lymphoid lineage (116, 120, 134, 139).

1.2.1.4 HSC descendants

Besides HSC regulation by the stromal compartment, differentiated progeny of HSC may also contribute to their regulation. Megakaryocytes are closely associated with sinusoids and therefore with HSCs in the BM (140). A major source of TGFb1, a HSC quiescence factor, is the megakaryocytic population (141). Studies have shown that conditional deletion of *Tgfb1* in megakaryocytes leads to HSC proliferation *in vivo* (142). Similarly, as megakaryocytes are the major source of CXCL4, gene deletion gave rise to increased HSC proliferation and activation (143). Lastly, megakaryocytes are also responsible for the generation of FGF1, a cytokine that directly affects HSCs in promoting regeneration after injury (144).

Macrophages in the BM are a major source of CXCL12 and consequently, depletion of this cell type led to HSPC mobilization (145, 146). Moreover, a subgroup of macrophages expresses CD234 which may regulate TFGb-SMAD3 signaling in HSC (147). Another subgroup expresses smooth muscle actin (SMA) and cyclooxygenase 2 (COX2) and localize close to HSCs. These cells proliferate in response to lipopolysaccharide stimuli and produce prostaglandin E2 which correlates with decreased ROS in HSC (148). Lastly, osteoclasts that differentiated from the monocyte lineage have been shown to regulate HSC maintenance in bone remodeling via modulating Ca^{2+} concentrations and releasing signals from the bone matrix (149-151).

A subset of T lymphocytes was initially thought to be contributing in successful allogeneic engraftment following BM transplantation (152, 153). Technological advances in intravital microscopy assisted in the discovery of the co-localization of allo-HSC with $FOXP3^+$ regulatory T (T_{reg}) cells in the endosteum following transplantation (154). T_{reg} cells secrete cytokine IL-10 which promotes donor-derived HSC survival. The depletion of $FOXP3^+$ T_{reg} cells resulted in rapid exhaustion of donor-derived HSC leading to the conclusion that T_{reg} cells are an essential immuneregulatory compartment of the HSC niche. Moreover, $CD150^{high}$ T_{reg} cells appear in close proximity to HSCs and contribute in maintaining their quiescence state at rest and therefore assisting in allo-HSC engraftment (155). In summary, T_{reg} cells protect the BM niche from immune attack and promote survival of transplanted allo-HSCs.

1.2.2 Localization of HSCs in the bone marrow

The term “stem cell niche” describes the local microenvironment within an organ in which stem cells maintain their undifferentiated, self-renewable state and receive signals that predispose their fate. Direct visualization and determination of the HSC niche via fluorescent microscopy has been a major challenge due to lack of exclusive markers and the calcified nature of bones. Initial studies were based on the transplantation of exogenous GFP-labeled HSPCs and tracking via intravital imaging. These methods revealed that HSPCs reside close to the endosteum (156-158). As the signaling lymphocytic activation molecule (SLAM) family was discovered as part of HSPC markers (CD48, CD150 and CD244), thin BM section imaging revealed that such cells are distributed broadly in close proximity to endothelial cells and nestin (Nes)-GFP^{+} perivascular cells (30, 118). Improvements in 3D imaging and visualization lead researchers to identify subsets of quiescent HSCs located adjacent to small arterioles. Loss of HSC quiescent state correlated with their distribution away from arterioles (29). A whole-mount 3D-imaging based study revealed the existence of a non-arteriolar niche associated with megakaryocytes secreting CXCL4 (143). On the other hand, a study using KIT immunostaining and Ctnnal1-GFP reporter mice concluded that HSC are randomly distributed in the BM rather than strategically placed in arteriolar niches (159). Finally, imaging of myeloid-biased HSCs using von Willebrand factor (vWf)-GFP determined that HSC-vWf^{+} and HSC-vWf^{-} dwell within megakaryocytic and arteriolar niches respectively (160). To summarize, the identification of quiescent HSC niches within the BM is very complex and often generates contradicting studies due to the variety of used markers and methodologies in bone processing and imaging.

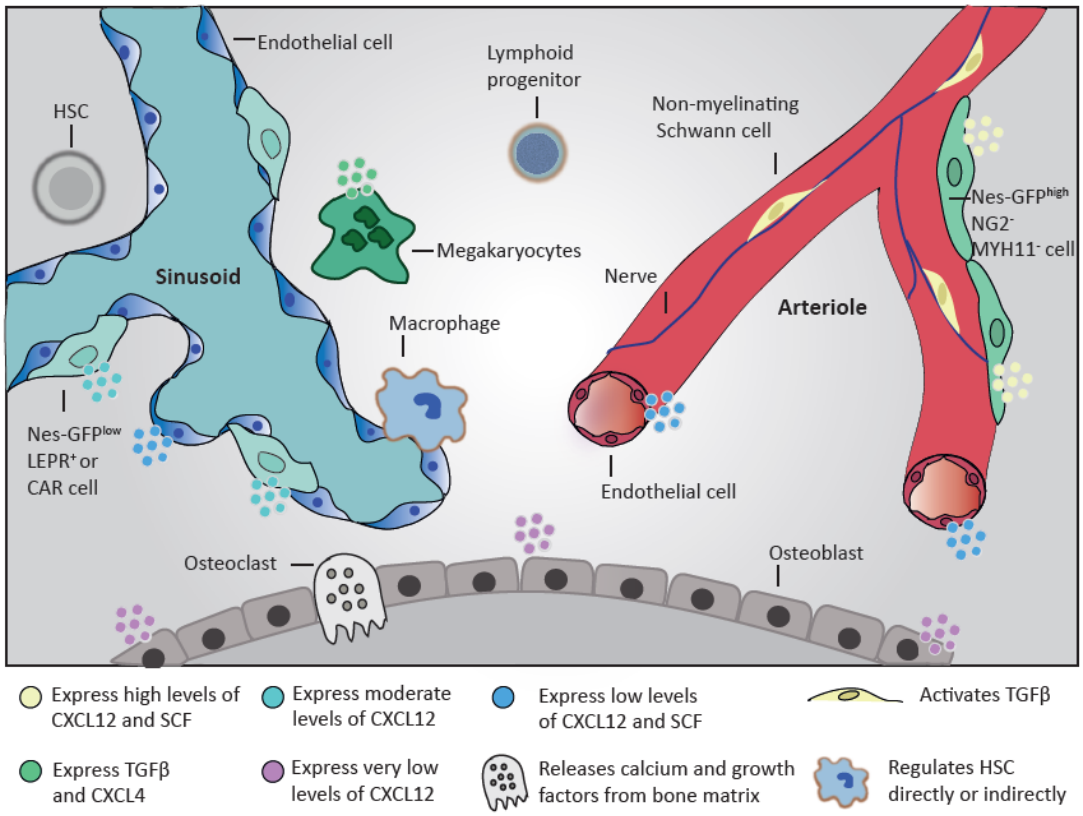

Figure 3: The bone marrow HSC niche at steady state in adults

Schematic representation of interactions between various cell types and HSC, at steady state. Blood vessels and stromal cells in the BM are considered key regulators of HSC activity and maintenance. Such cell types include periarteriolar nestin (Nes)-GFP^{high} cells, neural-glial antigen 2 (NG2)- positive cells, myosin heavy chain 11 (MYH11)-positive cell, perisinusoidal Nes-GFP^{low} cells, CXC-chemokine ligand 12 (CXCL12)- abundant reticular (CAR) cells and leptin receptor (LepR)-positive cells. Moreover, CXCL12-CAR and endothelial cells are sources of CXCL12 and stem cell factor (SCF) which are necessary for HSC maintenance (27, 29, 118, 125, 159). Nerve fibers (130) and associated non-myelinating Schwann cells (132), megakaryocytes (142, 143), macrophages (145-147, 161), and osteoclasts (149-151) have also been identified as regulators of HSC maintenance. The interactions of HSC and osteoblasts has yet to be elucidated, however it has been suggested that they may be implicated in the regulation of lymphoid progenitors (116).

1.3 STEM CELL MOBILIZATION AND TRANSPLANTATION

1.3.1 Hematological malignancies

The term leukemia derives from the Greek words for white (λευκός) and blood (αίμα) referring to a purely descriptive observation of elevated numbers of white blood cells (WBC). Leukemia is characterized by the term "blood cancer" which also encompasses lymphoma, myeloma, myelodysplastic syndrome and myeloproliferative neoplasm. Leukemia comprises a heterogeneous cluster of hematopoietic cancers consisting of biologically diverse subgroups. Leukemia types can be divided into acute and chronic depending on the differentiated state of abnormal cells. These groups can be further categorized into myeloid and lymphocytic depending on the type of the affected cells. Gene expression analysis and next generation sequencing (NGS) have significantly contributed in identifying unique biomarkers. These improve diagnosis, prognosis and dictate specific treatment approaches that have shaped the classification of leukemia types even further (162). According to the World Health Organization (WHO), cancer represents the second most prominent cause of mortality, with 8.2 million deaths (13% worldwide) in 2012 and around 14 million people affected every year. A recent study on cancer incidence and mortality rates estimated that in 2018 there were around 230,000 new cases and around 114,000 deaths due to leukemia and lymphoma in Europe (Fig. 4) (163).

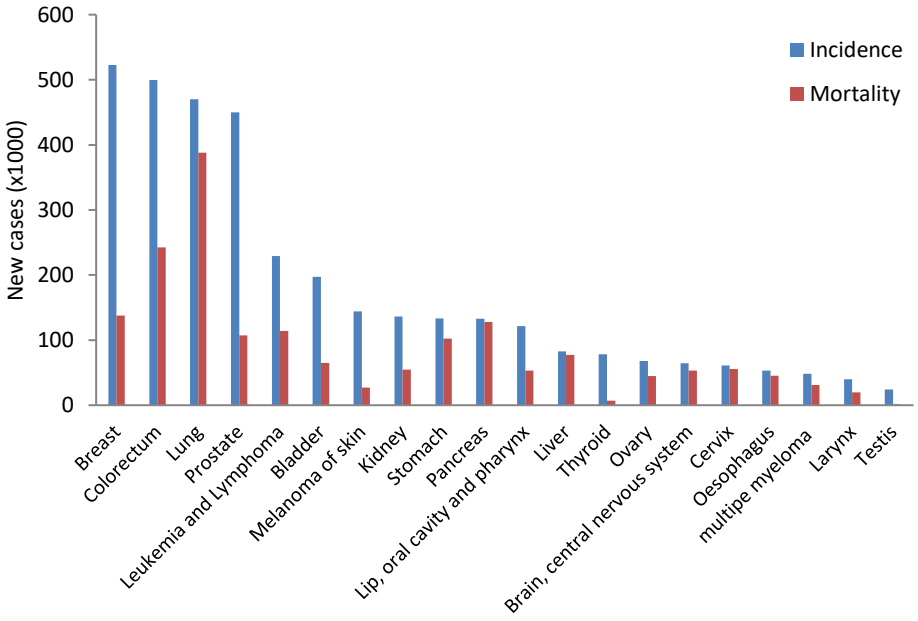

Figure 4: Estimated numbers of new cancer cases and deaths from cancer by cancer site in Europe in 2018
Adapted from (163).

Current treatment approaches for leukemia are determined depending on various patient factors such as overall health, rate of disease progression, classification etc. Treatment options include chemotherapy and other drug therapies, radiotherapy, immunotherapy, vaccine therapy, blood transfusion and stem cell transplantation.

1.3.2 Hematopoietic stem cell transplantation

BM transplantation is a curative therapy for hematological diseases involving the replacement of patient's immune system with healthy BM transplant. The first human BM transfusion was pioneered in 1939 followed by the first hematopoietic stem cell transplantation (HSCT) in 1957 by E Donnall Thomas carving the path towards a standard care procedure for hematologic malignancies (164, 165). There are two main approaches to hematopoietic stem cell transplantations namely autologous and allogeneic. The first approach involves patients receiving their own stem cells and in the latter stem cell graft is provided by a healthy donor. In 2017, out of all completed transplantations; autologous hematopoietic stem cell transplantations were carried out almost exclusively for the treatment of myeloma, non-Hodgkin's lymphoma and Hodgkin's lymphoma. On the other hand allogeneic transplantations were performed for the majority of acute myeloid leukemia (AML), acute lymphoid leukemia (ALL), myelodysplastic/myeloproliferative neoplasms (MDS/MPN), aplastic anemia, chronic myeloid leukemia (CML) and chronic lymphoid leukemia (CLL) (166).

1.3.3 Hematopoietic stem cell mobilization and homing

Under homeostatic conditions, HSPCs continuously egress out of the BM into the circulation. The boosted recruitment of HSPCs in the circulation in response to exogenous stimuli is termed as mobilization. HSPC mobilization is essential in treating patients with hematological malignancies or other diseases that require curative BM transplantation. The clinical benefit of targeting the BM endothelial barrier in the context of curative transplantations is to enhance cell mobilization of donor patients. Equally, patients would benefit from the improved homing of donor BM cells due to the loosening of the endothelial barrier. Finally, the opposite strategy would benefit in terms of expanding the pool of successfully lodged HSCs by tightening the vessel barrier and preventing their egress and differentiation (167).

The success of BM transplantation also depends on the ability of HSC/HSPC to successfully "home" and engraft into recipient's BM. In order for this to be completed, a number of serial processes take place including specific molecular recognition, cell-cell adhesion/disengagement, transendothelial migration and replenishment of the eradicated BM stem cell niche (168).

1.3.3.1 Granulocyte-colony stimulating factor (G-CSF)

In the past decades, granulocyte-colony stimulating factor (G-CSF) has been the mobilization agent of choice in clinical transplantation regimens (169). Yet, the incidence of insufficient G-CSF-mediated mobilization in certain individuals still remains significant and poorly explained. More specifically,

approximately 10% of allogeneic and 40% of autologous donor patients fails to mobilize sufficient amounts of HSPC resulting in treatment failure (170, 171). Endogenous G-CSF is released from monocytes, macrophages, endothelial cells and various BM stromal cell populations in response to sepsis and other inflammatory conditions (172, 173). It acts on the G-CSF receptor and its responding cell types are stromal cells and myeloid progenitors. Upon G-CSF stimulation, the CXCL12/CXCR4 signaling pathway is engaged for enhanced HSPC proliferation, migration and egress in circulation (174, 175). Initially, C-X-C Motif Chemokine Ligand 12 (CXCL12) levels decrease dramatically within the BM yet increase in blood circulation possibly due to re-secretion of scavenged CXCL12 levels (176). The sympathetic nervous system also plays important roles in G-CSF-mediated mobilization. This is apparent due to HSPC expression of both dopaminergic and adrenergic receptors and due to the fact that circadian epinephrine secretion affects CXCL12 levels within the BM microenvironment (130, 177). Moreover, mice with abnormal sympathetic nerve function fail to downregulate CXCL12, leading to unsuccessful mobilization in response to G-CSF (128).

Proteolytic functions of several factors are also important in HSPC mobilization. Notably, CXCL12 mediates the secretion of SCF via MMP-9 activation which results in enhanced HSPC egress (178). Moreover, the expression of membrane-bound type 1 MMP (MT1-MMP) on HSPC is increased upon G-CSF administration and actively contributes to the mobilization process by cleaving CD44 homing adhesion molecule (179). Finally, *in vitro* studies have highlighted the proteolytic activity of dipeptidylpeptidase 4 (DPP4) or CD26 and osteoclast-secreted cathepsin K by cleaving CXCL12 (150, 180). Both pharmaceutical inhibition and genetic deletion of CD26 resulted in hampering of HSPC in G-CSF-induced mobilization. This was attributed to the proteolytic activity of CD26 against a group of CSF proteins such as GM-CSF, G-CSF, IL-3 and erythropoietin (181-183). Notably, CD26 is expressed mainly in endothelial cells and its inhibition contributes to maintaining an intact barrier function during stress-induced conditions (184).

To date, G-CSF is available in several pharmaceutical variants. Most *in vivo* experimental studies have been carried out with filgrastim (Neupogen®). Filgrastim is structurally similar to endogenous G-CSF and is produced by recombinant DNA technology in an *E.coli* expression system. The PEGylated form of filgrastim is also available under the generic name PEG-filgrastim (Neulasta®). The advantage of PEG-filgrastim lies with its longer half-life making daily injections unnecessary. Lastly, another variant of recombinant human G-CSF named lenograstim is synthesized in Chinese Hamster Ovary cells (CHO cells) and is identical to the 174-amino acid natural human G-CSF.

1.3.3.2 Other mobilizing agents

As previously mentioned, the CXCL12/CXCR4 signaling pathway plays a pivotal role in HSPC mobilization. AMD3100 is a CXCR4 chemokine receptor antagonist that was discovered via serendipity in an HIV therapeutic targeting screening (185). AMD3100 or Plerixafor (Mobozil®) is indicated for use in combination with G-CSF for the collection of HSPC from the blood and subsequent autologous stem cell transplantation in patients with poor mobilization and non-Hodgkin's lymphoma (NHL) or multiple

myeloma (MM) (186). Other mobilizing agents that disrupt the CXCL12/CXCR4 pathway are CXCR4 antagonists T140 and T134 (187, 188). Administration of CXCR4 partial agonists such as met-SDF-1β, CTCE-0214 and CTCE-0021 has also been associated with mobilization due to desensitization and reduced surface expression of the CXCR4 receptor (189, 190).

The interaction between VLA-4 and VCAM-1 has also been shown to affect HSPC mobilization. Targeting strategies involve antibodies against VLA-4 (191, 192)and VCAM-1 (193, 194). Finally, monotherapy or combination of GM-CSF with G-CSF is contraindicated nowadays due to inadequate number of required mobilized $CD34^+$ cells and high toxicity (195-197).

1.3.4 Vascular regulation of HSPC trafficking

Endothelial cells are front-line responders to HSPC mobilizing agents due to the expression of sensory receptors which are majorly involved in the mobilization process (Fig. 5). CXCR4 and β-adrenergic receptors have been identified as key regulators of HSPC quiescence, BM retention, egress and mobilization processes (198-200).

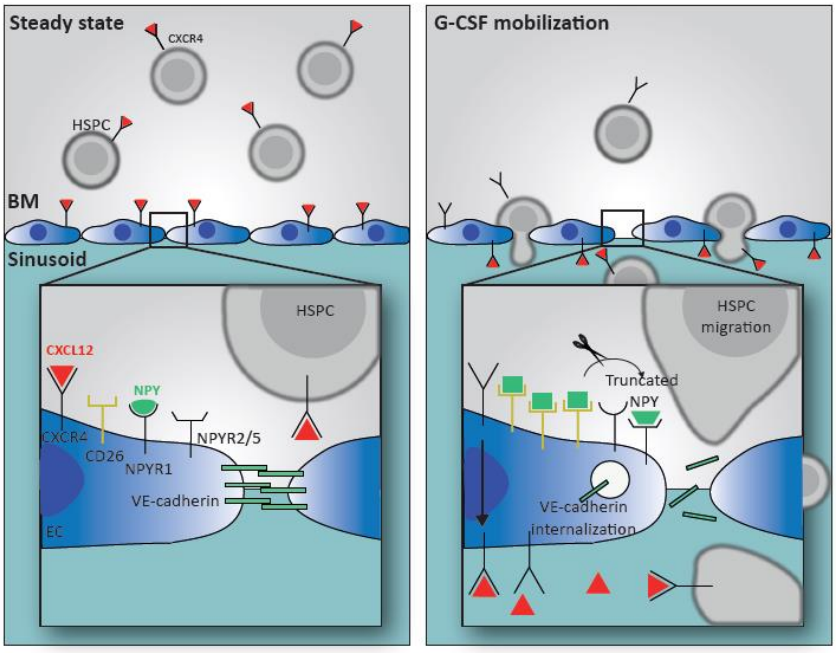

Figure 5: Steady state and G-CSF-induced HSPC mobilization

G-CSF administration favors HSPC migration to the periphery via the redelivery of CXCL12 from the BM to the sinusoid by the EC-expressed CXCR4 receptor. Meanwhile, CD26 receptor levels increase on ECs driving NPY cleavage into its truncated form and binds with higher affinity to NPYR2/5. NPY receptor activation leads to VE-cadherin internalization, degradation and therefore increased overall vascular permeability. The loosening of the vascular barrier further activates HSPCs by increasing intracellular ROS levels, HSPC motility and HSPC-expressed CXCR4 as a response to the CXCL12 gradient.

HSPC egress and mobilization has been suggested to be mediated by sinusoidal vessels due to their distinct properties compared to other types of vessels. In contrast to sinusoids, arterioles differ in integrity properties and higher expression of adherens junction (VE-cadherin) and tight junction

markers (ZO-1 and JAM-A) (25). Furthermore, sinusoids display higher permeability as shown by dye penetration assays and exhibit much lower blood flow and sheer rates compared to arteries (25). Cell trafficking processes such as deceleration, adhesion, rolling and transendothelial migration may only occur in low flow speed and shear rate environment such as the sinusoids.

Upon mobilization stimulus, ECs actively relocate CXCL12 from BM parenchyma to vessel lumen which is in direct contact with blood circulation (199, 200). Moreover, it was recently shown that BM vascular permeability plays an essential role in regulating activation and induction of HSPC motility via enhanced intracellular ROS in response to CXCL12 (25). Taken together, vascular permeability of the blood-BM barrier affects BM homeostasis and regulates HSPC fate.

2. AIMS OF THE THESIS

Hematopoietic stem (HSC) and progenitor cells (HSPC) represent a pool of ancestor cells which possess the ability of self-renewal and multi-lineage differentiation. Postnatally, the primary source of HSC resides within the bone marrow (BM) in a tightly controlled niche that regulates their quiescence, proliferation, and differentiation and subsequent mobilization (116, 201, 202). The recurrent localization of HSC in close proximity to blood vessels suggests the presence of a niche constituted of endothelial and perivascular cells throughout the BM. Consequently, several reports have emphasized the importance of the vascular component within the hematopoietic niche in regulating hematopoiesis through the expression of surface markers and upregulation of angiocrine factors (202). Previous studies revealed that the Ang1/Tie2 signaling pathway plays a critical role in maintaining the quiescent state of HSC (34). More recent data also revealed that deletion of *Angpt1* gene from HSC accelerated vascular and hematopoietic recovery following irradiation, while also inducing vessel leakiness.

The aim of the thesis was to investigate roles of Ang2 and Tie1 receptor in endothelial cells as well as hematopoietic stem and progenitor cells within the BM niche *in vivo*. Specifically, the aims focus on i) deciphering the roles of Ang2 in the context of G-CSF-induced mobilization and BM reconstitution and ii) investigating the roles of endothelial-specific and HSPC-specific Tie1 receptor in terms of HSPC mobilization, vascular function and BM reconstitution potential following lethal irradiation.

3. RESULTS

3.1 HSPC kinetics of G-CSF-induced mobilization in C57BL/6 mice

Prior to investigating of the roles of Angiopoietin-2 and Tie1, it was necessary to establish a robust working model of G-CSF-induced HSPC activation and mobilization to the periphery. For this purpose, 8-12 week old female C57BL/6 mice were subjected to a single subcutaneous injection of PEGylated recombinant G-CSF (Neulasta®) at a dose of 100 µg in 100 µl on day 0. Meanwhile, age-matched control mice received 100 µl saline solution (NaCl) subcutaneously. G-CSF exists in several pharmaceutical formulation variants; however, the choice of PEGylated formulation was made based on the longer half-life and therefore the advantage of single-dose administration. This prevented unnecessary dosing variations and animal burden entangled with daily injections. Several experimental time points were investigated in order to examine G-CSF kinetics and decide on the appropriate termination time-point. BM, spleen and blood were collected at the end of experiment and processed for analysis with flow cytometry. Gating strategies involved the isolation of viable immune single cells of which Lineage$^-$ (Lin$^-$), Lineage$^-$ Sca-1$^+$ c-Kit$^+$ (LSK), multipotent progenitors (MPP), short term HSC (ST-HSC) and HSC (or LSK-SLAM) were further distinguished. The term "lineage" refers to mature immune cells distinguished by the following surface markers: CD3, CD8a, Ter119, CD11b, CD45R. For the purpose of the thesis the term "hematopoietic stem progenitor cell" or "HSPC" corresponds to LSK population. The term "hematopoietic stem cell" or "HSC" corresponds to the LSK CD48$^-$ CD150$^+$ or LSK-SLAM population.

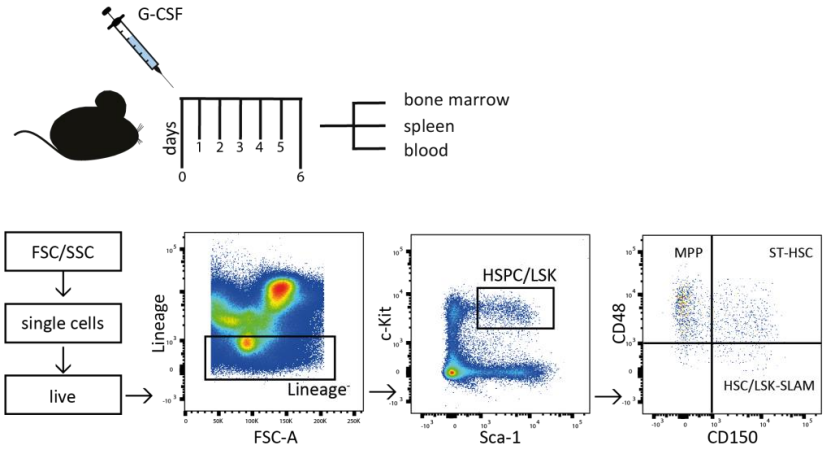

Figure 6: Experimental model and gating strategy of G-CSF-induced HSPC mobilization via flow cytometry

Experimental animals received one dose of 100 µg PEGylated recombinant G-CSF (Neulasta®) subcutaneously at day 0. BM, spleen and blood were collected at the end of experiment and underwent processing for analysis via flow cytometry. (abbreviations see text)

Upon G-CSF administration, the Lin^- population ratio in the BM gradually decreased suggesting a shift towards differentiation to more mature immune cells (Fig. 7A). The HSPC ratio gradually increased reaching a peak on day 3 which reflected an increase in HSPC proliferation and the subsequent mobilization to the circulation and spleen (Fig. 7B). Within the HSPC compartment, there was an increase in MPP cells at the expense of hierarchically primitive LSK $CD48^-$ $CD150^+$ cells (Fig. 7C-D). The Lin^- population in spleen was not significantly altered following G-CSF administration (Fig. 7E). However, within the Lin^- population, a gradual increase of HSPC compartment took place starting on day 3 due to the onset of mobilization from the BM (Fig. 7F). Total body weight and spleen weight were recorded. Upon G-CSF administration, mice developed splenomegaly which is one of the well-known side-effects of mobilizing agents (Fig. 7G-H). Finally, similar to BM, the detected Lin^- population ratio in the blood was significantly reduced on day 3 after G-CSF administration (Fig. 7I) whereas the HSPC population was significantly increased reflecting the onset of mobilization to the periphery. Notably, HSC reside within the BM and are therefore not found in spleen or blood even after G-CSF administration. Having established the HSPC activation and mobilization model, the experimental termination time-point (day 3) was also decided for the subsequent scientific experiments.

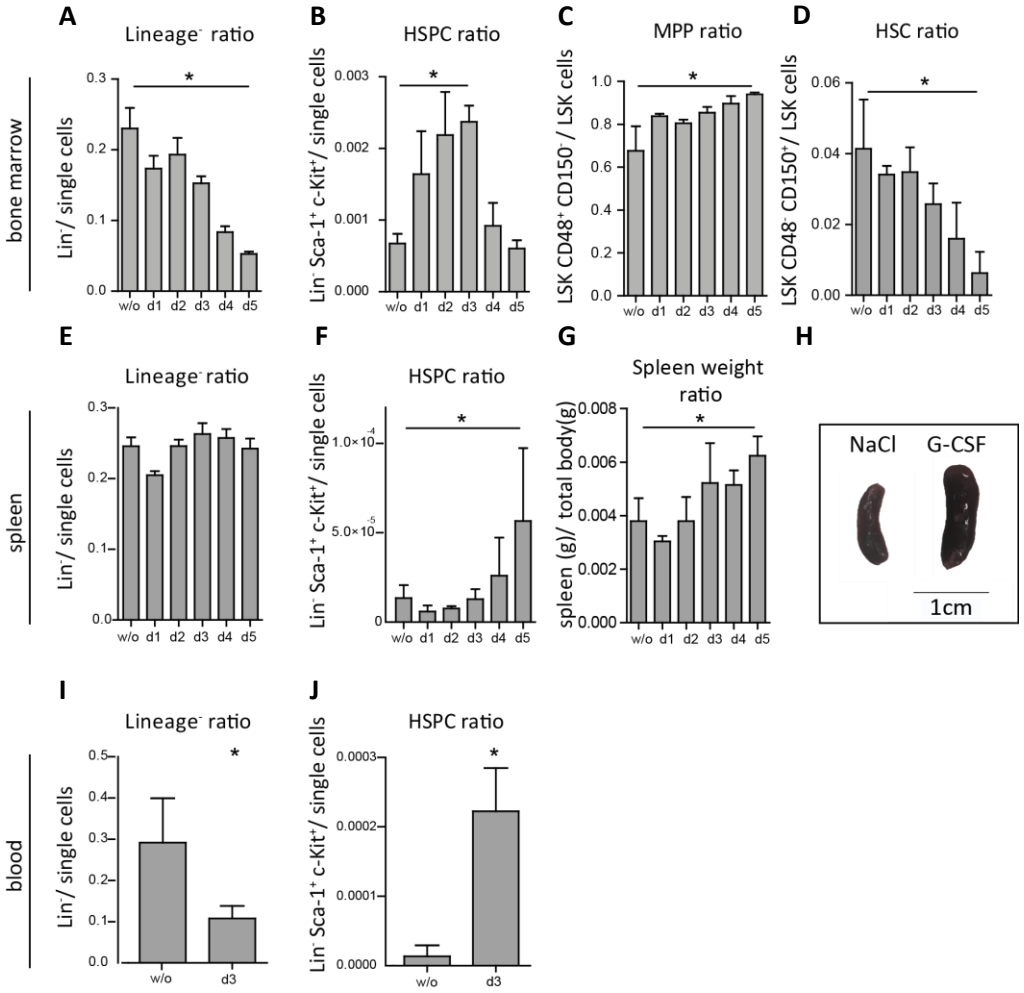

Figure 7: Establishment of G-CSF-mediated HSPC expansion in the bone marrow and mobilization

Analysis of **A)** Lineage⁻, **B)** HSPC, **C)** MPP and **D)** HSC population ratios in the BM via flow cytometry. Population ratios of **E)** Lineage⁻ and **F)** HSPC cells in spleen. **G)** Timeline of spleen weight increase upon G-CSF treatment and **H)** representative image of a spleen treated with NaCl and with G-CSF (d3). Population ratios of **I)** Lineage⁻ and **F)** HSPC cells in blood. Data are shown as mean±sd (n=3-4; Mann-Whitney test, *, $p<0.05$). (abbreviations see text)

In order to assess how G-CSF stimulation affects Ang/Tie signaling, blood serum and HSPCs were collected for C57BL/6N mice at different time-points (Fig. 8A). G-CSF administration resulted in the gradual increase of Angiopoietin-2 protein concentration from steady state to day 6 (Fig. 8B). Relative *Angpt1* expression was measured via qPCR in sorted HSPCs at different time-points upon G-CSF injection. Administration of G-CSF resulted in gradual downregulation of *Angpt1* on HSPCs (Fig. 8C). In conclusion, a G-CSF-induced HSPC activation and mobilization model was established in order to carry out further investigations concerning Ang/Tie signaling.

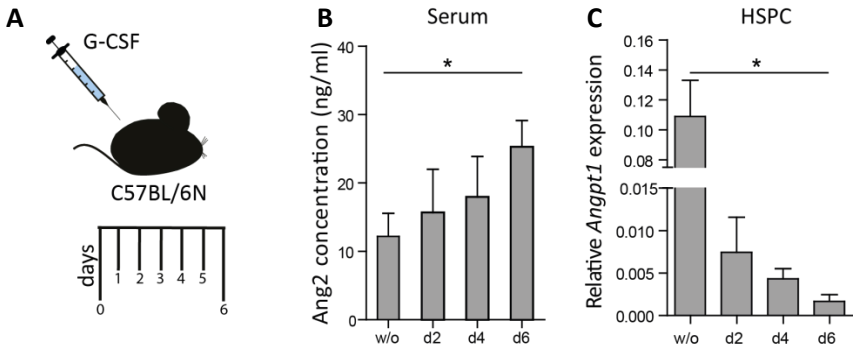

Figure 8: Further characterization of experimental model

A) Schematic representation of experimental model. C57BL/6N mice were treated with G-CSF and sacrificed at different time-points. **B)** Serum Ang2 protein concentration detected via ELISA (n=5-6; ANOVA-Kruskal-Wallis, *, $p<0.05$) and **C)** relative *Angpt1* expression in sorted HSPC (5000 LSK cells/mouse) at consecutive time-points upon G-CSF administration. Gene expression is normalized to *Hprt1* expression. (n=3-4; ANOVA-Kruskal-Wallis, *, $p<0.05$). Data are shown as mean±sd.

3.2 HSPC expansion is reduced in Ang2^{KO} mice treated with G-CSF

The strong increase in Ang2 protein concentration in the serum upon G-CSF administration hypothesized the possible contribution of the ligand to the mobilization process. In order to investigate this, mice with global deletion of the *Angpt2* gene in C57Bl/6N background (Ang2^{KO}), kindly provided by Dr. Gavin Thurston, were used. The Ang2^{KO} mouse line breeding strategy involved crossing heterozygotes (Ang2$^{+/-}$), which gave rise to further heterozygotes and homozygotes with and without the gene locus (Ang2$^{+/+}$ and Ang2$^{-/-}$). Ang2$^{+/+}$ littermates were used as controls (Wildtype, WT). The characterization of HSPC kinetics upon G-CSF stimulation was carried out (Fig. 9A).

At steady state, absolute numbers of BM HSPCs in WT and Ang2^{KO} mice were comparable (Fig. 9B). Moreover, hematological analysis via Hemavet counter on WT and Ang2^{KO} revealed comparable blood cell composition (Fig. 9 I-J). Whereas BM HSPC absolute numbers increased gradually in WT animals and peaked on day 3, the increase in HSPC absolute numbers in BM and spleen of Ang2^{KO} mice was reduced and delayed (Fig. 9B-C). This expansion and mobilization deficiency was not visible in blood until day 6 (Fig. 9D). Blood cell counts in WT and Ang2^{KO} littermates were comparable during both homeostasis and G-CSF-induced mobilization. This indicated that Ang2 affected HSPC expansion and mobilization, but not their differentiated progeny within the assessed time frame (Fig. 9E-G). Moreover, HSC numbers in G-CSF treated WT and Ang2^{KO} mice were also comparable (Fig9. H), suggesting that Ang2 was not critical for HSC expansion but rather that of multipotent progenitors (MPP).

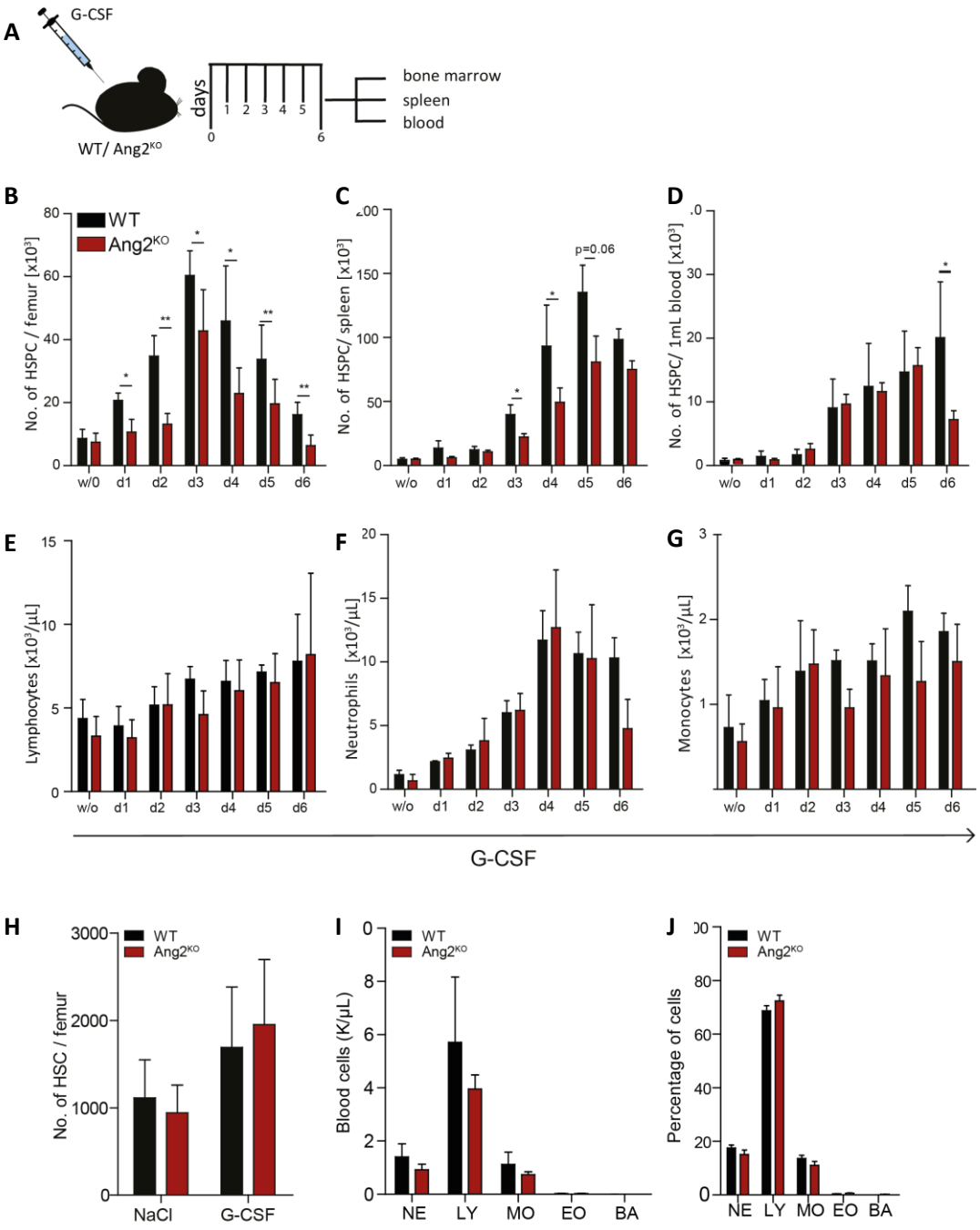

Figure 9: Loss of Ang2 decreases G-CSF induced HSPC expansion and mobilization

A) Schematic representation of experimental model. WT and Ang2^{KO} mice were treated with 100µg human PEGylated G-CSF and sacrificed at different time-points. Analysis was performed on BM, spleen and blood with flow cytometry. **(B)** Absolute number of HSPCs in WT and Ang2^{KO} mice at the indicated time-points post-treatment with G-CSF in the BM, **(C)** spleen and **(D)** blood (n=4-9; Mann-Whitney test,*, $p<0.05$ and **, $p<0.01$). **(E)** Absolute numbers of blood lymphocyte, **(F)** neutrophil and **(G)** monocyte populations in WT and Ang2^{KO} mice at steady state and G-CSF treatment timeline assessed by Hemavet counter (n=4; Mann-Whitney test). **(H)** Absolute number quantification of HSC in WT and Ang2^{KO} mice at steady state and treatment with G-CSF (day 3) (n=4-6; Mann-Whitney test). **(I)** Hematological profile of WT and Ang2^{KO} mice at steady state and **(J)** percentile representation of distinct blood cell types using Hemavet counter. Data are shown as mean±sd (n=8; Mann-Whitney test; *, $p<0.05$ and **, $p<0.01$).

The pharmacological inhibition of Ang2 was employed in order to validate the genetic approach. C57BL/6N mice were injected i.p. with either neutralizing mouse anti-Ang2 antibody or rat IgG (Eli Lilly) at 20mg/kg per mouse twice in a week (Fig. 10A). Similar to the Ang2^{KO} genetic mouse model, steady state absolute HSC and HSPC numbers were comparable in both WT and Ang2^{KO} mice. However, G-CSF stimulation resulted in the reduced expansion of HSC and HSPC within the BM (Fig. 10B-C). The pharmacological inhibition of Ang2 also resulted in a reduced number of HSPCs mobilizing to the spleen (Fig. 10D). Yet this phenomenon was not detectable in blood (Fig. 10E).

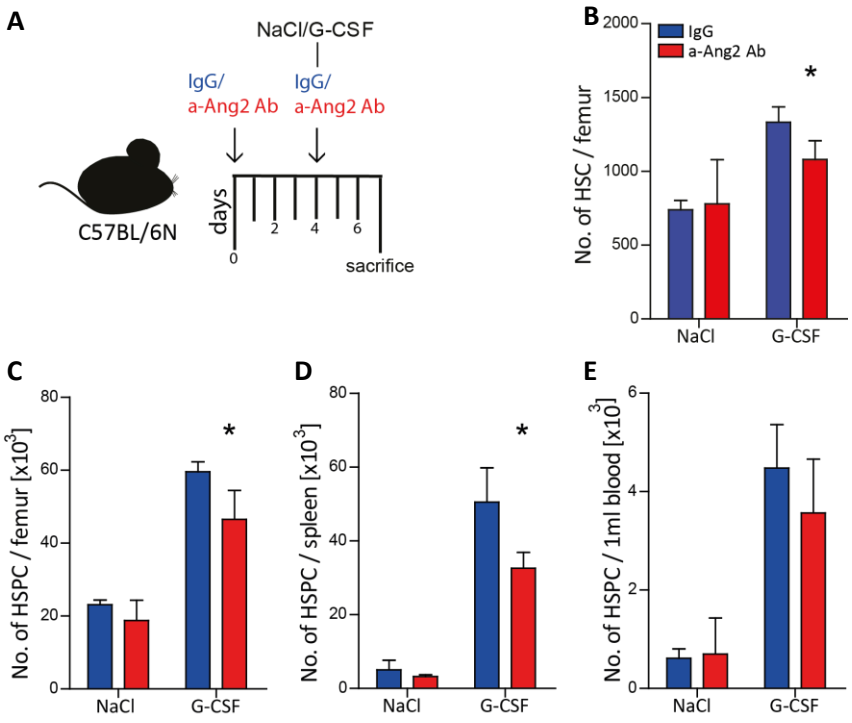

Figure 10: Pharmacological inhibition of Ang2 results in reduced HSPC and HSC in G-CSF-induced expansion and mobilization to the spleen

(A) Experimental setup of IgG/Ang2 neutralizing antibody administration at steady state and G-CSF induced mobilization (day3). **(B)** HSC and HSPC absolute number quantification in **(C)** BM, **(D)** spleen and **(E)** blood. Data are shown as mean±sd (n=6-10; Mann-Whitney test, *,p<0.05).

In conclusion, Ang2 affected HSPC within the BM resulting in delayed mobilization to the spleen up until day 4 prior to catching up. The reduced G-CSF-mediated HSPC activation in Ang2^{KO} mice supports the paracrine antagonistic role of Ang2 in the BM niche and pharmacological data could confirm these findings.

3.3 HSC and HSPC proliferation is reduced in Ang2^{KO} mice

To examine the underlying cause for the poor ability of Ang2^{KO} mice to trigger HSPC activation, the proliferative potential of HSPC and HSC was assessed in WT and Ang2^{KO} mice. Ki67/Hoechst33342 staining identified reduced fractions of HSPC and HSC in the S/G2/M phase in Ang2^{KO} mice during

steady state and upon G-SCF mobilization (Fig. 11A-B, D). Likewise, the HSC retention factor Cxcr4 was up-regulated in HSC and HSPC in $Ang2^{KO}$ (Fig. 11C-E). HSC sorted from $Ang2^{KO}$ mice also expressed more Cdkn1a at mRNA level (Fig. 11E), which interferes with cell cycle progression and has also been observed to be elevated in HSC upon Ang1 overexpression (203). HSPC of $Ang2^{KO}$ mice expressed enhanced levels of Tek/Tie2 (Fig. 11C), which might contribute to increased quiescence of HSPC and has also been shown to be increased in HSC cultured with Ang1 (102). Thus, absence of Ang2 reduced HSPC activation by restricting cell cycle entry. In order to investigate whether Ang2 affected the mobilization process, WT and $Ang2^{KO}$ mice were treated with AMD3100, a CXCR4 inhibitor and ,therefore, a rapid stem cell mobilizing agent. The absolute numbers of mobilized HSPC detected in blood was comparable in both groups suggesting that Ang2 did not affect the mobilization process.

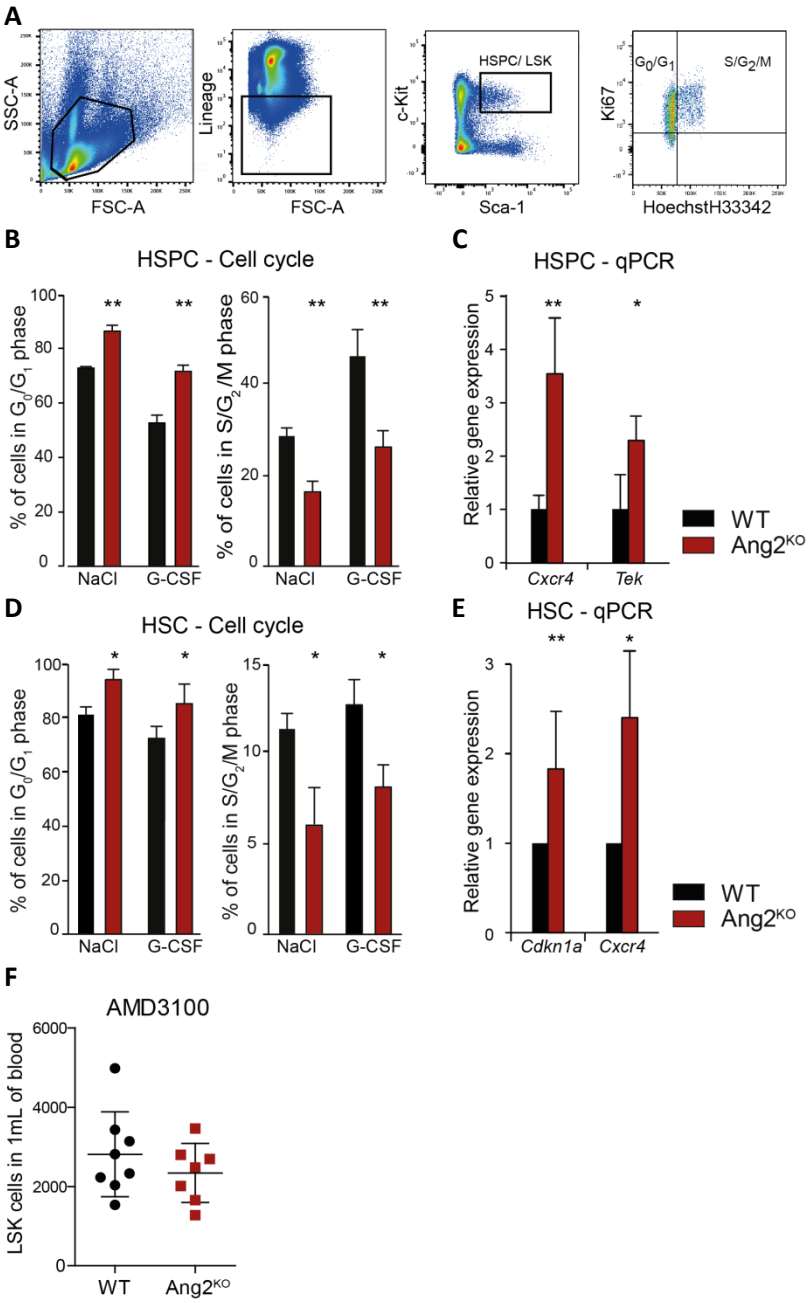

Figure 11: Loss of Ang2 disrupts HSPC and HSC quiescence

(A) Gating strategy for cell cycle analysis of HSPCs with Ki67/Hoechst. BM HSCs and HSPCs were analyzed for the presence of the proliferation marker Ki67 and counterstained with Hoechst H33342 for cell cycle analysis. **(B)** Percentages of sorted BM HSPCs and **(D)** HSCs in G0/G1 and S/G2/M phase in G-CSF-treated (day 2) and NaCl treated Ang2^{KO} and WT mice. **(C)** Target gene expression analysis in HSPCs and **(E)** HSCs at steady state (n≥ 3; Mann-Whitney test,*, p<0.05 and **, p<0.01). **(F)** Absolute numbers of HSPCs in blood of WT and Ang2^{KO} mice one hour after AMD3100 administration. Data are shown as mean±sd (n=7-8; Mann-Whitney test).

In order to exclude the possibility of vascular defects and further validate that Ang2 acts in a paracrine manner on the activated HSPC, we functionally assessed vessel leakiness ex vivo via dextran permeability assay. Sinusoidal vasculature characterization on G-CSF treated mice (day 3) yielded comparable vessel area and vessel density in WT and Ang2^{KO} mice (Fig. 12A). Merged confocal images demonstrate the co-localization of dextran-FITC with endomucin^{+} vessels in both experimental groups suggesting that Ang2 absence does not alter vessel area and density (Fig. 12B-C). Quantification of extravasated dextran-FITC in the diaphysis and epiphysis of femurs resulted in comparable extravasation effect in WT and Ang2^{KO} mice (Fig. 12D-E).

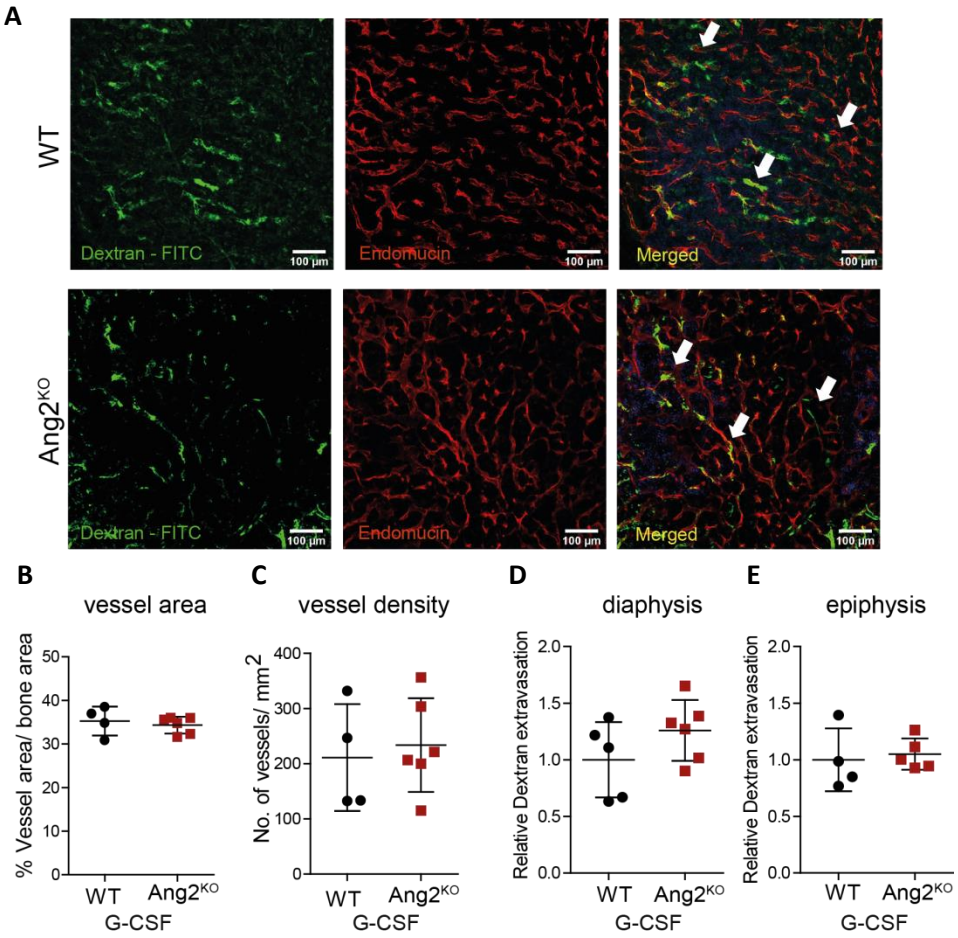

Figure 12: Bone marrow vasculature and dextran extravasation are unaffected by the absence of Ang2 upon G-CSF treatment

(A) Representative confocal images of dextran-FITC 70kD (green), endomucin+ (red) sinusoidal vessels in the femur diaphysis region. Scale bar indicates 100um. **(B)** Vessel area and **(C)** vessel density quantification. WT and Ang2^{KO} femur **(D)** diaphysis and **(E)** epiphysis quantification of extravasated dextran. White arrows indicate dextran-FITC and endomucin co-localization. Data are shown as mean±sd (n=4-6; Mann-Whitney test).

3.4 Niche derived Ang2 contributes to bone marrow reconstitution after irradiation.

To further investigate the role of paracrine Ang2 signaling, transplantation experiments were carried out in order to assess the hematopoietic reconstitution efficiency. Donor BM cells from CD45.1 mice were transplanted into lethally irradiated WT and Ang2^{KO} congenic mice (Fig. 13A). This resulted in overall reduced reconstitution efficiency in the Ang2^{KO} mice translating in fewer circulating WBC (Fig. 13B) as shown by Hemavet counter. More specifically, in the absence of stromal Ang2, the repopulating lymphocytes (Fig. 13D) and monocytes (Fig. 13E) were fewer in absolute numbers compared to WT mice. This effect was not observed in neutrophils (Fig. 13C). These results were further validated by blood flow cytometry analysis with neutrophilic, T-cell and B-cell markers (Fig. 13F-H). Furthermore, engraftment efficiency was quantified by flow cytometry in blood (Fig. 13I).

Percentages of donor-derived (CD45.1$^+$) immune cells were not significantly altered in CD45.2$^+$ recipients 18 weeks after transplantation (Fig. 13J). Within the donor-derived immune cells, there was no selective advantage in myeloid or lymphoid population fractions (Fig. 13K-L). These data demonstrate that the absence of Ang2 from BM stroma resulted in defects in hematopoietic reconstitution, but did not play a role in hematopoietic engraftment.

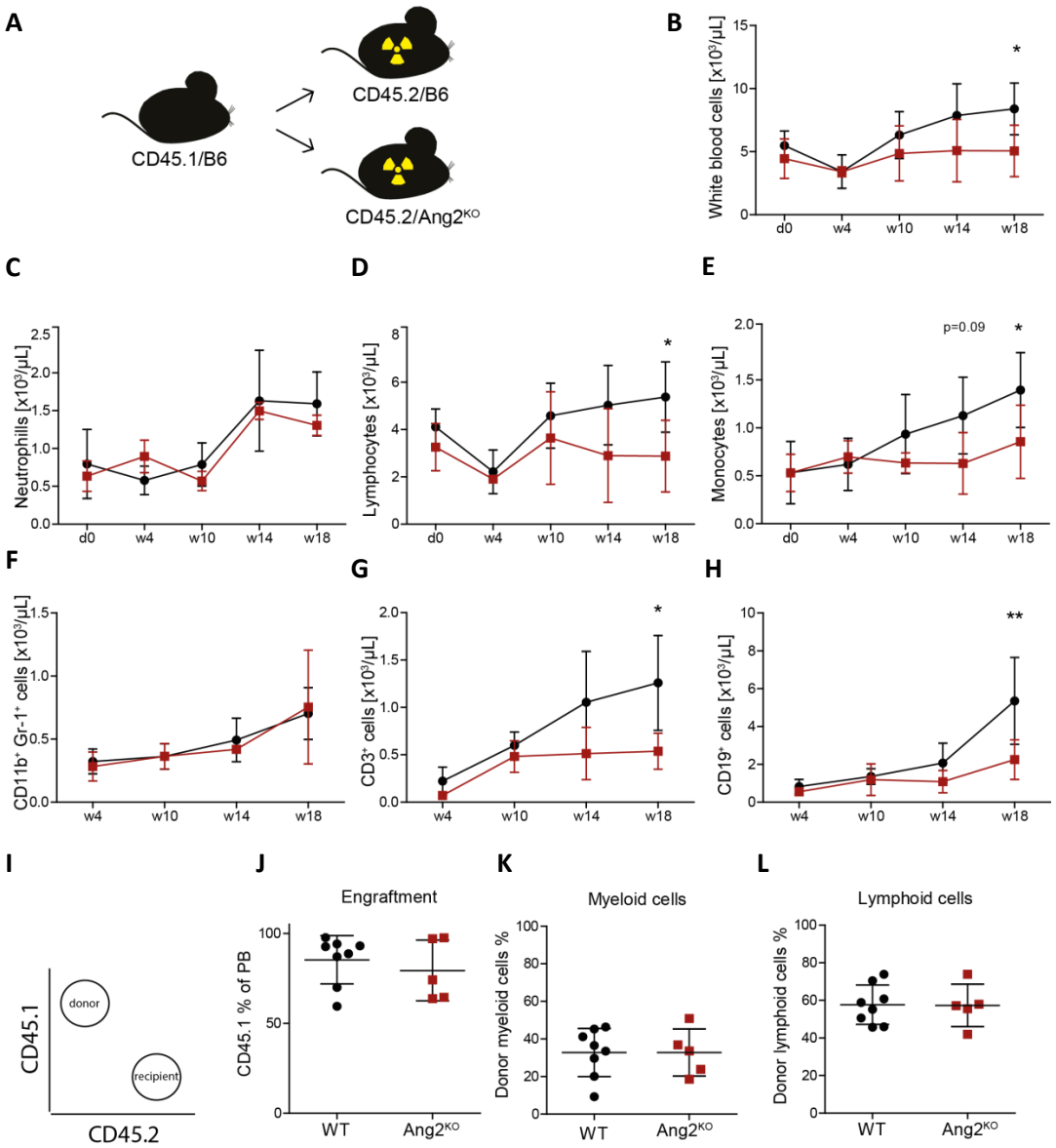

Figure 13: Niche-derived Ang2 affects bone marrow reconstitution in lethally irradiated mice

(A) BM cells from CD45.1 donor were transplanted into WT and Ang2^{KO} lethally irradiated recipient mice. **(B)** Total white blood cell count in WT and Ang2^{KO} mice throughout BM reconstitution process. **(C)** Neutrophil, **(D)** lymphocyte and **(E)** monocyte populations assessed via Hemavet counter. Blood **(F)** CD45$^+$, CD11b$^+$, Gr-1$^+$, **(G)** CD45$^+$, CD3$^+$ and **(H)** CD45$^+$,CD19$^+$ cell populations assessed by flow cytometry throughout BM reconstitution. **(I)** Gating strategy for assessment of engraftment efficiency. **(J)** Engraftment efficiency percentage indicating CD45.1$^+$ donor derived cells in blood at the end of the experiment (week 18). **(K-L)** Donor derived myeloid (CD45.1$^+$, CD11b$^+$, Gr-1$^+$) and lymphoid (CD45.1$^+$, B220$^+$, CD4$^+$, CD8$^+$) cell population percentages. Data are shown as mean±sd (n=5-8; Mann-Whitney test, $p<0.05$ and **, $p<0.01$).

3.5 Endothelial Tie1 deletion delays HSPC egress and G-CSF-induced mobilization

The approach for investigating the role of BM endothelial Tie1 in HSPC egress and mobilization involved the breeding and use of an inducible EC-specific Tie1 knock-out mouse line ($Tie1^{iECKO}$). Since constitutive Tie1 deletion is embryonically lethal, $Tie1^{flox/flox}$ mice were generated by Dr. Scott Baldwin using the Cre/loxP system to induce conditional deletion of the first coding exon of Tie1 (204). In order to obtain Tie1 endothelial specific deletion following tamoxifen administration, $Tie1^{flox/flox}$ mice were crossed with inducible Tg(Cdh5-cre/ERT2)1Rha($Cdh5Cre^{ERT2}$) mice (205). $Tie1^{flox/flox}$ mice were used as controls (Wildtype, WT). For all experiments, Tie1 deletion efficiency was evaluated by qPCR in total tissue RNA lysates. Mice with less than 35% Tie1 deletion were excluded from analyses.

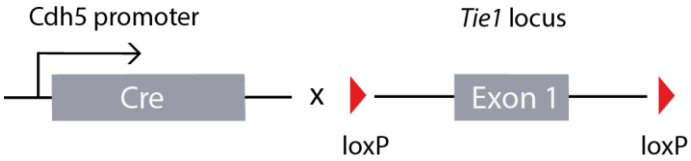

Figure 14: Targeting strategy of the Tie1 locus
Ve-$CadherinCre^{ERT2}$ mice were bred with $Tie1^{flox/flox}$ mice to achieve EC-specific receptor deletion.

In the attempt to assess the importance of endothelial cell Tie1 in the process of HSPC egress and G-CSF-induced mobilization, mice were induced with tamoxifen and either saline or G-CSF was administered subcutaneously. On day 3, mice were sacrificed and flow cytometry analysis was performed in BM, spleen and blood (Fig. 15A).

At steady state, the absolute number of HSPCs in BM was unchanged in $Tie1^{iECKO}$ mice compared to WT littermates (Fig. 15B). However, a reduced number of HSPCs egressed to the spleen (Fig. 15C). Similarly, upon endothelial cell *Tie1* deletion and G-CSF stimulation, the number of HSPCs within the BM remained comparable between the groups (Fig. 15D). Yet, in the case of HSPC mobilization to the periphery, there was a significant decrease in the number of HSPCs in $Tie1^{iECKO}$ mice (Fig. 15E-F). It was previously showed that Ang2 affected HSPC expansion. In the case of $Tie1^{iECKO}$ an HSPC mobilization phenotype was observed. This suggested that *Tie1* deletion affected BM vasculature in restricting access of HSPC to the blood stream and eventually the spleen during G-CSF-induced mobilization.

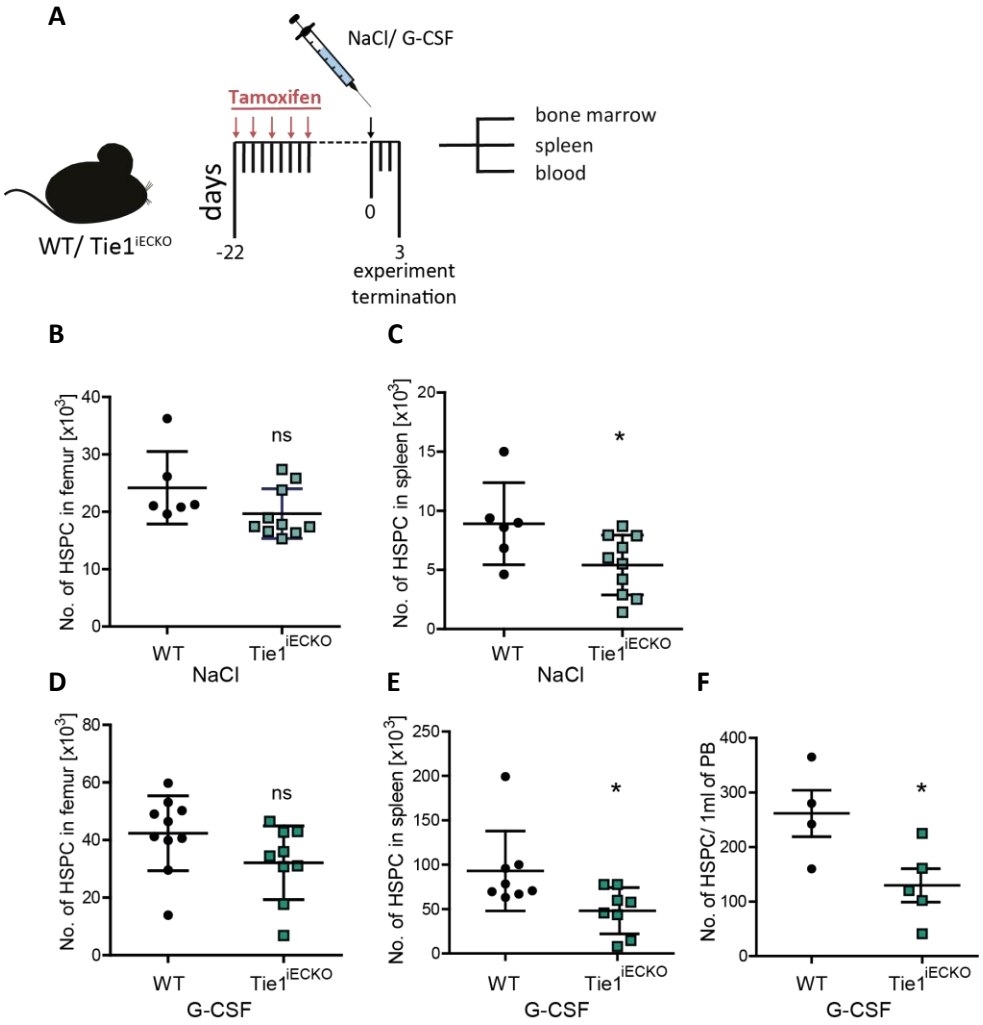

Figure 15: Endothelial specific* Tie1 *deletion reduces mobilization at steady state and G-CSF-induced stimulus yet does not affect HSPC expansion

(A) Schematic representation of experimental model. Endothelial-specific *Tie1* deletion was induced via tamoxifen administration. Mice received either G-CSF or equal volume of NaCl at d0 and sacrificed at day 3. **(B)** Absolute HSPC numbers in BM and **(C)** spleen at steady state (n=6-10; Mann-Whitney test, *; p<0.05). **(D)** Absolute HSPC numbers in BM, **(E)** spleen and **(F)** blood at G-CSF stimulation. Data are shown as mean±sd (n=4-10; Mann-Whitney test, *; p<0.05).

In order to explore the roles of Tie1 receptor in HSPC egress and mobilization, tamoxifen was administered according to the established protocol (Fig. 16A) and Cre/Lox recombination efficiency was determined by Tie1 gene expression analysis in whole bone marrow (WBM) (Fig. 16D). Upon endothelial *Tie1* deletion, Ang2 protein levels in serum was elevated at steady state as well as in G-CSF-treated Tie1^{iECKO} mice (Fig. 16B-C). Moreover, gene expression analysis in the WBM was carried out in order to investigate the behavior of Tie2 receptor and Angiopoietin-1 ligand upon G-CSF stimulation and endothelial cell Tie1 deletion. Similar to Tie1, Tie2 receptor was upregulated upon G-CSF stimulation and downregulated in the absence of Tie1 (Fig. 16E). The gene expression of the

agonistic ligand Ang1, was downregulated upon G-CSF stimulus and even more so in Tie1^{iECKO} mice compared to WT (Fig. 16F). Moreover, the panvascular gene, *Pecam1* (CD31) was significantly increased upon G-CSF stimulus indicating the vascular compartment's involvement in the process of HSPC activation and mobilization. However, *Pecam1* was significantly downregulated in Tie1^{iECKO} mice compared to WT mice upon G-CSF treatment (Fig. 16G). The gene expression of the intercellular junction marker, VE-Cadherin (*Cdh5*) and the tight junction marker, Claudin 5 (*Cldn5)*, did not significantly differ between WT and Tie1^{iECKO} mice. However, upon G-CSF stimulus, gene expression of VE-Cadherin was downregulated whereas the opposite occurred for Claudin 5 (Fig. 16H-I).

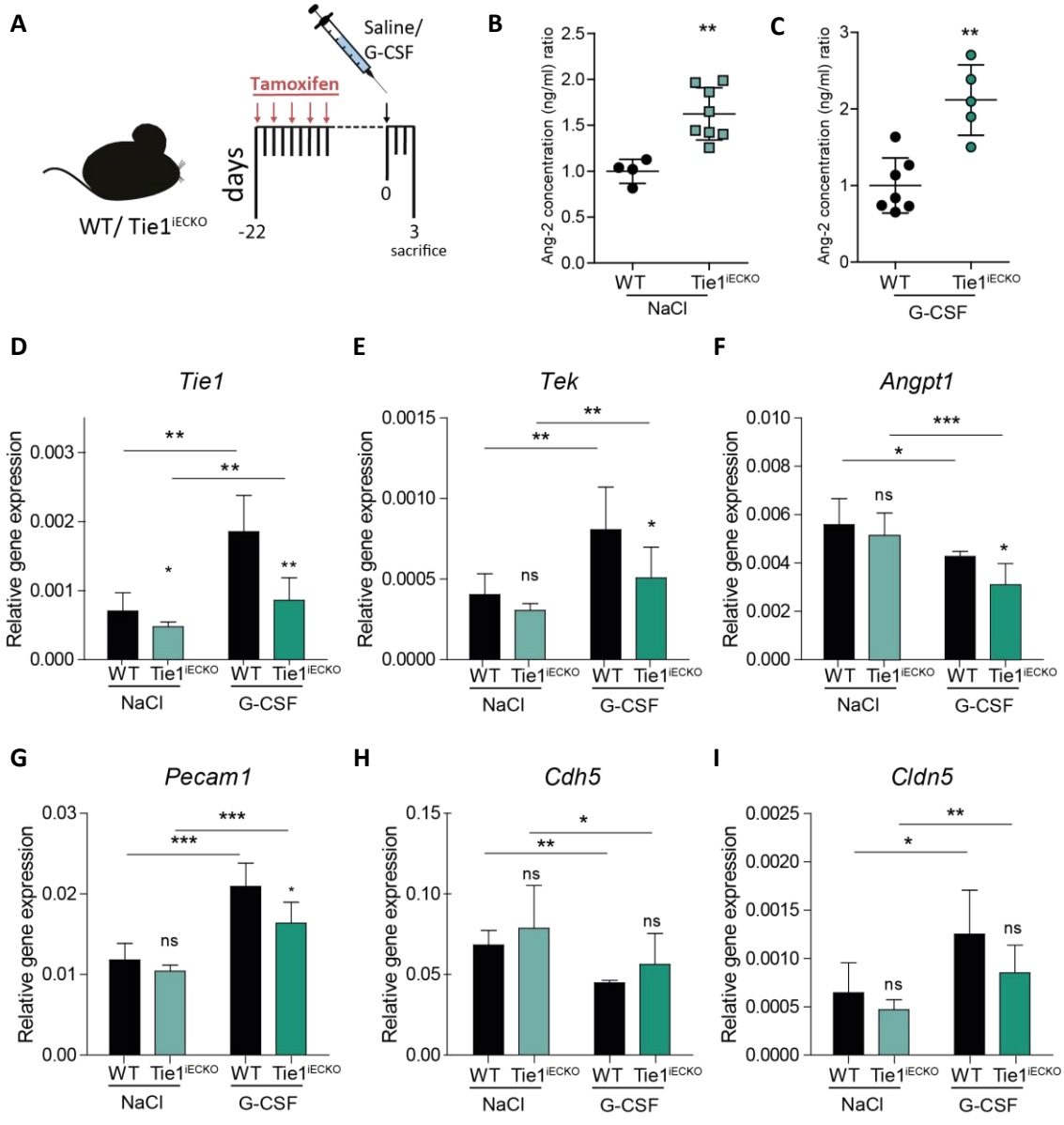

Figure 16: Endothelial specific* Tie1 *affects gene expression at steady state and G-CSF mobilization in the bone marrow

(A) Schematic representation of experimental model. Endothelial-specific *Tie1* deletion was induced via tamoxifen administration. Mice received either G-CSF or equal volume of NaCl at d0 and were sacrificed at d3.

(B) Ang2 protein concentration in serum of WT and Tie1^{iECKO} mice at steady state and **(C)** G-CSF stimulation (n=4-8; Mann-Whitney test, **, p<0.01). Whole bone marrow gene expression via RT-qPCR of **(D)** *Tie1*, **(E)** *TEK,* **(F)** *Angpt1* and vascular and adherens markers **(G)** *Pecam1,* **(H)** *Cdh5,* **(I)** *Cldn5*. Data are shown as mean±sd n=4-8; Mann-Whitney test, *; p<0.05, **; p<0.01, ***; p<0.001).

In order to assess HSPC proliferation, mice were induced with tamoxifen, mobilized with G-CSF and received EdU (1mg/mouse) intraperitoneally 24h prior to sacrifice (Fig. 17A). Bone marrow HSPCs were analyzed using "LSK" markers by flow cytometry. EdU incorporation into dividing LSK cells showed no difference between WT and Tie1^{iECKO} mice (Fig. 17B).

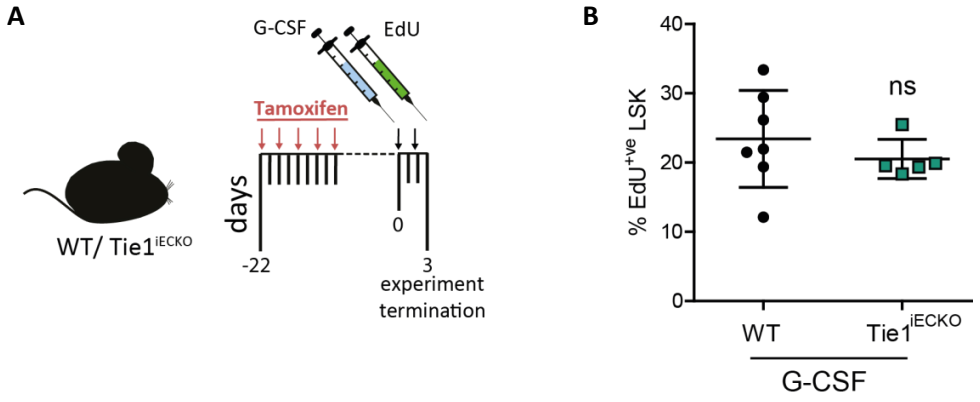

Figure 17: Endothelial specific Tie1 deletion does not affect HSPC proliferation

(A) Schematic representation of experimental model. Endothelial-specific Tie1 deletion was induced via tamoxifen administration. Mice received either G-CSF or equal volume of NaCl at d0 and sacrificed at day 3. Mice receive EdU (1mg/mouse) 24 h prior to sacrifice for HSPC proliferation quantification. **(B)** Quantification of EdU positive LSK cells in WT and Tie1^{iECKO} mice at G-CSF (day 3) stimulation determined via flow cytometry. Data are shown as mean±sd (n=5-7; Mann-Whitney test).

BM vascular endothelial barrier function was assessed using the Evans Blue Dye (EBD) assay. Here, extravasation of the circulating low molecular weight dye Evans Blue from BM vessels to the surrounding tissue is analyzed by measuring the absorbance of the dye extracted from femurs. Upon G-CSF stimulus, there was no detectable difference in absorbance ratio between WT and Tie1^{iECKO} mice.

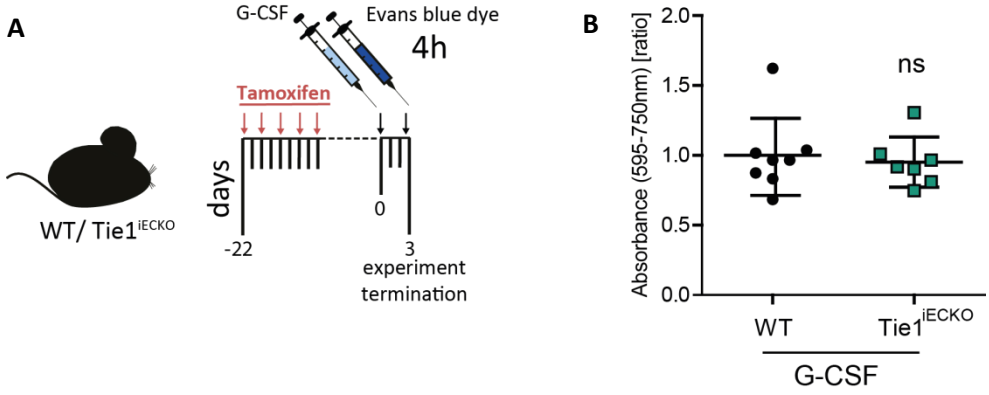

Figure 18: Endothelial specific Tie1 deletion does not alter vessel permeability to EBD

(A) Schematic representation of Evans Blue dye i.v. administration in induced WT and Tie1^{iECKO} mice. Mice were sacrificed 4h later and femurs were harvested for colorimetric quantification. **(B)** Extravasated Evan's Blue dye quantification at G-CSF stimulation. Data are shown as mean±sd (n=7-8; Mann-Whitney test).

The vasculature was also functionally assessed by performing an HSPC homing assay. Transplanted HSC and HSPC have the ability to successfully lodge and reach the recipient's BM. This property can be used as an indication of HSC and HSPC functionality as well as an assessment of the recipient's vasculature. Equal numbers of BM Lin$^-$ cells were injected intravenously into WT and Tie1^{iECKO} mice 4 hours prior to sacrifice at G-CSF day 3. Flow cytometry analysis of the BM indicated that a reduced number of Lin$^-$ cells reached the recipient Tie1^{iECKO} BM further supporting the notion that Tie1 acts as a vascular gate-keeper for HSPC.

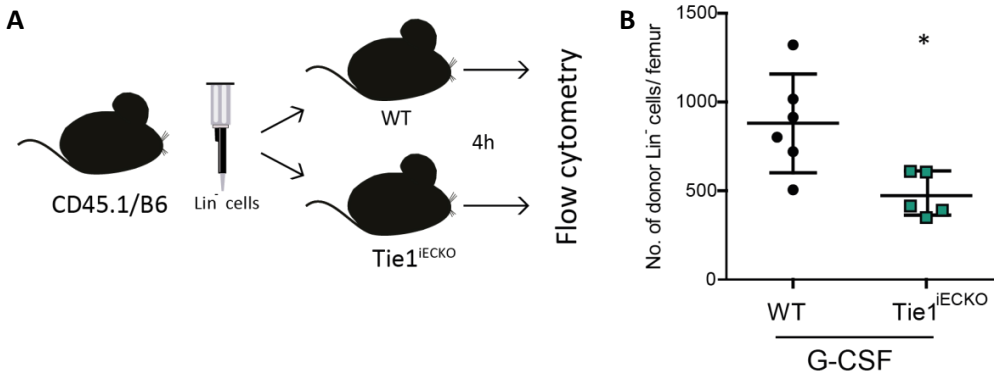

Figure 19: Absence of endothelial Tie1 reduces efficient homing of donor undifferentiated cells
(A) Schematic representation of homing experiment in WT and Tie1^{iECKO} mice at steady state. Lineage$^-$ BM cells from CD45.1 donor mice were collected and transplanted in WT and Tie1^{iECKO} (CD45.2) mice. Recipient mice were sacrificed after 4h and femurs were processed for flow cytometry. **(B)** Flow cytometry quantification of donor Lineage$^-$ cells in recipient mice femurs. Data are shown as mean±sd (n=5-6; Mann-Whitney test, *; $p<0.05$).

Finally, the femur diaphysis and epiphysis were chosen for imaging and analysis of vascular area and dextran-FITC extravasation. WT and Tie1^{iECKO} mice received 10mg/mouse dextran-FITC 70 kDa intravenously 4 h before sacrifice. This timeframe allowed for dextran-FITC extravasation from BM vessels to surrounding tissues. Endomucin was the vascular marker of choice in the BM due to high specificity in sinusoidal vasculature. At steady state, neither diaphysis nor epiphysis had evident differences in endomucin staining. Upon G-CSF however, vascular area in Tie1^{IECKO} mice was reduced in both regions. In the case of extravasated dextran-FITC, there was no difference between WT and Tie1^{iECKO} mice in both steady state and G-CSF models in the diaphysis. In the epiphysis however, there was a detectable increase in dextran-FITC extravasation to peripheral tissue upon G-CSF stimulation in Tie1^{iECKO} mice.

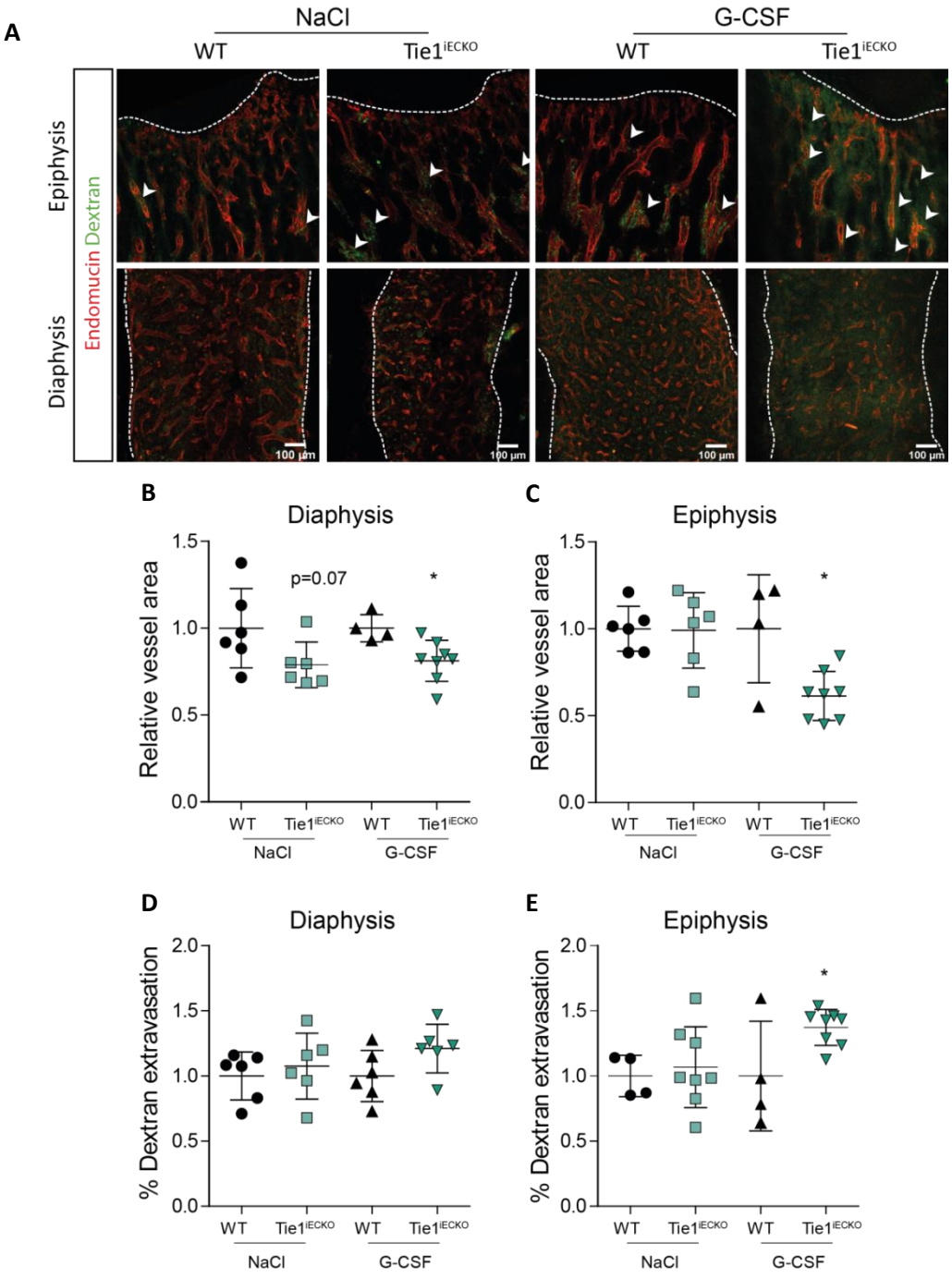

Figure 20: Bone marrow vasculature and dextran extravasation in Tie1^{iECKO} mice at steady state and upon G-CSF treatment

(A) Representative confocal images of dextran-FITC 70kD (green), endomucin^{+} (red) sinusoidal vessels in the femur diaphysis and epiphysis. Scale bar indicates 100 µm. Relative vessel area in steady state and G-CSF treated **(B)** diaphysis and epiphysis. Dextran extravasation quantification at steady state and G-CSF treatment in **(C)** diaphysis and epiphysis. White arrows indicate dextran-FITC and endomucin co-localization. Arrows indicated extrasazated dextran-FITC. Data normalized to WT. Data are shown as mean±sd (n=4-8; Mann-Whitney test).

3.6 Tie1 deletion on HSPC reduces short-term BM reconstitution in lethally irradiated mice

Since the receptor's discovery in the early 90s, it was well accepted that Tie1 is expressed by both endothelial cells and immature hematopoietic cells. This study would therefore be incomplete without the investigation of the roles of Tie1 expressed in HSPC. In order to get a glimpse of how Ang/Tie expression is distributed among separate HSC and multipotent progenitor (MPP) populations I reanalyzed the bulk sequencing data produced by Cabezas-Wallscheid et al. (35) and focused on gene expression of the components of Ang/Tie signaling family (Fig. 21). The different populations were grouped hierarchically according to loss or gain of surface markers. Multipotent HSC with long-term self-renewal were followed by multipotent MPP1 with short-term self-renewal. MPP2 population was characterized by the presence of CD48, whereas MPP3 and MPP4 represented progeny with myeloid and lymphoid bias respectively. Mean reads per kilobase of transcript per million mapped reads (RPKM) of *Angpt1* and *Tie1* demonstrated a clear correlation between higher gene expression and hierarchical order.

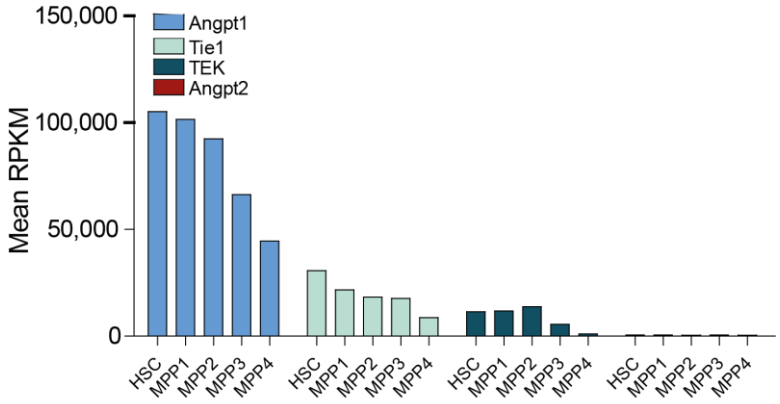

	HSC	MPP1	MPP2	MPP3	MPP4
CD34	-	+	+	+	+
CD48	-	-	+	+	+
CD150	+	+	+	-	-
CD135	-	-	-	-	+

Figure 21: Ang/Tie gene expression of different hematopoietic stem and progenitor cell populations obtained by bulk RNA sequencing

Mean RPKM of *Angpt1*, *Tie1*, *TEK* and *Angpt2* in hematopoietic stem and progenitor cell populations sorted according to surface markers (lower panel). All groups above are also encompassed by the Lineage$^-$ Sca-1$^+$ c-Kit$^+$ population.

Although both Tie receptors have been associated with HSC and HSPC, most studies have focused on Tie2 as an important receptor for HSC quiescence. In order to investigate the roles of Tie1 expressed on HSPC, Tie1$^{flox/flox}$ mice were crossed with inducible Gt(ROSA)26Sortm1(cre/ERT2)Tyj (Rosa-CreERT2) mice (Fig. 22). Tie1$^{flox/flox}$ mice were used as controls (Wildtype, WT). For all experiments, Tie1 deletion efficiency was evaluated by qPCR in sorted HSPC. Mice with less than 90% *Tie1* deletion were excluded from analyses.

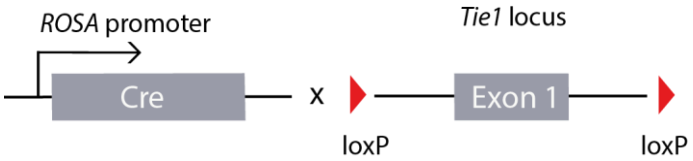

Figure 22: Targeting strategy of the Tie1 locus

ROSACre^{ERT2} mice were bred with *Tie* $^{flox/flox}$ mice to achieve global Tie1 receptor deletion.

Having established that Tie1 expression occured not only on EC but also on HSC and HSPC, the next step was to investigate the biological function of the receptor. For this purpose, Tie1 deletion was induced on Tie1^{KO} mice and HSPCs were sorted using the "LSK" markers and plated at a concentration of 1000 cells per well with two technical replicates per mouse (Fig. 23A). The LSK cell-derived colonies were counted on week 1 showing a clear decrease in absolute numbers of colonies in the absence of Tie1 (Fig. 23B). The colonies were further categorized according to their appearance, size and color. Interestingly, colonies composed of macrophage progenitors (CFU-M) and the combination of multi-potential granulocyte, macrophage and megakaryocyte progenitor cells (CFU-GEMM) did not show a significant difference in colony numbers. However, in the case of granulocyte progenitor cells, a decreased number of colonies was counted in cells derived from Tie1^{KO} mice suggesting that Tie1 has a role in the granulocytic progenitor differentiation (Fig. 23C). On week 2, the re-plated cells generated fewer colonies due to diminishing hematopoietic potential of stem cells. However, the result of fewer colonies in Tie1 deleted progenitors was still evident further supporting the notion that Tie1 is important in granulocytic differentiation (Fig. 23D-E).

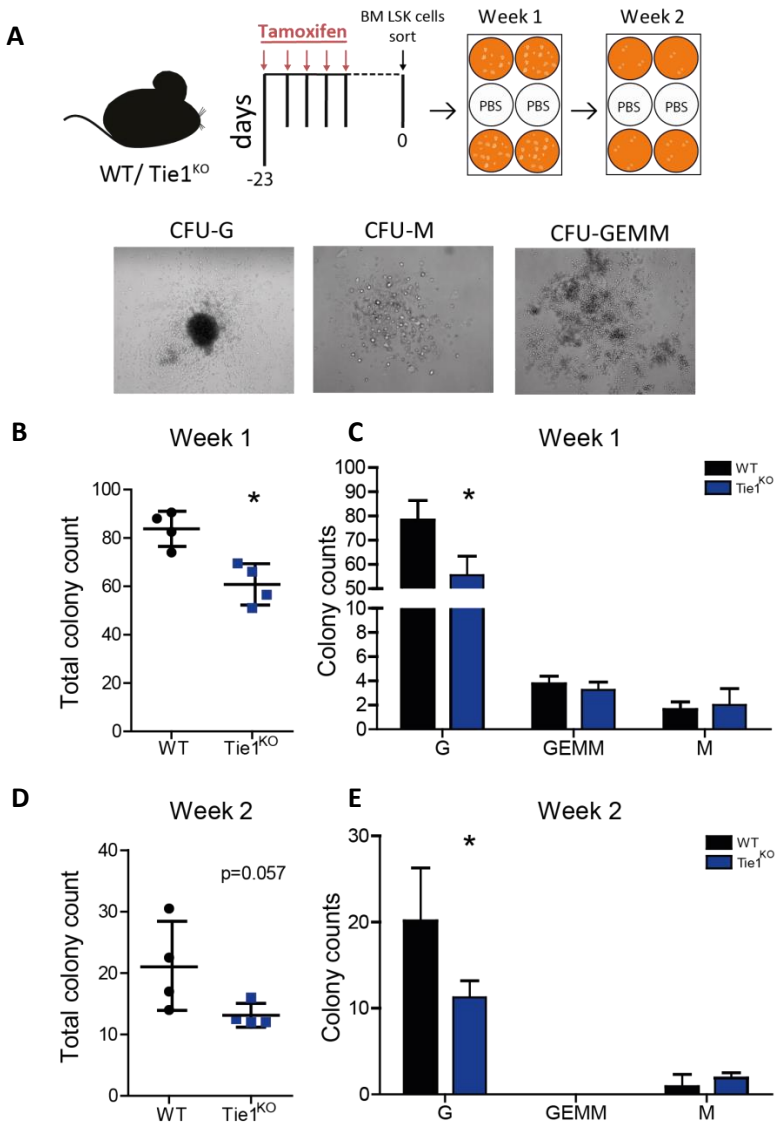

Figure 23: Deletion of Tie1 on HSPC leads to reduced colony formation

(A) Global Tie1 deletion was induced in Tie1^{KO} mice with the administration of tamoxifen every other day (5 times in total). After a washout period of 15 days, mice were sacrificed and their BM was processed and stained for FACS. Sorted HSPCs were plated at a concentration of 1000 cells/1mL MethoCult^{TM} medium within 6-well plates. Derived colonies were counted after 1 week. Cells were then re-plated a concentration of 10.000 cells/well and derived colonies were counted 1 week later. **(B)** Total colony counts and **(C)** absolute number of identified colony type. **(D)** Total colony counts and **(E)** absolute number of identified colony type on week 2. Data are shown as mean±sd (n=4; Mann-Whitney test, *; p<0.05). (abbreviations see text)

The next step was to assess the functional roles of Tie1 *in vivo*. One of the most important properties of hematopoietic stem and progenitor cells is that when transplanted into an irradiated recipient they possess the ability to reinitiate blood cell production. The *in vivo* clonal repopulating assay was established by Till and McCulloch and since then it has been altered and evolved according to scientific questions (206). Global Tie1 deletion was induced as described before and BM HSPCs were sorted from WT and Tie1^{KO} mice. There are two identifiable alleles for *Ptprc* (CD45 leukocyte antigen), which can be distinguished by surface marker antibodies (CD45.1 and CD45.2 isoforms). CD45.1 and

CD45.2 mice were used for *in vivo* tracking of donor and host immune cells. Primary transplantation took place as equal numbers of either WT or $Tie1^{KO}$ HSPCs were intravenously injected into lethally irradiated (9Gy) CD45.1/B6 mice. Blood was withdrawn every 4 weeks and processed for FACS. Donor-derived cells were distinguished from recipient cells due to CD45.1/CD45.2 isoform difference. The next goal was to assess the long-term reconstitution efficacy of *Tie1*-deleted hematopoietic stem cells by means of secondary transplantation. After 12 weeks, recipient mice were sacrificed and sorted for CD45.2 WT and $Tie1^{KO}$ HSPCs. Equal numbers of these cells were intravenously injected into a second cohort of lethally irradiated (9Gy) CD45.1/B6 mice. Similar to the first recipient cohort, blood was withdrawn every 4 weeks and processed for FACS and Hemavet counter analysis (Fig. 24A). *Tie1* deletion efficiency was evaluated via qPCR of sorted HSPCs before transplantation. In order to analyze distinct immune cell populations, fluorescent antibodies against CD45, CD3, CD11b, Gr-1 and CD19 epitopes were used. The cell population characterized by $CD45^+$, $CD11b^+$ and $Gr\text{-}1^+$ staining encompassed neutrophils and monocytes. Although no difference was detectable up until week 8, *Tie1* deletion on transplanted HSPC led to decreased ratio of $CD11b^+Gr\text{-}1^+$ population (Fig. 24B). Upon secondary transplantation of WT and $Tie1^{KO}$ HSPCs, the same effects is demonstrated by week 8. However, it was not detectable at further time-points (Fig. 24B).

Blood analysis via Hemavet counter was performed during secondary transplantation in order to support flow cytometry findings. $Tie1^{KO}$ HSPC transplanted recipient mice had significantly fewer WBC compared to control recipients (Fig. 24C). This effect was due to neutrophils (Fig. 24D) and monocytes (Fig. 24F) and not apparent in lymphocytes (Fig. 24E), also isolated by $CD45^+$ and $CD3^+$ flow cytometry-based analysis.

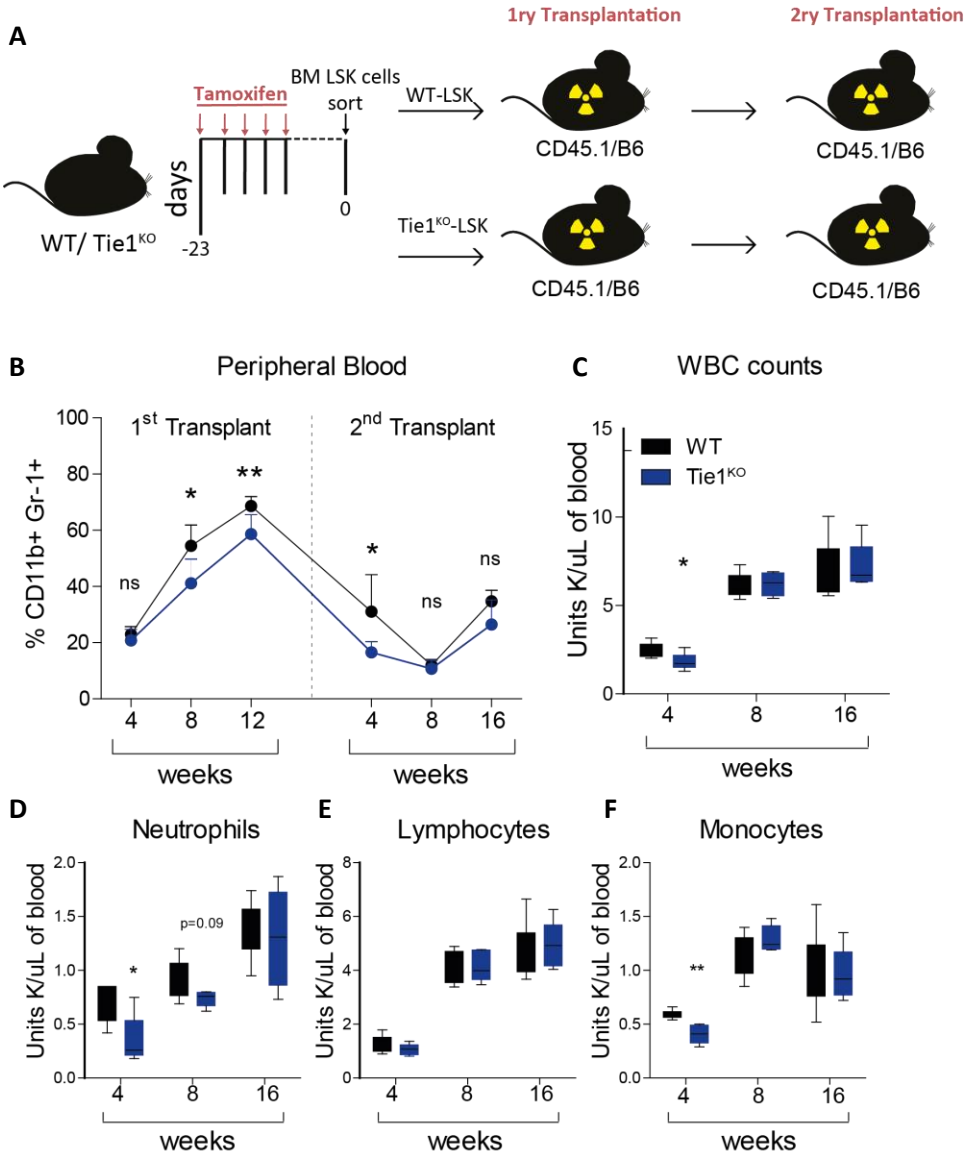

Figure 24: Tie1-deficient HSPC are capable of BM reconstitution yet have reduced efficiency in generating myeloid cells

(A) Global Tie1 deletion was induced in Tie1^{KO} mice with the administration of tamoxifen. CD45.1/B6 lethally irradiated mice (9Gy) received either 5000 WT or Tie1^{KO} sorted HSPCs. In order to assess long-term reconstitution efficiency of Tie1^{KO} HSPCs, secondary (2ry) transplantation was performed and the blood of recipient mice was examined for immune cell markers. **(B)** Flow cytometry analysis of recipient mice blood during primary (1ry) and 2ry transplantation. Hemavet counter analysis during 2ry transplantation of **(C)** WBC, **(D)** neutrophils, **(E)** lymphocytes, **(F)** monocytes. Data are shown as mean±sd (n=5-6; Mann-Whitney test, *; p<0.05, **; p<0.01).

Competitive transplantation experiments are functional assays that compare hematopoietic stem and progenitor cell capacities of two different cell populations within the same BM. Lethally irradiated CD45.1/B6 mice received 10.000 sorted HSPCs composed of 1:1 ratio of WT (CD45.1) and Tie1^{KO} (CD45.2) cells. The control group was transplanted with 10.000 sorted HSPCs composed of 1:1 ratio of

WT (CD45.1) and WT (CD45.2) cells (Fig. 25A). Throughout 16 weeks after transplantation, blood was withdrawn in order to determine engraftment efficiency using cell surface markers that distinguished donor cells (CD45.2) from the recipient, or host (CD45.1). Deletion of Tie1 on HSPC did not have an effect on engraftment compared to the control (Fig. 25B). However, further immune cell marker analysis via flow cytometry confirmed previous finding the deficiency of Tie1^{KO} derived immune cells to generate myeloid lineages. The percentages of CD11b^{+}F4/80^{+}, CD11b^{+}Ly6G^{+} and CD11b^{+}Ly6C^{+}, also described as macrophages, neutrophils and monocytes respectively, were significantly decreased on week 16 compared to the control group.

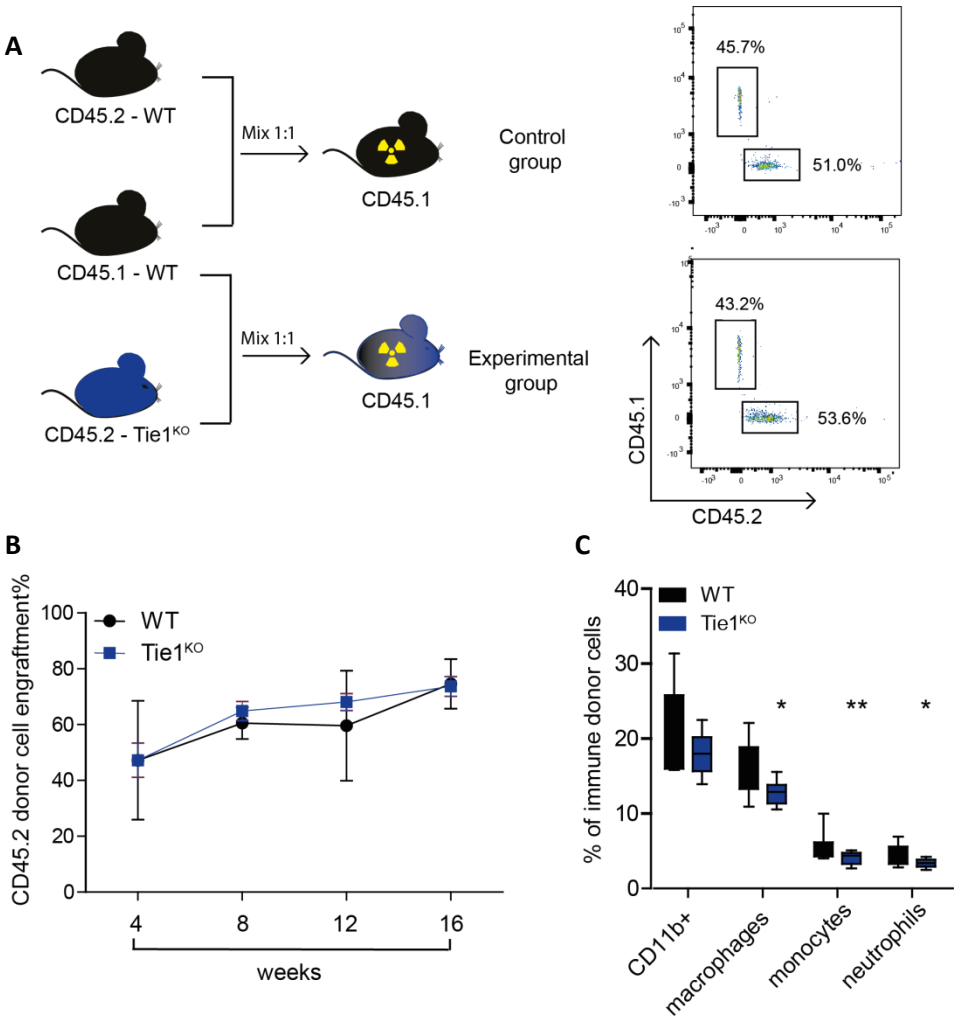

Figure 25:* Tie1 *deletion on HSPC does not affect engraftment efficiency in lethally irradiated mice
(A) Schematic illustration and representative FACS plots of engraftment efficacy. **(B)** Contribution of WT and Tie1^{KO} donor cells (CD45.2) to the blood cells of lethally irradiated WT recipients (CD45.1) over 16 weeks after transplantation. **(C)** Percentages of different lineages derived from donor cells in the blood of recipient mice at 16 weeks post transplantation. Data are shown as mean±sd (n=10; Mann-Whitney test, *; p<0.05, **; p<0.01).

4. DISCUSSION

The BM is a very complex microenvironment in which numerous cell types reside and interact in developmental and pathological settings. Historically, scientists acknowledged the importance of EC in steady state hematopoiesis and cell trafficking. However, technical obstacles in visualizing the tissue's location within calcified bone hindered further insight. The evolution of modalities, microscopy and hematopoietic markers substantially contributed in providing newer evidence in terms of blood vessel and BM interactions. Angiopoietin/Tie signaling has been recognized as crucial regulator of development, pathological angiogenesis and inflammation. Partially conflicting studies have attempted to elucidate the roles of Angiopoietin/Tie signaling in HSC and HSPC maintenance and quiescence in the BM (34, 93). Interestingly, Tie receptors are not confined to EC but also on hematopoietic stem and progenitor cells as well as a subset of fully differentiated immune cells such as macrophages (37, 38, 53). Employing a range of cellular and functional experiments as well as genetic mouse models, the present study demonstrates that i) Ang2 facilitates HSPC activation and mobilization, yet, vascular integrity and function remains unchanged; ii) Ang2 is important for hematopoietic reconstitution after irradiation; iii) *Tie1* deletion increases Ang2 in the serum, yet, hinders HSPC mobilization and iv) *Tie1* deletion in HSPC delays myeloid hematopoiesis in irradiated BM.

4.1 Ang/Tie signaling at steady state and G-CSF stimulus

G-CSF has been the mobilization agent of choice in clinical transplantation regimens for the past three decades (169). The process of BM transplantation by intravenous infusion depends on the ability of HSC/HSPC to "home" and engraft in the recipient's BM. This procedure entails a sequence of events including specific molecular recognition, cell-cell adhesion/disengagement, transendothelial migration and effective reconstitution of the eradicated BM stem cell niche (168). The process of rolling is mediated by adhesion molecules on HSPC such as VLA-4 (CD49d), LFA-1 (CD11α) and HCAM (CD44). The complementary binding partners of these molecules such as VCAM-1 (CD106), ICAM-1 (CD54), E- and P-selectin (CD62E and CD62P) are found on the surface of BMECs (207). This suggests that BMECs play important roles in BM transplantation on a molecular level.

The Ang/Tie signaling system is poorly studied in the context of BM vasculature and even more so regarding HSPC mobilization. A recent study on human data concluded that G-CSF administration led to decreased soluble Tie2 level in aphaeresis samples compared to pre-mobilization blood. The significant decrease in Tie2 suggests suppression of Angiopoietin-1/Tie2 signaling, ultimately assisting in release of HSPC from hematopoietic niches to blood (208). Another patient study evaluating several cytokines showed that VEGF concentration increased upon G-CSF administration, whereas Tie2, Ang1 and Ang2 levels decreased in the blood serum (209). A more recent study established that

low base-line levels of Angiopoietin-2 in patients' blood correlates with poor mobilization. On the other hand, Angiopoietin-1 levels did not differ between good and poor mobilizers (210).

To investigate the effects of G-CSF stimulus with respect to Ang/Tie signaling in WT mice, blood was collected and hematopoietic stem progenitor cells (HSPC) were sorted via flow cytometry at different time-points following G-CSF administration. In contrast to Yang et al. (209), an increase rather than decrease of Ang2 was observed in blood serum upon G-CSF stimulation. This was expected since it had already been reported that Ang2 is profoundly involved in inflammation (31, 211) and recruitment of myeloid cells in a β2 integrin-dependent manner (212). Moreover, this finding is in line with the Szmigielska-Kapłon et al. study in which the mobilization procedure demonstrates opposing development of Ang1 and Ang2 with a decrease and an increase respectively (210). When looking at the gradual decrease of *Angpt1* expression on HSPCs during the mobilization process, there are several aspects that need to be addressed. Initially, this finding fits nicely to the notion that Ang1 serves as a mediator for HSPC quiescent state (34, 210) which is disturbed by G-CSF leading to HSPC detachment, differentiation and mobilization. However, the gradual *Angpt1* expression decrease can also be attributed to a shift towards more differentiated immune cells populations due to G-CSF. Notably, RNA sequencing data from Cabezas-Wallscheid et al. demonstrated the presence of *Angpt1*^{high} HSC at the top of hematopoietic hierarchy. On the other hand, progenitor stem cell populations were associated with lower levels of *Angpt1* expression (35). The findings of this thesis as well as previously-mentioned studies support the notion that upon G-CSF stimulation, Angiopoietin-2 dominates binding to the Tie2 receptor against Ang1 leading to the disruption of chemotactic interaction within HSPC and stromal cells of the BM and the consequent release to the blood.

4.2 The absence of Ang2 hinders HSPC activation and BM reconstitution after lethal irradiation

Angiopoietins are highly associated with angiogenesis and inflammation. Initially, Ang1 was characterized for the ligand's anti-inflammatory properties and their contribution to maintaining vascular integrity and reducing plasma leakage (213, 214). Later on, the stabilizing functions of Ang1 were also investigated in terms of pericyte coverage and tightening of EC junctions by preventing VEGF-induced VE-cadherin phosphorylation (215). The role of Ang2 was historically projected on the assumption that it opposes the anti-inflammatory effect of Ang1 and on the fact that it is upregulated in many inflammatory diseases including cancer (216-218). However, subsequent mechanistic data showed that Ang2 sensitized Tie2^{+} EC towards inflammatory stimuli such as tumor necrosis factor α (TNF-α) (57). In fact, the authors also showed that the absence of Ang2 in mice led to failure of leukocyte arrest. Moreover, Ang2 has also been shown to mediate leukocyte trafficking via the transformation of capillaries to venules in a mouse airway inflammatory model (219). Previous *in vitro* and *in vivo* studies have attempted to elucidate the importance of Ang/Tie signaling in HSC functions.

BM transplantation assays following *in vitro* cultivation of HSCs with angiopoietins showed that Ang1 maintained long-term repopulating activity of HSCs, whereas the addition of Ang2 drastically inhibited with the effects of Ang1 (102). Colony formation assays, on the other hand, showed no Ang1 or Ang2-induced effects on HSCs (102).

Previously discussed data and literature on Ang2 in relation to inflammation pose the question: How is Ang2 affecting the process of HSPC activation and mobilization upon G-CSF stimulus? To address this, WT and $Ang2^{KO}$ mice were treated with G-CSF. The absolute numbers of HSPCs in the BM, spleen, blood as well as circulating immune cells were recorded at different time-points (day 1-6) upon G-CSF administration. At steady state there was no apparent difference between WT and $Ang2^{KO}$ mice. This involved the absolute number of HSPC in different organs as well as the number of immune cells and composition of blood. Ang2 deficient mice have been studied in the past for complex lymphatic and vascular phenotypes (56). Depending on genetic background, Ang2 related defects involved development of chylous ascites, abnormal vessel architecture, malfunctioning lymphatic valves, defective vascular remodeling in the eye, dysmorphogenesis of cortical peritubular capillaries in the kidney and premature death (56, 220, 221).

Evidently, Ang2 is not essential for HSC and HSPC maintenance and immune cell generation at steady state. Under G-CSF stimulation however, $Ang2^{KO}$ mice showed a reduced response of HSPC activation in the BM compared to WT mice. This translates to reduced mobilization from day 3 until slowly catching up at day 5 as shown in data obtain from the spleen. This phenomenon could not be captured when looking at blood until day 6. This could be attributed to very low numbers of HSPCs identified in blood and therefore a higher risk for variability and cell contamination.

G-CSF affects the survival, proliferation and differentiation of all cells within the neutrophil lineage ranging from the HSC to mature neutrophil. Although there is an evident increase in numbers of neutrophils in blood through day 6, $Ang2^{KO}$ mice do not present any defects in generating neutrophils. This suggests that Ang2 hinders HSPC activation initially, yet does not affect subsequent differentiation of neutrophil progenitors as they eventually catch up. Similarly, Ang2 deficiency does not significantly affect activation of HSC suggesting that the population affected is restricted to MMP cells. On the other hand, when WT mice were pretreated with Ang2 blocking antibody, G-CSF-treated mice showed reduced HSPC expansion compared to control mice. This discrepancy between the two models may be attributed to the fact that in the genetic model compensatory mechanisms may have resulted in a more stable HSC pool. The pharmacological inhibition on the other hand constitutes a better representation of a clinical scenario. Besides, it has been shown that Ang2 deficient mice display defects in rapid inflammatory response and more specifically, the processes of leukocyte firm adhesion and transmigration are affected (31, 57). However, what remains uncertain is whether angiogenic signals directly regulate inflammatory processes, or simply mediate and/or amplify previous proinflammatory stimuli.

The co-staining of cells with Ki67 and Hoechst 33342 provide information on proliferation and cell cycle status, respectively. The higher percentage of HSPCs and HSCs in G0/G1 phase in $Ang2^{KO}$ mice

describes a more quiescent state irrespective of mobilization status. Naturally, the absence of Ang2 results in a smaller percentage of HPSCs and HSCs in S/G2/M phase regardless of the mobilization state. Notably, the discrepancy in cell cycle phases between WT and $Ang2^{KO}$ mice at steady state does not affect the overall HSPC and HSC numbers as shown earlier. This may be attributed to the fact that the cell cycle population differences are slight and may be insufficient for the detection of smaller HSC and HSPC steady state populations. The focus of the study involved two very different, yet challenging to distinguish processes: HSPC activation and mobilization. The absence of Ang2 affects HSPC activation by hindering the cell cycle. However, the process of retention and mobilization should be further discussed. The Cxcl12/Cxcr4 signaling axis is regarded essential for neutrophil homeostasis and mobilization (222). Ccxr4 negatively regulates neutrophil release in a cell-autonomous manner and therefore its higher expression in HSPCs and HSCs in the absence of Ang2 suggests a higher retention capability in the BM stroma. In order to study the process of mobilization alone and whether the increased Cxcr4 expression is functionally involved in the retention of HSPCs in the BM, AMD3100 was administered to WT and $Ang2^{KO}$. Notably, the inhibition of Cxcr4 did not hinder HSPC mobilization to the periphery. It was therefore evident that Ang2 hindered activation and not mobilization of HSPC. Moreover, increased expression levels of Tie2 and Cdkn1a suggest that HSPCs are more quiescent in $Ang2^{KO}$ mice. This is in agreement with two landmark studies on Tie2 and Cdkn1a in hematopoietic stem cells (34) (223). Finally, the BM vasculature was assessed in terms of structure and functionality in the attempt to further validate that Ang2 affected HSPC cell cycle rather than BMEC. Developmentally, Ang2 is important for the lymphangiogenic process, yet not critical for embryonic survival (224). In adulthood, the roles of Ang2 are studied in pathological contexts such as cancer and inflammation. In physiological conditions, Ang2 expression is very low and well-established vasculatures are not affected. Unsurprisingly, the absence of Ang2 in the BM had not affected vasculature structure and leakiness.

HSC and HSPC are defined by their functional ability to reconstitute a depleted BM. Having shown that Ang2 affects HSC and HSPC activation rather than their retention and mobilization, reconstitution experiments were also carried out in order to further characterize the importance of the ligand. One important yet unavoidable weakness of this model is that irradiation inflicted damage to sinusoidal vessels within the BM (225, 226). In patient transplantation research, the roles of neovascularization in hematopoietic recovery after irradiation are increasingly recognized (227). The results indicated that Ang2 is important, yet not critical for BM reconstitution following lethal irradiation. Hemavet counter as well as flow cytometry data show that Ang2 is involved in both branches of hematopoiesis: myelopoiesis and lymphopoiesis. Although Ang2 promotes prompt BM reconstitution in terms of myeloid and lymphoid immune cells, it is worth considering that the administration of recombinant Ang2 in BM ablated patients may involve risks due to the ligand's association with inflammation and metastasis (228). Zhou et al demonstrated that Ang1 secreted by HSC/HSCP and $LepR^{+}$ cells reduced vascular leakiness, yet hindered niche replenishment upon lethal irradiation (93) . Similarly, the thesis data suggest that the absence of Ang2 also hinders niche recovery.

4.3 Tie1 on endothelial cells controls HSPC egress and mobilization

The incomplete knowledge of functions of Tie1 receptor and the context-dependent roles of Ang2 had been limiting progress in understanding how the Ang/Tie system orchestrates vascular stability and remodeling in physiological and pathological settings. Yet, the notion that Tie2 signaling is highly dependent on the presence and interaction of Tie1 is well accepted (80). Loss of endothelial cell Tie1 prevents the agonistic actions of Ang1 and Ang2 as shown by Korhonen et al. The authors also described that upon inflammation and loss of Tie1, Tie2 and Ang1 expression were downregulated whereas, Ang2 was upregulated. The findings of this thesis follow exactly the same pattern as Korhonen et al. upon G-CSF stimulation in WBM gene expression analyses.

Upon steady state, WBM CD31 gene expression is unaffected by endothelial cell Tie1 deletion. Yet, at G-CSF stimulation CD31 gene expression was reduced upon endothelial cell Tie1 deletion. Similarly, a decreased vessel area in diaphysis and epiphysis was identified in G-CSF-induced Tie1^{iECKO} mice as shown by endomucin staining. La Porta et al. has previously described this phenomenon in tumor angiogenesis arguing that endothelial cell Tie1 deletion promoted vascular normalization in mouse tumors (229). Moreover, the association of decreased vascular markers due to Tie1 deletion has also been described as an endothelial-mesenchymal transition (EndMT) (230). Tie1 deletion does not play a role in regulating the gene expression of the tight junction molecules, Claudin5 and adherens marker VE-Cadherin. Yet, along the lines of the thesis findings, literature has previously described the mechanism of G-CSF induced blood-brain barrier stabilization via Claudin 5 reduction (231) and VE-Cadherin increase (232).

In the attempt to elucidate the role of BMEC Tie1 regarding HSPC egress and mobilization, the G-CSF model was implemented as described earlier. Within the BM compartment, BMEC Tie1 deletion did not induce changes in terms of HSPC activation at steady state and mobilization. These findings were confirmed by flow cytometry analysis indicating total HSPC numbers as well as EdU incorporation and detection were unchanged. Interestingly, BMEC Tie1 deletion resulted in decreased numbers of egressed or mobilized cells in the periphery suggesting that the BM vasculature acts as gatekeeper for HSPC. As discussed above, several studies support the notion that BM vascular permeability and HSC cell cycle status are not correlated. Similarly, data on mobilized Tie1^{iECKO} mice also demonstrate a “tighter” vasculature with no EdU incorporation effect on HSPCs. Data on egressed HSPCs at steady state in blood are not shown. Previous analyses showed that egressed HSPCs are very low in number in the absence of mobilization stimulus and therefore prone to cell population contaminations and errors in interpretation.

Evans blue dye (EBD) has been traditionally applied for various diagnostic purposes as well as estimations of blood volume and vascular permeability. EBD properties stem from its high water solubility, slow excretion and its tight binding to serum albumin resulting to a 69kDA protein tracer (233). In the attempt to further characterize BM vascular permeability in G-CSF-mobilized Tie1^{iECKO} mice, EBD was intravenously injected in experimental and control mice 4 hours prior to sacrifice.

Formamide extraction of EBD from femurs and photometric estimation showed no difference in vascular leakiness based on EBD extravasation. This finding can be attributed to several factors. As mentioned earlier, BM vasculature is fenestrated and EBD bound to albumin constitute a molecular weight of 69kDa. HSPC as significantly larger in size (3-7µm) and alterations in BM vasculature that restrict HSPC trafficking might not be identifiable by EBD extravasation (234). Moreover, EBD assays have traditionally been assessing functionality of continuous blood vessels especially during pathological settings such as tumor and inflammation (235, 236). Reduced functional integrity is associated with leakier phenotypes. In the contrary, this thesis discusses that Tie1^{iECKO} mice possess a "tighter" vasculature which reduces but does not exclusively prohibit HSPC trafficking.

Besides having the capacity to dynamically egress and mobilize, HSPC are also able to return to the BM. The homing process is a good indication of HSPC functionality as well as BM vasculature permeability (25, 237, 238). The decreased number of successfully homed Lin^{-} donor cells in Tie1^{iECKO} compared to WT mice enhances the evidence that EC Tie1 deletion leads to a "tighter" vasculature. In comparison to the EBD assay, this approach is more sensitive to changes in vasculature and therefore more representative due the assessment of vessel permeability with BM cells rather than low molecular weight dyes.

At first glance, both mobilization phenotypes observed in Ang2^{KO} and Tie1^{iECKO} mice may appear similar due to reduced numbers of HSPC in the periphery. Based on the reduced activity of HSPC in Ang2^{KO} mice, the increase of Ang2, both at mRNA as well as protein level in the serum in Tie1^{iECKO} mice suggests that HSPC mobilization would be enhanced. On the contrary, data show that Tie1^{iECKO} mice have reduced numbers of HSPCs in the periphery. These seemingly unfitting results may be attributed to the fact that Ang2^{KO} and Tie1^{iECKO} mice exert mobilization phenotypes on different cell types. Initially, the lack of Ang2 affected HSPC whereas deletion of EC Tie1 primarily affected the vasculature. Therefore, an increase in Ang2 protein levels may not be sufficient for the HSPC to surpass the less penetrable sinusoids in Tie1^{iECKO} mice.

Tie1 targeting has previously been described in the context of primary tumor therapy by D' Amico et al. The authors assessed the combination of Tie1 deletion and VEGF/VEGFR blocking antibodies and saw no additive effect on tumor angiogenesis inhibition. On the other hand, the targeting of Tie1 and Tie2 resulted in tumor vessel normalization and growth inhibition (239). La Porta et al also showed that Tie1 inhibition not only leads to normalization of primary tumor vasculature, but also hinders post-surgical lung metastasis (229). Capillary leak syndrome (CLS) is a potentially life-threatening disease induced by endothelial cell damage. G-CSF can cause extravasation of plasma proteins and fluid from the blood vessels to extracellular space resulting in the presentation of symptoms of CLS. Current treatment regimens focus on alleviating symptoms since there is no known cure. Manipulation of vascular permeability may therefore be a desirable prospect since therapeutic targeting of Tie1 on endothelial could be an attractive approach for the treatment of CLS.

4.4 Tie1 deletion on HSPC delays myelopoiesis

Tie2 became known as a receptor located on the surface of EC as well as HSC and several studies attempted to elucidate its roles in hematopoiesis (34, 38, 240). In addition to that, Tie2-Cre mouse lines were established and used to investigate attributes of HSC in mice (241-243). In contrast to Tie2, the presence of the orphan receptor Tie1 on HSC has not been investigated in depth. Rodewald et al. described Tie1 as dispensable for HSC engraftment and self-renewal (53), yet the significance of the receptor's high expression on HSC remained unexplained. Moreover, the aforementioned study was carried out on fetal liver of Tie1-deficient mice due to embryonic lethality. In the present thesis, conditional deletion of Tie1 under the ROSA promoter ($Tie1^{KO}$) was induced via tamoxifen treatment. Conditional deletion of the receptor circumvented the issue of embryonic lethality and facilitated the study of Tie1 in adult mice. HSPCs were isolated via FACS using the LSK markers. $Tie1^{KO}$ and WT HSPC were used in a series of functional experiments including *in vitro* serial colony forming unit (CFU) assays and *in vivo* serial and competitive BM transplantations. The purpose to these experiments was to investigate the importance of Tie1 receptor on HSPC in the processes of differentiation and BM replenishment after lethal irradiation.

Colony-forming unit assays are the most common *in vitro* manipulation for hematopoietic progenitor cells. $Tie1^{KO}$ HSPC appeared to have a disadvantage in clonal colony expansion compared to WT HSPC. This effect was mostly detectable in granulocyte progenitor cells. Long-term assessment of $Tie1^{KO}$ and WT HSPC resulted in a less pronounced difference in the overall number of colonies, yet $Tie1^{KO}$ granulocytic progenitor colony counts remained significantly fewer than WT HSPC-derived colonies. These findings constituted the building ground for the consequent *in vivo* functional assays. BM transplantation experiments designed to evaluate relative fitness of donor HSPC against known competitor HSPC are a widely used tool for assessing stem cell fitness. Competitive transplantations are highly sensitive making it more likely to detect moderate changes in stem cell fitness and benefit from having an internal technical control regarding the efficiency of irradiation and injection (244). Yet, results can be misleading as the competitor cells can rescue leading to the survival of all recipient mice. Therefore, results should be complemented with a non-competitive setting as shown in the present thesis. In the serial transplantation scenario, lethally irradiated recipient mice received either WT or $Tie1^{KO}$ HSPCs. Interestingly, Tie1 absence of HSPC is more pronounced during primary than secondary transplantation. Notably, the $CD11b^{+}$ $Gr1^{+}$ population which describes a variety of myeloid cells such as monocytes, granulocytes and neutrophils is significantly decreased during primary transplantation. This effect diminished during the progression of secondary transplantation suggesting that Tie1 does not affect long-term BM reconstitution. Throughout 16 weeks of competitive transplantation, $Tie1^{KO}$ HSPC did not show a disadvantage compared to WT HSPC in terms of engraftment efficiency. This suggests that Tie1 is not essential for the reconstitution of an ablated BM. Yet, further flow cytometry analysis of different immune populations showed that $Tie1^{KO}$ HSPC-derived myeloid populations were decreased compared to the control in blood. These data along with

the serial transplantation data confirm that Tie1 on HSPC contributes to myeloid differentiation of HSPC.

5. MATERIALS

5.1 Chemicals

Table 1 Chemicals

Company
PanReac AppliChem (www.itwreagents.com)
Carl Roth (www.carl-roth.de)
Merck (www.merk.de)
Roche (www.roche-apllied-science.com)
StemCell Technologies (www.stemcell.com)
Thermo Fisher Scentific (www.thermofisher.com)

5.2 Cell culture reagents

Table 2 Cell culture reagents

Reagent	Company
MethoCult™ GF M3434	StemCell Technologies
Dulbecco's phosphate buffered saline (PBS)	PAA Laboratories
Fetal calf serum (FCS), heat inactivated	PAA Laboratories
Trypan blue	Thermo Fisher Scientific

5.3 Primers and Oligonucleotides

5.3.1 Genotyping primers

Table 3 Genotyping primers

Genotype	Primer name	Sequence
$Ang2^{KO}$	mL2-5' GTD	CTG GGA TCT TGT CTT GGC C
	mL2-intron1US1	CTT CTC TCT GTG ACT GCT TTG C
	Neo3'ds85	GAG ATC AGC AGC CTC TGT TTC
$Tie1^{flox/flox}$	LoxP1 for	ATGCCTGTTCTATTTATTTTTCCAG
	LoxP1 rev	TCGGGCGCGTTCAGAGTGGTAT
$Cdh5\text{-}Cre^{ERT2}$	Cre for	CAGGGTGTTATAAGCAATCCC
	Cre rev	CCTGGAAAATGCTTCTGTCCG
	Actin for	CAATGGTAGGCTCACTCTGGGAGATGATA
	Actin rev	AACACACACTGGCAGGACTGGCTAGG
$Rosa\text{-}Cre^{ERT2}$	AU-RCE -1	AAA GTC GCT CTG AGT TGT TAT
	AU-RCE -2	GGA GCG GGA GAA ATG GAT ATG
	AU-RCE -3	CCT GAT CCT GGC AAT TTC G

5.3.2 TaqMan™ probes for RT-qPCR

All TaqMan™ probes were purchased from Thermo Fisher Scientific

Table 4 TaqMan™ probes for RT-qPCR

Target gene (ms)	Ordering number
B2m	Mm00437762_m1
Cdh5 (VE-Cadherin)	Mm03053719-s1
Pecam	Mm01242584_m1
Tie1	Mm00441786_m1
Tek	Mm00443254_m1
Angpt1	Mm00456503_m1
Cldn5 (Claudin5)	Mm00727012_s1
Cxcr4	Mm01996749_s1
Cxcl12	Mm00445553_m1

5.4 PCR/RT-qPCR reagents, nucleotides and buffers

Table 5 PCR/RT-qPCR reagents, nucleotides and buffers

Reagent	Company
100 bp DNA Ladder plus	Fermentas
10 x Coral Load PCR buffer	Qiagen
Direct PCR Lysis Reagent	PeqLab
DNase/RNase free H2O	Gibco
dNTP mix (10mM each)	Fermentas
Ethidium bromide	Roth
Taq DNA polymerase (5U/µl)	Qiagen
TaqMan® Fast Advanced PCR Master Mix	Thermo Fisher Scientific

5.5 Company kits

Table 6 Company kits

Reagent	Company
Arcturus PicoPure RNA Isolation Kit	Thermo Fisher Scientific
EdU-Click 488	Baseclick
Fixation/Permeabilization Solution Kit	BD Biosciences
Lineage cell depletion kit	BD Biosciences
Mouse/Rat Angiopoietin-2 Quantikine ELISA Kit	R&D systems
Pierce Bicinchoninic acid (BCA) Protein Assay Kit	Thermo Fischer Scientific
Quantitect Reverse Transcription Kit for cDNA Synthesis	Qiagen
GenElute™ Total RNA purification Kit	Merck

5.6 Immunohistochemistry

5.6.1 Primary antibodies

Table 7 Primary antibodies

Antigen	Reactivity	Species	Conjugate	Dilution	Source (cat.no)
C-kit (CD117)	mouse	rat	APC	1:400	BD Biosciences (553356)
Sca-1	mouse	rat	APC-Cy7	1:200	Biolegend (108125)
CD48	mouse	rat	PE-Cy7	1:200	Biolegend (103423)
CD150	mouse	rat	PE-Cy5	1:100	Biolegend (115912)
CD45	mouse	rat	FITC	1:400	BD Biosciences (553080)
CD11b	mouse	rat	PE-Cy7	1:200	Thermo Fisher Scientific (25-0112)
Gr-1	mouse	rat	APC	1:200	Biolegend (108412)
CD19	mouse	rat	PE	1:200	BD Biosciences (557399)
CD3	mouse	rat	APC-Cy7	1:50	Thermo Fisher Scientific (470032)
CD45.1	mouse	rat	FITC	1:400	BD Biosciences (553775)
CD45.2	mouse	rat	APC	1:400	BD Biosciences (558702)
Endomucin	mouse	rat	-	1:100	Santa-Cruz (65495)
Sca-1	Mouse	rat	APC	1:100	Thermo Fisher Scientific (17598183)
DAPI	mouse	rat	-	1:2000	Thermo Fisher Scientific (D1306)
CD8a	mouse	rat	Pacific Blue	1:200	Biolegend (100725)
CD45R/B220	mouse	rat	Pacific Blue	1:200	Biolegend (103227)
CD11b	mouse	rat	Pacific Blue	1:200	Biolegend (101224)
Ter-119	mouse	rat	Pacific Blue	1:200	Biolegend (116232)
CD3	mouse	rat	Pacific Blue	1:200	Biolegend (100214)
Ly-6G/Ly-6C	mouse	rat	Pacific Blue	1:200	Biolegend (108430)

5.6.2 Secondary antibodies

Table 8 Secondary antibodies

Reactivity	Species	Conjugate	Dilution	Source (cat.no)
Rat IgG	Goat	AF-546	1:200	Life technologies (A11081)

5.6.3 Staining reagents

Table 9 Staining reagents

Staining	Company
BSA	Gerbu
EDTA 0.5M pH 8.0	Thermo Fisher Scientific
Fluorescence mounting medium	DAKO
Gelatin	Merck
Hoechst Dye 33258, 1mg/ml	Merck
Normal goat serum ready-to-use (10%)	Zymed
Roti-Histofix 4% (pH 7)	Carl Roth
Sucrose	Merck
Polyvinylpyrrolidone (PVP)	Merck
Tissue-Tek O.C.T.™ Compound	Scigen
Triton X-100	Thermo Fisher Scientific

5.7 Reagents for animal experimentation

Table 10 Reagents for animal experimentation

Reagent	Company
AMD3100	Merck
Mouse anti-human Ang2 ab /IgG	Eli Lilly
Dextran -70	Merck
Evans Blue dye	Merck
Formamide	Merck
G-CSF (Neulasta)	Amgen
Ketavet	Pfizer
NaCl solution	Braun
Rompun	Bayer

5.8 Solutions and Buffers

Table 11 Solutions and buffers

Buffer		Composition
Ammonium chloride potassium buffer (ACK)	150 mM 10 M 100 mM	NH4Cl KHCO3 Na2EDTA adjust pH 7.2-7.4
Phosphate buffered saline (PBS)	1.34 M 27 mM 200 mM 4.7 mM	NaCl KCl Na2HPO4 KH2HPO4 adjust pH 7.4
Tris-Borate-EDTA buffer (TBE)	89 mM 89 mM 1 mM	Tris-HCL pH 7.5 NaCl Tween-20
Tris-Buffered Saline Tween-20 (TBS-T)	10 mM	Tris/HCl, pH 7.5

	100 mM	NaCl
	0.1%	Tween-20
Sucrose preservation solution (SPS)	20%	Sucrose
	2%	PVP
		Prepared in PBS
Embedding solution (ES)	20%	Sucrose
	2%	PVP
	8%	Gelatin
		Prepared in PBS

5.9 Consumables

Table 12 Consumables

Consumables	Company
96 well plates	Steinbrenner Laborsystem
384 well plates	4titute
6-well plates	Sarstedt
12- well plates	Sarstedt
Cannula (18G, 19G, 27G, 30G)	BD
Cell culture dishes (10cm, 15cm)	TPP
Cryotubes	Carl-Roth
FACS tubes	BD Biosciences
Filter containing pipette tips	Biozym
Freezing box	Thermo Scientific
Hematocrit capillaries Na-hep	Hirschmann
Insulin syringe	BD
Lancets Solofix	Braun
LS Columns MACS®	Thermo Fisher Scientific
Microscope cover glasses	VWR international
Microscope glass slides	Menzel-Gläser
Pipette tips	Nerbe
qPCR plates (96-well)	Biozyme
qPCR plates (384-well)	Roche
Reaction tubes (0.5ml, 1.5ml, 2ml)	Eppendorf
Reaction tubes (15ml, 50 ml)	Greiner
Round bottom 96 well plate	Greiner
Sealing foil	Applied Biosystems
Sterile pipettes	Corning
Sterile filters	Renner
Syringes	Dispomed
Tissue cultures 6-well plates	Greiner
Tissue freezing medium (Tissue TEK)	Sakura

5.10 Equipment

Table 13 Equipment

Equipment	Company
Canto II	BD
Cell culture hood	Thermo Fisher Scientific
Cell culture incubator	Thermo Fisher Scientific
ConfoCor 3 LSM 710	Zeiss
Centrifuge	Thermo Fisher Scientific
Countess™ automated cell counter	Thermo Fisher Scientific
Hyrax C50 Microtome Cryostat	Zeiss
FACS Aria II	BD
FACS Aria Fusion	BD
Heating block	Eppendorf
Hemavet 950 FS	Drew Scientific
iMark™ Microplate Reader	BioRad
Light cycler 480	Roche
LSM710	Zeiss
LSR Fortessa	BD
Mortar/Pestle 150mm	Thermo Fisher Scientific
MACS Magnetic separators	Miltenyi
Multistep pipette	Eppendorf
NanophotometerR N60	INTAS
Olympus IX 71	Olympus
Pipettes	ErgoOne
QIAxcel Advanced System Qiagen	Qiagen
Special accuracy weighing scale	Mettler Toledo
StepOnePlus Real-Time PCR System	Thermo Fisher Scientific
Surgery and dissection tools	Fine Science Tools
Table centrifuge (5417R)	Eppendorf
Thermocycler	Applied Biosystems
Tubes and adapters for flow incubation	Carl Roth
Vortex	Neolab
Water bath	Julabo

5.11 Miscellaneous

Table 14 Miscellaneous reagents

Reagent	Company
Collagenase A	Merck
Dispase	Roche
Ki67	BD Biosciences
Lysis Solution	Merck

5.12 Software

Table 15 software

Software	Company
Fiji	ImageJ
FlowJo	Miltenyi Biotec
Illustrator CS6	Adobe
Light Cycler 480 software	Roche
Microsoft office	Microsoft
Prism	Graph Pad
ZEN blue	Zeiss

6. METHODS

6.1 Mouse experimentation

6.1.1 Animal welfare

Angpt2-deficient mice in C57Bl/6 background were kindly provided by Dr. Gavin Thurston. Mice in C57Bl/6 background with inducible deletion of *Tie1* gene were kindly provided by Dr. Scott Baldwin and the B6-Gt(ROSA)26Sortm1(cre/ERT2)Tyj (Rosa-CreERT2) mouse line was kindly provided by Dr Thomas Hoffman. To generate $Tie1^{flox/flox}$ mice, a Tie1 floxed targeting vector was constructed based on the 129-Sv mouse genomic fragment used by Puri et al. (245). $Tie1^{flox/flox}$ mice were crossed with *Tg(Cdh5-cre/ERT2)1Rha* (Cdh5CreERT2) mice (205) to specifically delete endothelial *Tie1* gene and B6-Gt(ROSA)26Sortm1(cre/ERT2)Tyj (Rosa-CreERT2) for inducible global deletion (Table 1). Induction of Cre recombination was carried out by administration of tamoxifen according the protocol indicated on each experiment. C57BL/6-Ly5.1 and C57BL/6N mice were purchased from Charles River. Female 8-12-week old mice were used in all experiments unless stated otherwise.

Animals were housed in sterile cages maintained in temperature controlled rooms and had access *ab libitum* autoclaved food and water. All animals were monitored daily for signs of illness. Mice were euthanized via rapid cervical dislocation of spinal cord unless stated otherwise. Part of the tail was taken for re-genotyping.

All animal experiments were carried out according to the guidelines of the local Animal Use and Care Committees and were approved by the local regulatory committee Bezirksregierung Karlsruhe, Germany (G82/18 and G78/19).

Table 16 In-house mouse lines

GOI	Short name	Full name	Induction	Purpose
Angpt2	$Ang2^{KO}$	B6-Angpttm1Gdy	-	Global *Angpt2* deletion
Tie1	$Tie1^{iECKO}$	B6.Cg-Tie1tm1Scba Tg(Cdh5-cre/ERT2)1Rha /Aug	5x2mg tamoxifen	Endothelial cell-specific *Tie1* deletion
	$Tie1^{KO}$	B6.Cg-Tie1tm1Scba Gt(ROSA)26Sortm1(cre/ERT2)Tyj/Aug	5x2mg tamoxifen	Global *Tie1* deletion

6.1.2 Cre recombination induction

To induce *Tie1* deletion in the $Tie1^{iECKO}$ and $Tie1^{KO}$ mouse lines, both control and mutant animals were intraperitoneally treated with five doses of 2mg tamoxifen (Merck) dissolved in ethanol/peanut oil.

6.1.3 HSPC expansion and mobilization

6.1.3.1 G-CSF-induced expansion and mobilization

For HSPC expansion and mobilization, mice were received a single subcutaneous dose of 100 µg PEGylated human recombinant G-CSF (Neulasta®, Amgen) solution in 100 µL. Control mice were treated with 100 µL NaCl subcutaneously. Animals were euthanized at indicated time-points via

intraperitoneal (i.p) injection of Ketamin/Xylazin (120mg/16mg per kg). Blood was collected via heart puncture. The spleen and two femurs were also collected for analysis via flow cytometry.

6.1.3.2 AMD3100-induced mobilization

AMD3100 (Merck) was diluted in NaCl and administered i.p. at a dose of 5 mg/kg 1hour prior to sacrifice. As in section 6.1.3.1, mice were euthanized via Ketamin/Xylazin and blood was collected for analysis via flow cytometry.

6.1.4 Ang2 antibody treatment

Neutralizing rat anti-Ang2 antibody or rat IgG (Eli Lilly) was injected i.p. twice in a week at 20 mg/kg per mouse. As in section 6.1.3.1 mice were euthanized via Ketamin/Xylazin administration. Blood, the spleen and two femurs were then collected for flow cytometry analysis.

6.1.5 Proliferation assay

BM cells were isolated from mice 2 days after G-CSF treatment and stained for LSK, CD150 and CD48. Cells were fixed and permeabilized with the BD Cytofix/Cytoperm Kit and stained for Ki67 (BD Biosciences). After counterstaining with Hoechst33342, BM HSCs and HSPCs were analyzed via flow cytometry.

6.1.6 EdU proliferation assay

HSPC cell proliferation in induced female 8-12 week old WT and $Tie1^{iECKO}$ mice was measured performing an EdU incorporation assay. A Click-iT™ reaction is performed as proliferating cells incorporate 5-ethyl-2'-deoxyuridine (EdU) instead of thymidine during DNA synthesis. EdU can be detected due to a fluorescent label. Two days after G-CSF administration, EdU-AF488 was injected intraperitoneally at a dose of 1mg/mouse 24h prior to sacrifice. Two femurs were collected and processed for staining with LSK markers. Acquisition was performed on a BD Canto II and results were quantified using Flowjo software.

6.1.7 Dextran permeability assay

Dextran-FITC 70 kDa (Merck) was injected intravenously at a dose of 10mg/mouse 4h prior to sacrifice. Femurs were collected and processed for cutting and staining. Stained slides were mounted in DAKO fluorescence mounting medium and fluorescent images were acquired on Zeiss LSM710 confocal microscope. Images were analyzed using Fiji/Image J software.

6.1.8 Bone marrow transplantation

6.1.8.1 $Ang2^{KO}$ serial BM transplantation

Lethally irradiated (2 x 4.5 Gy) 8-12 week old female WT and $Ang2^{KO}$ (C57BL/6N background, CD45.2) recipient mice were transplanted with $2x10^6$ BM cells from CD45.1 donor mice. Blood was obtained at indicated time-points to determine BM reconstitution via flow cytometry analysis. Recipient mice were euthanized at 18 weeks post transplantation to determine engraftment levels via flow cytometry analysis.

6.1.8.2 $Tie1^{KO}$ serial BM transplantation

Cre recombination was induced via tamoxifen administration to female 8-12 week old WT and $Tie1^{KO}$ mice. Mice were sacrificed via cervical dislocation and BM cells from were collected following induction. These cells were then processed and stained for LSK staining and sorting. Lethally irradiated (2 x 4.5 Gy) 8-12 week old female WT (CD45.1) received 10.000 sorted HSPC from either WT or $Tie1^{KO}$ mice. Blood was collected every 4 weeks via the submandibular vein. Equal volumes of blood underwent erythrocyte lysis and staining with the appropriate antibodies for the determination

of BM reconstitution and engraftment. In order to determine long-term HSPC reconstitution efficacy, after 16 weeks mice were sacrificed and their BM cells were collected for HSPC sorting in order to perform a secondary transplantation. BM reconstitution and engraftment were determined as described above. Mice were euthanized via cervical dislocation.

6.1.8.3 Competitive BM transplantation

Lethally irradiate (2 x 4.5 Gy) 8-12 week old female WT (C57BL/6N background, CD45.1) recipient mice were transplanted with 1:1 ratio of WT (CD45.1):Tie1^{KO} HSPCs. The control branch received a 1:1 ratio of WT (CD45.1): Tie1^{KO} (CD45.2) HSPCs. Transplantations were carried out via i.v. administration of 5000:5000 sorted HSPCs in 200uL NaCl. Blood was collected every 4 weeks via the submandibular vein. Equal volumes of blood underwent erythrocyte lysis and staining with the appropriate antibodies for the determination of engraftment efficacy. Mice were euthanized after 16 weeks via cervical dislocation.

6.1.9 Evans Blue Dye Permeability assay

WT and Tie1^{iECKO} mice were injected with 200 µL of 2% EBD/NaCl solution intravenously into the tail vein. After 4 h of circulation of the dye, mice were anesthetized by intraperitoneal injection of ketamine (120mg/kg) xylazine (16mg/kg) in NaCl. Completely anesthetized mice were then perfused with NaCl via the heart for 5min. Two tibias were used for *Tie1* knock-out validation via qPCR and 2 femurs were collected for crushing in formamide dye extraction at 60^{o}C overnight. The crushed fractions were then centrifuged at 2000g for 30min and 70 µL of supernatant was used to measure absorption at 620nm and 750nm using an iMark^{TM} Microplate Reader. Haem pigment correction and sample normalization were carried out by subtracting control measurements.

6.1.10 BM homing assay

Female 8-12 week old donor WT mice (CD45.1) were euthanized via cervical dislocation and their femurs and tibias were collected and crushed using a mortar and pestle. Crushed fraction was digested in 3ml of 0.1% Dispase and 0.1% Collagenase A for 15min at 37 degrees and underwent negative selection for Lineage^{-} BM fraction. Lineage^{-} BM cells were then injected intravenously into the tail of induced WT and Tie1^{iECKO} mice. Mice were euthanized 4h later via cervical dislocation and both femurs were collected for crushing, ACK buffer incubation and staining for flow cytometry analysis.

6.2 Cellular assays

6.2.1 Ex vivo culture of sorted HSPCs for CFU assay

Induced WT and Tie^{KO} mice were euthanized via cervical dislocation and their femurs and tibias were collected and crushed with a mortar and pestle. Lineage^{-} BM cells were negatively selected via the Direct Lineage Cell Depletion kit (MACS, Miltenyi) and further processed for staining and FACS sorting. Sorted HSPCs were plated at a concentration of 1000 cells/1mL MethoCult^{TM} medium within 6-well plates. After 1 week, colonies were assessed and counted using an Olympus IX71 microscope. Cells were then re-plated a concentration of 10.000 cells/well and new colonies were assessed and counted 1 week later. Each biological sample had two technical replicates. The total number of colonies and per plate was quantified manually in ≥2 plates for each biological sample on an Olympus IX71 microscope.

6.3 Immunohistochemistry

6.3.1 Sample preparation

For confocal microscopy, femurs were fixed for 2h in 4% paraformaldehyde which was then replaced with 0.5M EDTA for 24h followed by 20% sucrose 2% PVP prepared in PBS. Femurs were then embedded in EBM medium (8% gelatin, 20% sucrose, 2% PVP in PBS) and kept in -80°C. For immunostaining, femurs were trimmed longitudinally until the marrow was visible from highest to lowest point using a Zeiss Hyrax C50 Microtome Cryostat.

6.3.2 Immunostaining

0.3% Triton X-100 solution was added on the slides and kept at RT for 10 min. After discarding the Triton X-100 solution and washing once with PBS, blocking solution was added and slides were kept at RT for 30min. After blocking solution was removed, 200 µL of primary antibody solution was added to each section and incubated at RT for 2 h. Next, three washes were carried out with PBS at RT. The secondary antibody was then added at 200 µL per slide and kept at RT for 1 h. Next, three washes were carried out with PBS at RT. Nuclei were stained with DAPI and after three final washes with PBS, slides were mounted with appropriate cover slips avoiding bubbles.

6.3.3 Image acquisition and analysis

Fluorescent imaged were acquired via Zeiss LSM 710 (10x objective) confocal microscope at the imaging core facility of the DFKZ. Image analysis was performed with Fiji/Image J software.

6.4 Molecular biology methods

6.4.1 Genotyping PCR

Genotyping from mouse tissue was performed by PCR of genomic DNA. Tail tips were incubated in 100 µL Direct PCR Reagent + 10µg Proteinase K at 55°C overnight followed by 20min at 95°C for enzyme inactivation. Tail tip lysates were used directly or were stored at -20°C until genotyped.
Genotyping PCRs for different alleles were carried out using REDTaq® ReadyMix™ and primers as listed on tables 17 and 19. Alternatively, the PCR mix was prepared manually as in table 18 and 20. Agarose gel was prepared by dissolving 1% (w/v) agarose in 0.5x TBE buffer by heating. Ethidium bromide (5 µl/100 ml) was added and the solution was transferred into a cast tray for solidification. Samples were loaded onto the gel, which run at 140V for 45min. The 100 bp Generuler Plus DNA-Ladder (7 µl/well) was used as a size reference. DNA was visible under UV-light and the band size was determined relative to the DNA ladder. Alternatively, PCRs were analyzed via QIAxcel Advanced system according to manufacturer's protocol.

Table 17 Ang2^{KO} genotyping PCR mix and program

Ang2^{KO} genotyping PCR mix		**Genotyping PCR Program**			
	1x	Step	Temperature	Time	
dd H2O	9.15 µL	1	94°C	4’	
RedTaq Mix	2 µL	2	94°C	30”	x39
Primer loxp1 for (10µM)	0.25 µL	3	60°C	45”	
Primer loxp1 rev (10µM)	0.25 µL	4	72°C	45’”	
Primer loxp2 rev (10µM)	0.25 µL	5	72°C	7’	
DNA	1 µL	6	4°C	hold	

Table 18 Tie1$^{flox/flox}$ genotyping PCR mix and program

Tie1$^{flox/flox}$ genotyping PCR mix		**Genotyping PCR Program**			
	1x	Step	Temperature	Time	
dd H2O	10.8 µL	1	95 °C	4’	
Q-Solution	2.60 µL	2	95 °C	30”	x35
10X Buffer	1.93 µL	3	53 °C	1’	
MgCl2	0.64 µL	4	72°C	1’	
dNTP	0.64 µL	5	72 °C	5’	
Primer Tie1fl/fl-5 (5µM)	0.64 µL	6	10 °C	hold	
Primer Tie1fl/fl-3 (5µM)	0.64 µL				
Taq	0.13 µL				
DNA	4 µL				

Table 19 Cdh5-CreERT2 genotyping PCR mix and program

***Cdh5-CreERT2* genotyping PCR mix**		**Genotyping PCR Program**			
	1x	Step	Temperature	Time	
dd H2O	7.50 µL	1	94°C	2’	
RedTaq Mix	12.50 µL	2	94°C	30”	x35
MB182R Actin (10µM)	1 µL	3	58°C	45”	
MB182R Actin (10µM)	1 µL	4	72°C	2’	
MB183R Cre (10µM)	1 µL	5	72°C	2’	
MB183F Cre (10µM)	1 µL	6	4°C	hold	
DNA	2 µL				

Table 20 ROSA-CreERT2 genotyping PCR mix and program

***ROSA-CreERT2* genotyping PCR mix**		**Genotyping PCR Program**			
	1x	Step	Temperature	Time	
dd H2O	19.4 µL	1	94°C	3’	
10 x Buffer	2.5 µL	2	94°C	30”	x35
25mM MgCl2	0.75 µL	3	60°C	30”	
dNTP Mix (10mM each)	0.5 µL	4	72°C	30”	
AU-RCE-1 (100µM)	0.2 µL	5	72°C	3’	
AU-RCE-2 (100µM)	0.2 µL	6	4°C	hold	

AU-RCE-3 (100µM)	0.2 µL			
Taq	0.25 µL			
DNA	1 µL			

6.4.2 RNA isolation

6.4.2.1 RNA isolation from WBM

RNA from whole BM cells was isolated using the GenElute™ kit according manufacturer's instructions. Femurs and tibias were collected and crushed with a mortar and pestle in the presence of 2ml PBS/FCSF 5%. Crushed fraction was then passed through a 100 µm nylon mesh into fresh Eppendorf tubes. Following centrifugation at 400 g and 4°C for 10min, the pellet is lysed with 350 µL lysis solution. Eventually, RNA was eluted in 30 µL RNase free H_2O and stored at -80°C.

6.4.2.2 RNA isolation from sorted HSPCs

RNA isolation on sorted HSPCs was performed with the Arcturus™ PicoPure™ RNA isolation Kit. Sorted cells were centrifuged at 400 g and 4°C for 10min to form a pellet which was then lysed by 100 µL Arcturus PicoPure extraction buffer. The protocol was performed according to manufacturer's instructions. RNA was eluted in 11 µL RNase free H_2O and concentration was measured via NanoPhotometer® N60.

6.4.3 cDNA synthesis

cDNA generation was carried out using the Quantitect® Reverse Transcription Kit (Qiagen) according to manufacturer's instructions. Template RNA was thawed on ice and 1 µg RNA was incubated with 2 µL x DNA Wipeout buffer for 2min at 42°C and the total volume was adjusted to 14 µL adding RNase-free H_2O. The mixture was further incubated with 1 µL reverse transcriptase, 4 µL 5xRT-buffer and 1 µL RT Primer mix at 42°C for 30min for reverse transcription and 95°C for 3min for inactivation of the enzyme. The cDNA was diluted 1:10 in H2O for qPCR reaction. cDNA was kept in -20°C for short term storage.

6.4.4 Quantitative Real Time-PCR (RT-qPCR)

Relative gene expression was quantified by RT-qPCR based on synthesized cDNA. mRNA transcription levels were determined based on TaqMan™- based RT-qPCR. The Taqman™ mono-color hydrolysis method is based on probes labeled with a fluorophore (6-carboxyfluorescein, FAM) at the 5' end and a fluorescence quencher at the 3' end. The Taq polymerase cleaves the probe resulting in FAM fluorescence detection. Reactions were taking place in either 96 or 384-well plates. The reaction mix components are listed on Table 6.

Table 21 TaqMan™ RT-qPCR reaction mix

TaqMan™ RT-qPCR reaction mix	
cDNA (1:10 dilution)	3 µL
Taqman™ Fast Advanced Master Mix	5 µL

TaqMan™ probe	0.5 µL
ddH_2O	1.5 µL

Each reaction was performed in technical triplicates. The RT-qPCR was performed using the Lightcycler® 480 System (for the 384-well plates) or the StepOnePlus Real-Time PCR System (for 96-well plates).

Table 22 TaqMan™ RT-qPCR program

TaqMan™ RT-qPCR program		
Step	Temperature (°C)	Time (sec)
Pre-denaturation	95	30
Denaturation	95	2
Amplification	60	20

For analysis, the ΔΔCt method was applied as described in literature(246). This is done by normalizing CT values of the genes of interest to the CT values of the housekeeping gene for each sample (ΔCT).

$$\Delta CT = CT_{\text{gene of interest}} - CT_{\text{housekeeping gene}}$$

The normalized CT valued were then further normalized to CT values of control samples (ΔΔCT).

$$\Delta\Delta CT = \Delta CT_{\text{sample of interest}} - \Delta CT_{\text{control sample}}$$

Respective fold changes were calculated from the ΔΔCT values.

$$\text{Fold change} = 2^{-\Delta\Delta CT}$$

6.5 Protein chemical methods

6.5.1 Preparation of blood serum

Blood was collected into 1.5ml Eppendorf tubes is either from the submandibular vein or from the heart of anesthetized mice. The tubes were left undisturbed for 30min at RT and then centrifuged at 1.500 x g for 10min at 4°C. The resulting supernatant was removed and stored at -20°C until used for the ELISA assay.

6.5.2 Protein concentration measurement

The protein concentration of blood serum was determined by the BCA-assay (Pierce) according to manufacturer's instructions for microplate formats. The working reagent (WR) was incubated with the samples for 30min at 37°C protected from light. The microplate was then inserted into an iMark™ Microplate Reader and measured at 562nm. Standard values were plotted in order to generate the standard curve according to which sample concentrations were determined.

6.5.3. ELISA

Serum was collected from C57BL/6N mice injected with either NaCl or G-CSF at different time-points. The concentration of Ang2 in mouse serum was determined with the mouse Angiopoietin-2 Quantikine ELISA Kit (R&D systems). Absorbance at 450 nm was recorded on an iMark™ Microplate Reader.

6.5.4 Fluorescence activated cell sorting (FACS)

6.5.4.1 Analysis and sorting of HSPCs

To isolate BM or spleen cell populations, bones were crushed with mortars and pestles and spleens were grinded. Crushed and grinded fractions were filtered through a 100 µm nylon mesh. Blood was withdrawn from the heart or the submandibular vein using heparinized capillaries. Blood leukocytes were purified by erythrocyte lysis (ACK). Total white blood cell (WBC) counts were assessed using a Hemavet 950FS cell counter. For HSC or HSPC flow analysis via flow cytometry, immature cells were enriched by erythrocyte lysis and selected via lineage (Lin) markers: CD3, CD8a, Ter119, CD11b, CD45R (Biolegend) and LSK-SLAM markers: CD117 [2B8] (BD Biosciences), Sca-1 [7H4L3] (Thermo Fisher Scientific), CD150 [TC15-12F12.2] and CD48 [HM48-1] (Biolegend). The Mouse Lineage Depletion kit (Miltenyi Biotec) was used for HSPC and HSC sorting. BM sinusoidal endothelial cells (BM-SEC) were enriched by lineage depletion as described above and identified by negative selection for CD45 and positive staining for CD31 (BD Bioscience) and VEGFR-3 (Thermo Fisher Scientific). Osteoblasts and osteoprogenitors were isolated by bone crushing and digestion with collagenase P, dispase, DNaseI and trypsin. For blood analysis in BM reconstituted mice, antibodies against CD45 [30-F11], CD19 [1D3], CD11b (BD Biosciences), CD3 [17A2] (Thermo Fisher Scientific), CD4 [RM4-5] (Thermo Fisher Scientific), CD8a [5H10] (Thermo Fisher Scientific), B220 [RA3-6B2] (Thermo Fisher Scientific) and Ly-6G/Ly-6C (Gr-1) [RB6-8C5] (Biolegend) were used. For the discrimination of donor-derived and resident immune cells, rat anti-mouse CD45.1 and CD45.2 (BD Biosciences) antibodies were used. Live/dead cells discrimination was achieved via Fx Cycle Violet staining (Thermo Fisher Scientific). Cell populations were analyzed on BD LSR Fortessa and sorted using FACS Aria cell sorter. Single stained and unstained controls were used for compensation and correct gating strategy. Cells were pre-gated to distinguish debris and doublets using FSC and SSC. Acquisition was carried out using either a BD Canto II or BD LSR Fortessa and quantification of the analysis using FlowJo software.

6.6 Statistical analysis

Statistical analysis was carried out via GraphPad Prism 7 (GraphPad Software). Data are illustrated as mean ±SD. Statistical significance between experimental groups was determined using two-tailed Student's t-test, Mann-Whitney test as indicated in figure legends. T-test values ≤0.05 were considered statistically significant. *=P<0.05, **= P<0.01 and ***= P<0.001.

7. ABBREVIATIONS

3D	3-dimensions
Ab	Antibody
ABIN2	A20-binding inhibitor of NF-kappa-B activation 2
ACTA2	Alpha-smooth muscle actin
ADAM	a disintegrin and metalloproteases
AF	Alexa-Fluor
ALL	Acute lymphoid leukemia
AML	Acute myeloid leukemia
Ang	Angiopoietin
$Ang2^{KO}$	Ang2 global knock out
Angptl4	Angiopoietin like 4
ATP	Adenosine Triphosphate
B	B-cell
BCA	Bicinchoninic acid
BFU-E	Burst-forming unit-erythrocytes
BM	Bone marrow
BRAF	B-Raf-proto-oncogene Serine/Threonine Kinase
C	Celsius
C57BL/6J	C57 Black 6
CAR	CXCL12 Abundant Reticular
CCL	C-C motif chemokine ligand
CD31	Cluster of differentiation 31
Cdh5	Cadherin 5
cDNA	Complementary DNA
CFU	Colony forming unit
CFU-E	Colony forming unit-erythroid
CFU-G	Colony forming unit-granulocyte
CFU-GEMM	Colony forming unit-granulocyte, erythrocyte, megakaryocyte, monocyte
CFU-GM	Colony forming unit-granulocyte, megakaryocyte
CFU-M	Colony forming unit-monocyte
CFU-Mk	Colony forming unit-megakaryocyte
CLL	Chronic lymphoid leukemia
CLP	Common lymphoid progenitor
CLS	Capillary leak syndrome
CML	Chronic myeloid leukemia
CMP	Common myeloid progenitor
COL1	Collagen Type I
COL2	Collagen Type II
COMP-Ang1	cartilage oligomeric matrix protein-Angiopoietin 1

COX2	Cyclooxygenase 2
CT	Threshold Cycle
CXCL12	CXC-chemokine ligand 12
DMSO	Dimethylsulfoxide
DNA	Desoxyribonucleic acid
DNase	Deoxyribonuclease
dNTP	Desoxy nucleotide triphosphate
DPP4	Dipeptidylpeptidase 4
E	Embrionic day
EBD	Evans blue dye
EC	Endothelial cell
ECM	Extrcellular matrix
EGF	Epidermal Growth factor
EMCN	Endomucin
EndMT	Endothelial-Mesenchymal transition
eNOS	endothelial nitric oxide synthase
ERK	Extracellular signal regulated kinase
ES	Embedding solution
FACS	Fluorescent activated cell sorting
FAK	Focal Adhesion kinase
Fc	Fusion construct
FCS	Fetal Calf Serum
FDA	Food and Drugs Administration
FGF	Fibroblast growth factor
FITC	Fluorescein thioisocyanate
FOXO-1	Forkhead Box protein O1
For	Forward
FSC	Forward scatter
FSP	Fibroblast-Specific Protein
g	Gram
g	Gravity (centrifugation context)
G-CSF	Granulocyte colony stimulating factor
GFP	Green fluorescent protein
GMP	Granulocyte-monocyte progenitor
GOI	Gene of interest
GRB2	Growth factor receptor-bound protein2
h	Hour(s)
H&E	Hematoxylin/Eosin
H_2O	Water
HB-EGF	Heparin binding-epidermal growth factor
HSCT	Hematopoietic stem cell transplantation

HGF	Hepatocyte growth factor
HIF1	Hypoxia Inducible Factor 1a
HRP	Horseradish peroxidase
HSC	Hematopoietic stem cell
HSPC	Hematopoietic stem progenitor cell
HUVEC	Human Umbilical Vein Endothelial Cells
i.p	Intraperitoneally
i.v	Intravenously
ICAM	Intercellular adhesion molecule
iECKO	Inducible endothelial cell knock-out
Ig	Immunoglobulin
IGF	Insulin growth factor
IgG	Immunoglobulin G
IHC	Immunohistochemistry
Il	Interleukin
ILK	Integrin Linked Kinase
kDa	Kilo Dalton
KO	Knock Out
l	Liter
LepR	Leptin Receptor
LOX	Lysyl oxidase
LPS	Lipopolysaccharide
LSK	$Lineage^{-}$ $Sca\text{-}1^{+}$ $c\text{-}Kit^{+}$
LT-HSC	Long term hematopoietic stem cells
Ly6d	Lymphocyte antigen 6D G6D
Ly6g	Lymphocyte antigen 6D
M	Molar
mAb	Monoclonal antibody
MAPK	Mitogen-activated protein kinase
MDS/MPN	Myelodysplastic/myeloproliferative neoplasms
MET	Mesenchymal-Epithelial Transition
min	Minute(s)
mm	Millimeter
MMP	Matrix metalloproteinase
MPP	Multipotent progenitors
ms	Mouse
MSC	Mesenchymal stem cell
MSPC	Mesenchymal stem and progenitor cell
MYH11	Myosine heavy chain 11
n	Nano
Nes	Nestin
NFKB	Nuclear Factor kappa-light chain enhancer of activated B cells

NG-2	Neural-glial antigen-2
NK	Natural Killer cell
nm	Nanometer
OPN	Osteopontin
PAR1	Protease activated receptor 1
PBS	Phosphate buffered saline
PCNA	Proliferating cell nuclear antigen
PCR	Polymerase chain reaction
PDGF	Platelet derived growth factor
PDGFR	Platelet derived growth factor receptor
PFA	Paraformaldehyde
pH	Power of hydrogen
PI3K	Phosphatidylinositol-3-kinase
PKC	Protein kinase C
PMA	para-methoxyanfethamine
POC	Primary ossification centre
PTEN	Phosphatase and tensin homologue
qRT-PCR	Quantitative real time polymerase chain reaction
Rac1	Ras-related C3 botulinum toxin substrate 1
rev	Reverse
Rho A	Ras homolog gene family, member A
RNA	Ribonucleic acid
RNase	Ribonuclease
ROS	Reactive oxygen species
RPKM	Reads Per Kilobase of transcript, per Million mapped reads
rpm	Rounds per minute
RT	Room temperature
RTK	Receptor Tyrosine Kinase
SCF	Stem cell factor
SD	Standard deviation
MA	Smooth muscle actin
SNS	Sympathetic nervous system
SPS	Sucrose preservation solution
SOC	Secondary ossification centre
SSC	Side scatter
ST-HSC	Short term hematopoietic stem cell
T	T cell
TAM	Tumor associated macrophages
TBS	Tris buffered saline
TBS-T	Tris buffered saline with Tween
TGF	Transforming growth factor

THPO	Thrombopoietin
Tie	Tyrosin kinase with immunoglobulin-like and EGF-like domain
$Tie1^{iECKO}$	Tie1 inducible endothelial cells knock out
$Tie1^{KO}$	Tie1 global knock out
$Tie2^{KO}$	Tie2 global knock out
TNF-α	Tumor necrosis factor α
TSP1	Thrombospondin 1
U	Unit
v/v	Volume/Volume
VE-Cadherin	Vascular endothelial cadherin
VEGF	Vascular endothelial growth factor
VEGFR	Vascular endothelial growth factor receptor
Vwf	Von Wilebrand factor
w/v	Mass volume (mass concentration)
WB	Western blot
WBM	Whole bone marrow
WHO	World health organization
WBC	White blood cell
WR	Working reagent
WT	Wildtype

8. PUBLICATIONS

Freire Valls A, Knipper K, Giannakouri E, Sarachaga V, Hinterkopf S, Wuehrl M, Shen Y, Radhakrishnan P, Klose J, Ulrich A, Schneider M, Augustin HG, Ruiz de Almodovar C, Schmidt T. (2019) VEGFR1(+) metastasis-associated macrophages contribute to metastatic angiogenesis and influence colorectal cancer patient outcome. Clin Cancer Res.

Schlereth K, Weichenhan D, Bauer T, Heumann T, Giannakouri E, Lipka D, Jaeger S, Schlesner M, Aloy P, Eils R, Plass C, Augustin HG. (2018) The transcriptomic and epigenetic map of vascular quiescence in the continuous lung endothelium. eLife.

9. REFERENCES

1. Adams RH, Alitalo K. Molecular regulation of angiogenesis and lymphangiogenesis. Nat Rev Mol Cell Biol. 2007;8(6):464-78.

2. Herbert SP, Stainier DY. Molecular control of endothelial cell behaviour during blood vessel morphogenesis. Nat Rev Mol Cell Biol. 2011;12(9):551-64.

3. Tammela T, Alitalo K. Lymphangiogenesis: Molecular mechanisms and future promise. Cell. 2010;140(4):460-76.

4. Risau W, Flamme I. Vasculogenesis. Annu Rev Cell Dev Biol. 1995;11:73-91.

5. Geudens I, Gerhardt H. Coordinating cell behaviour during blood vessel formation. Development. 2011;138(21):4569-83.

6. Potente M, Gerhardt H, Carmeliet P. Basic and therapeutic aspects of angiogenesis. Cell. 2011;146(6):873-87.

7. Carmeliet P, Jain RK. Molecular mechanisms and clinical applications of angiogenesis. Nature. 2011;473(7347):298-307.

8. Maes C, Kobayashi T, Selig MK, Torrekens S, Roth SI, Mackem S, et al. Osteoblast precursors, but not mature osteoblasts, move into developing and fractured bones along with invading blood vessels. Dev Cell. 2010;19(2):329-44.

9. Kronenberg HM. Developmental regulation of the growth plate. Nature. 2003;423(6937):332-6.

10. Abzhanov A, Rodda SJ, McMahon AP, Tabin CJ. Regulation of skeletogenic differentiation in cranial dermal bone. Development. 2007;134(17):3133-44.

11. Olsson AK, Dimberg A, Kreuger J, Claesson-Welsh L. VEGF receptor signalling - in control of vascular function. Nat Rev Mol Cell Biol. 2006;7(5):359-71.

12. Bentovim L, Amarilio R, Zelzer E. HIF1alpha is a central regulator of collagen hydroxylation and secretion under hypoxia during bone development. Development. 2012;139(23):4473-83.

13. Lu P, Takai K, Weaver VM, Werb Z. Extracellular matrix degradation and remodeling in development and disease. Cold Spring Harb Perspect Biol. 2011;3(12).

14. Murshed M, Schinke T, McKee MD, Karsenty G. Extracellular matrix mineralization is regulated locally; different roles of two gla-containing proteins. J Cell Biol. 2004;165(5):625-30.

15. Coutu DL, Francois M, Galipeau J. Inhibition of cellular senescence by developmentally regulated FGF receptors in mesenchymal stem cells. Blood. 2011;117(25):6801-12.

16. Kozhemyakina E, Lassar AB, Zelzer E. A pathway to bone: signaling molecules and transcription factors involved in chondrocyte development and maturation. Development. 2015;142(5):817-31.

17. Kusumbe AP, Ramasamy SK, Starsichova A, Adams RH. Sample preparation for high-resolution 3D confocal imaging of mouse skeletal tissue. Nat Protoc. 2015;10(12):1904-14.

18. Acar AH, Yolcu U, Gul M, Keles A, Erdem NF, Altundag Kahraman S. Micro-computed tomography and histomorphometric analysis of the effects of platelet-rich fibrin on bone regeneration in the rabbit calvarium. Arch Oral Biol. 2015;60(4):606-14.

19. Trueta J, Morgan JD. The vascular contribution to osteogenesis. I. Studies by the injection method. J Bone Joint Surg Br. 1960;42-B:97-109.

20. Kusumbe AP, Ramasamy SK, Adams RH. Coupling of angiogenesis and osteogenesis by a specific vessel subtype in bone. Nature. 2014;507(7492):323-8.

21. Kusumbe AP, Adams RH. Osteoclast progenitors promote bone vascularization and osteogenesis. Nat Med. 2014;20(11):1238-40.

22. Kopp HG, Avecilla ST, Hooper AT, Rafii S. The bone marrow vascular niche: home of HSC differentiation and mobilization. Physiology (Bethesda). 2005;20:349-56.

23. Aird WC. Phenotypic heterogeneity of the endothelium: I. Structure, function, and mechanisms. Circ Res. 2007;100(2):158-73.

24. Ramasamy SK, Kusumbe AP, Wang L, Adams RH. Endothelial Notch activity promotes angiogenesis and osteogenesis in bone. Nature. 2014;507(7492):376-80.

25. Itkin T, Gur-Cohen S, Spencer JA, Schajnovitz A, Ramasamy SK, Kusumbe AP, et al. Distinct bone marrow blood vessels differentially regulate haematopoiesis. Nature. 2016;532(7599):323-8.

26. Ding L, Saunders TL, Enikolopov G, Morrison SJ. Endothelial and perivascular cells maintain haematopoietic stem cells. Nature. 2012;481(7382):457-62.

27. Sugiyama T, Kohara H, Noda M, Nagasawa T. Maintenance of the hematopoietic stem cell pool by CXCL12-CXCR4 chemokine signaling in bone marrow stromal cell niches. Immunity. 2006;25(6):977-88.

28. Kusumbe AP, Ramasamy SK, Itkin T, Mae MA, Langen UH, Betsholtz C, et al. Age-dependent modulation of vascular niches for haematopoietic stem cells. Nature. 2016;532(7599):380-4.

29. Kunisaki Y, Bruns I, Scheiermann C, Ahmed J, Pinho S, Zhang D, et al. Arteriolar niches maintain haematopoietic stem cell quiescence. Nature. 2013;502(7473):637-43.

30. Mendez-Ferrer S, Michurina TV, Ferraro F, Mazloom AR, Macarthur BD, Lira SA, et al. Mesenchymal and haematopoietic stem cells form a unique bone marrow niche. Nature. 2010;466(7308):829-34.

31. Augustin HG, Koh GY, Thurston G, Alitalo K. Control of vascular morphogenesis and homeostasis through the angiopoietin-Tie system. Nat Rev Mol Cell Biol. 2009;10(3):165-77.

32. Partanen J, Armstrong E, Makela TP, Korhonen J, Sandberg M, Renkonen R, et al. A novel endothelial cell surface receptor tyrosine kinase with extracellular epidermal growth factor homology domains. Mol Cell Biol. 1992;12(4):1698-707.

33. Dumont DJ, Yamaguchi TP, Conlon RA, Rossant J, Breitman ML. tek, a novel tyrosine kinase gene located on mouse chromosome 4, is expressed in endothelial cells and their presumptive precursors. Oncogene. 1992;7(8):1471-80.

34. Arai F, Hirao A, Ohmura M, Sato H, Matsuoka S, Takubo K, et al. Tie2/angiopoietin-1 signaling regulates hematopoietic stem cell quiescence in the bone marrow niche. Cell. 2004;118(2):149-61.

35. Cabezas-Wallscheid N, Klimmeck D, Hansson J, Lipka DB, Reyes A, Wang Q, et al. Identification of regulatory networks in HSCs and their immediate progeny via integrated proteome, transcriptome, and DNA methylome analysis. Cell Stem Cell. 2014;15(4):507-22.

36. Turrini R, Pabois A, Xenarios I, Coukos G, Delaloye JF, Doucey MA. TIE-2 expressing monocytes in human cancers. Oncoimmunology. 2017;6(4):e1303585.

37. Chen L, Li J, Wang F, Dai C, Wu F, Liu X, et al. Tie2 Expression on Macrophages Is Required for Blood Vessel Reconstruction and Tumor Relapse after Chemotherapy. Cancer Res. 2016;76(23):6828-38.

38. Ito K, Turcotte R, Cui J, Zimmerman SE, Pinho S, Mizoguchi T, et al. Self-renewal of a purified Tie2+ hematopoietic stem cell population relies on mitochondrial clearance. Science. 2016;354(6316):1156-60.

39. Brindle NP, Saharinen P, Alitalo K. Signaling and functions of angiopoietin-1 in vascular protection. Circ Res. 2006;98(8):1014-23.

40. Saharinen P, Kerkela K, Ekman N, Marron M, Brindle N, Lee GM, et al. Multiple angiopoietin recombinant proteins activate the Tie1 receptor tyrosine kinase and promote its interaction with Tie2. J Cell Biol. 2005;169(2):239-43.

41. Schnurch H, Risau W. Expression of tie-2, a member of a novel family of receptor tyrosine kinases, in the endothelial cell lineage. Development. 1993;119(3):957-68.

42. Shewchuk LM, Hassell AM, Ellis B, Holmes WD, Davis R, Horne EL, et al. Structure of the Tie2 RTK domain: self-inhibition by the nucleotide binding loop, activation loop, and C-terminal tail. Structure. 2000;8(11):1105-13.

43. Procopio WN, Pelavin PI, Lee WM, Yeilding NM. Angiopoietin-1 and -2 coiled coil domains mediate distinct homo-oligomerization patterns, but fibrinogen-like domains mediate ligand activity. J Biol Chem. 1999;274(42):30196-201.

44. Davis S, Papadopoulos N, Aldrich TH, Maisonpierre PC, Huang T, Kovac L, et al. Angiopoietins have distinct modular domains essential for receptor binding, dimerization and superclustering. Nat Struct Biol. 2003;10(1):38-44.

45. Kim KT, Choi HH, Steinmetz MO, Maco B, Kammerer RA, Ahn SY, et al. Oligomerization and multimerization are critical for angiopoietin-1 to bind and phosphorylate Tie2. J Biol Chem. 2005;280(20):20126-31.

46. Leppanen VM, Saharinen P, Alitalo K. Structural basis of Tie2 activation and Tie2/Tie1 heterodimerization. Proc Natl Acad Sci U S A. 2017;114(17):4376-81.

47. Yuan HT, Khankin EV, Karumanchi SA, Parikh SM. Angiopoietin 2 is a partial agonist/antagonist of Tie2 signaling in the endothelium. Mol Cell Biol. 2009;29(8):2011-22.

48. Maisonpierre PC, Suri C, Jones PF, Bartunkova S, Wiegand SJ, Radziejewski C, et al. Angiopoietin-2, a natural antagonist for Tie2 that disrupts in vivo angiogenesis. Science. 1997;277(5322):55-60.

49. Sato TN, Tozawa Y, Deutsch U, Wolburg-Buchholz K, Fujiwara Y, Gendron-Maguire M, et al. Distinct roles of the receptor tyrosine kinases Tie-1 and Tie-2 in blood vessel formation. Nature. 1995;376(6535):70-4.

50. Suri C, Jones PF, Patan S, Bartunkova S, Maisonpierre PC, Davis S, et al. Requisite role of angiopoietin-1, a ligand for the TIE2 receptor, during embryonic angiogenesis. Cell. 1996;87(7):1171-80.

51. Dumont DJ, Gradwohl G, Fong GH, Puri MC, Gertsenstein M, Auerbach A, et al. Dominant-negative and targeted null mutations in the endothelial receptor tyrosine kinase, tek, reveal a critical role in vasculogenesis of the embryo. Genes Dev. 1994;8(16):1897-909.

52. Patan S. TIE1 and TIE2 receptor tyrosine kinases inversely regulate embryonic angiogenesis by the mechanism of intussusceptive microvascular growth. Microvasc Res. 1998;56(1):1-21.

53. Rodewald HR, Sato TN. Tie1, a receptor tyrosine kinase essential for vascular endothelial cell integrity, is not critical for the development of hematopoietic cells. Oncogene. 1996;12(2):397-404.

54. Puri MC, Partanen J, Rossant J, Bernstein A. Interaction of the TEK and TIE receptor tyrosine kinases during cardiovascular development. Development. 1999;126(20):4569-80.

55. Ward NL, Van Slyke P, Sturk C, Cruz M, Dumont DJ. Angiopoietin 1 expression levels in the myocardium direct coronary vessel development. Dev Dyn. 2004;229(3):500-9.

56. Gale NW, Thurston G, Hackett SF, Renard R, Wang Q, McClain J, et al. Angiopoietin-2 is required for postnatal angiogenesis and lymphatic patterning, and only the latter role is rescued by Angiopoietin-1. Dev Cell. 2002;3(3):411-23.

57. Fiedler U, Reiss Y, Scharpfenecker M, Grunow V, Koidl S, Thurston G, et al. Angiopoietin-2 sensitizes endothelial cells to TNF-alpha and has a crucial role in the induction of inflammation. Nat Med. 2006;12(2):235-9.

58. Shimoda H, Bernas MJ, Witte MH, Gale NW, Yancopoulos GD, Kato S. Abnormal recruitment of periendothelial cells to lymphatic capillaries in digestive organs of angiopoietin-2-deficient mice. Cell Tissue Res. 2007;328(2):329-37.

59. Lobov IB, Brooks PC, Lang RA. Angiopoietin-2 displays VEGF-dependent modulation of capillary structure and endothelial cell survival in vivo. Proc Natl Acad Sci U S A. 2002;99(17):11205-10.

60. Holash J, Maisonpierre PC, Compton D, Boland P, Alexander CR, Zagzag D, et al. Vessel cooption, regression, and growth in tumors mediated by angiopoietins and VEGF. Science. 1999;284(5422):1994-8.

61. DeBusk LM, Hallahan DE, Lin PC. Akt is a major angiogenic mediator downstream of the Ang1/Tie2 signaling pathway. Exp Cell Res. 2004;298(1):167-77.

62. Kim I, Kim HG, So JN, Kim JH, Kwak HJ, Koh GY. Angiopoietin-1 regulates endothelial cell survival through the phosphatidylinositol 3'-Kinase/Akt signal transduction pathway. Circ Res. 2000;86(1):24-9.

63. Kwak HJ, So JN, Lee SJ, Kim I, Koh GY. Angiopoietin-1 is an apoptosis survival factor for endothelial cells. FEBS Lett. 1999;448(2-3):249-53.

64. Papapetropoulos A, Fulton D, Mahboubi K, Kalb RG, O'Connor DS, Li F, et al. Angiopoietin-1 inhibits endothelial cell apoptosis via the Akt/survivin pathway. J Biol Chem. 2000;275(13):9102-5.

65. Daly C, Wong V, Burova E, Wei Y, Zabski S, Griffiths J, et al. Angiopoietin-1 modulates endothelial cell function and gene expression via the transcription factor FKHR (FOXO1). Genes Dev. 2004;18(9):1060-71.

66. Tsigkos S, Zhou Z, Kotanidou A, Fulton D, Zakynthinos S, Roussos C, et al. Regulation of Ang2 release by PTEN/PI3-kinase/Akt in lung microvascular endothelial cells. J Cell Physiol. 2006;207(2):506-11.

67. Seegar TC, Eller B, Tzvetkova-Robev D, Kolev MV, Henderson SC, Nikolov DB, et al. Tie1-Tie2 interactions mediate functional differences between angiopoietin ligands. Mol Cell. 2010;37(5):643-55.

68. Dejana E, Orsenigo F, Lampugnani MG. The role of adherens junctions and VE-cadherin in the control of vascular permeability. J Cell Sci. 2008;121(Pt 13):2115-22.

69. Gavard J, Gutkind JS. VEGF controls endothelial-cell permeability by promoting the beta-arrestin-dependent endocytosis of VE-cadherin. Nat Cell Biol. 2006;8(11):1223-34.

70. Kanda S, Miyata Y, Mochizuki Y, Matsuyama T, Kanetake H. Angiopoietin 1 is mitogenic for cultured endothelial cells. Cancer Res. 2005;65(15):6820-7.

71. Kim I, Kim HG, Moon SO, Chae SW, So JN, Koh KN, et al. Angiopoietin-1 induces endothelial cell sprouting through the activation of focal adhesion kinase and plasmin secretion. Circ Res. 2000;86(9):952-9.

72. Hughes DP, Marron MB, Brindle NP. The antiinflammatory endothelial tyrosine kinase Tie2 interacts with a novel nuclear factor-kappaB inhibitor ABIN-2. Circ Res. 2003;92(6):630-6.

73. Tadros A, Hughes DP, Dunmore BJ, Brindle NP. ABIN-2 protects endothelial cells from death and has a role in the antiapoptotic effect of angiopoietin-1. Blood. 2003;102(13):4407-9.

74. Kobayashi H, DeBusk LM, Babichev YO, Dumont DJ, Lin PC. Hepatocyte growth factor mediates angiopoietin-induced smooth muscle cell recruitment. Blood. 2006;108(4):1260-6.

75. Iivanainen E, Nelimarkka L, Elenius V, Heikkinen SM, Junttila TT, Sihombing L, et al. Angiopoietin-regulated recruitment of vascular smooth muscle cells by endothelial-derived heparin binding EGF-like growth factor. FASEB J. 2003;17(12):1609-21.

76. Sullivan CC, Du L, Chu D, Cho AJ, Kido M, Wolf PL, et al. Induction of pulmonary hypertension by an angiopoietin 1/TIE2/serotonin pathway. Proc Natl Acad Sci U S A. 2003;100(21):12331-6.

77. Heldin CH, Westermark B. Mechanism of action and in vivo role of platelet-derived growth factor. Physiol Rev. 1999;79(4):1283-316.

78. Fiedler U, Augustin HG. Angiopoietins: a link between angiogenesis and inflammation. Trends Immunol. 2006;27(12):552-8.

79. Kim M, Allen B, Korhonen EA, Nitschke M, Yang HW, Baluk P, et al. Opposing actions of angiopoietin-2 on Tie2 signaling and FOXO1 activation. J Clin Invest. 2016;126(9):3511-25.

80. Korhonen EA, Lampinen A, Giri H, Anisimov A, Kim M, Allen B, et al. Tie1 controls angiopoietin function in vascular remodeling and inflammation. J Clin Invest. 2016;126(9):3495-510.

81. Souma T, Thomson BR, Heinen S, Carota IA, Yamaguchi S, Onay T, et al. Context-dependent functions of angiopoietin 2 are determined by the endothelial phosphatase VEPTP. Proc Natl Acad Sci U S A. 2018;115(6):1298-303.

82. Felcht M, Luck R, Schering A, Seidel P, Srivastava K, Hu J, et al. Angiopoietin-2 differentially regulates angiogenesis through TIE2 and integrin signaling. J Clin Invest. 2012;122(6):1991-2005.

83. del Toro R, Prahst C, Mathivet T, Siegfried G, Kaminker JS, Larrivee B, et al. Identification and functional analysis of endothelial tip cell-enriched genes. Blood. 2010;116(19):4025-33.

84. Chen-Konak L, Guetta-Shubin Y, Yahav H, Shay-Salit A, Zilberman M, Binah O, et al. Transcriptional and post-translation regulation of the Tie1 receptor by fluid shear stress changes in vascular endothelial cells. FASEB J. 2003;17(14):2121-3.

85. Marron MB, Singh H, Tahir TA, Kavumkal J, Kim HZ, Koh GY, et al. Regulated proteolytic processing of Tie1 modulates ligand responsiveness of the receptor-tyrosine kinase Tie2. J Biol Chem. 2007;282(42):30509-17.

86. Yabkowitz R, Meyer S, Black T, Elliott G, Merewether LA, Yamane HK. Inflammatory cytokines and vascular endothelial growth factor stimulate the release of soluble tie receptor from human endothelial cells via metalloprotease activation. Blood. 1999;93(6):1969-79.

87. Yabkowitz R, Meyer S, Yanagihara D, Brankow D, Staley T, Elliott G, et al. Regulation of tie receptor expression on human endothelial cells by protein kinase C-mediated release of soluble tie. Blood. 1997;90(2):706-15.

88. Singh H, Hansen TM, Patel N, Brindle NP. The molecular balance between receptor tyrosine kinases Tie1 and Tie2 is dynamically controlled by VEGF and TNFalpha and regulates angiopoietin signalling. PLoS One. 2012;7(1):e29319.

89. Yuan HT, Venkatesha S, Chan B, Deutsch U, Mammoto T, Sukhatme VP, et al. Activation of the orphan endothelial receptor Tie1 modifies Tie2-mediated intracellular signaling and cell survival. FASEB J. 2007;21(12):3171-83.

90. Savant S, La Porta S, Budnik A, Busch K, Hu J, Tisch N, et al. The Orphan Receptor Tie1 Controls Angiogenesis and Vascular Remodeling by Differentially Regulating Tie2 in Tip and Stalk Cells. Cell Rep. 2015;12(11):1761-73.

91. Kontos CD, Cha EH, York JD, Peters KG. The endothelial receptor tyrosine kinase Tie1 activates phosphatidylinositol 3-kinase and Akt to inhibit apoptosis. Mol Cell Biol. 2002;22(6):1704-13.

92. Xu J. LECT2, a Ligand for Tie1, Plays a Crucial Role in Liver Fibrogenesis. Cell. 2019;178(178):1–15.

93. Zhou BO, Ding L, Morrison SJ. Hematopoietic stem and progenitor cells regulate the regeneration of their niche by secreting Angiopoietin-1. Elife. 2015;4:e05521.

94. Schliemann C, Bieker R, Padro T, Kessler T, Hintelmann H, Buchner T, et al. Expression of angiopoietins and their receptor Tie2 in the bone marrow of patients with acute myeloid leukemia. Haematologica. 2006;91(9):1203-11.

95. Hintsala E, Bono P, Andersson S, Kivivuori SM. Quantification of plasma and bone marrow VEGF and angiopoietin-2 levels in pediatric malignancies. J Pediatr Hematol Oncol. 2012;34(7):503-10.

96. Koenecke C, Kumpers P, Lukasz A, Dammann E, Verhagen W, Gohring G, et al. Shedding of the endothelial receptor tyrosine kinase Tie2 correlates with leukemic blast burden and outcome after allogeneic hematopoietic stem cell transplantation for AML. Ann Hematol. 2010;89(5):459-67.

97. Belloni D, Marcatti M, Ponzoni M, Ciceri F, Veschini L, Corti A, et al. Angiopoietin-2 in Bone Marrow milieu promotes Multiple Myeloma-associated angiogenesis. Exp Cell Res. 2015;330(1):1-12.

98. Cheng CL, Hou HA, Jhuang JY, Lin CW, Chen CY, Tang JL, et al. High bone marrow angiopoietin-1 expression is an independent poor prognostic factor for survival in patients with myelodysplastic syndromes. Br J Cancer. 2011;105(7):975-82.

99. Min Y, Ren X, Vaught DB, Chen J, Donnelly E, Lynch CC, et al. Tie2 signaling regulates osteoclastogenesis and osteolytic bone invasion of breast cancer. Cancer Res. 2010;70(7):2819-28.

100. Doan PL, Russell JL, Himburg HA, Helms K, Harris JR, Lucas J, et al. Tie2(+) bone marrow endothelial cells regulate hematopoietic stem cell regeneration following radiation injury. Stem Cells. 2013;31(2):327-37.

101. Jeong BC, Kim HJ, Bae IH, Lee KN, Lee KY, Oh WM, et al. COMP-Ang1, a chimeric form of Angiopoietin 1, enhances BMP2-induced osteoblast differentiation and bone formation. Bone. 2010;46(2):479-86.

102. Gomei Y, Nakamura Y, Yoshihara H, Hosokawa K, Iwasaki H, Suda T, et al. Functional differences between two Tie2 ligands, angiopoietin-1 and -2, in regulation of adult bone marrow hematopoietic stem cells. Exp Hematol. 2010;38(2):82-9.

103. Laurenti E, Gottgens B. From haematopoietic stem cells to complex differentiation landscapes. Nature. 2018;553(7689):418-26.

104. Kaushansky K. Lineage-specific hematopoietic growth factors. N Engl J Med. 2006;354(19):2034-45.

105. Wilson A, Laurenti E, Oser G, van der Wath RC, Blanco-Bose W, Jaworski M, et al. Hematopoietic stem cells reversibly switch from dormancy to self-renewal during homeostasis and repair. Cell. 2008;135(6):1118-29.

106. Essers MA, Offner S, Blanco-Bose WE, Waibler Z, Kalinke U, Duchosal MA, et al. IFNalpha activates dormant haematopoietic stem cells in vivo. Nature. 2009;458(7240):904-8.

107. Baldridge MT, King KY, Boles NC, Weksberg DC, Goodell MA. Quiescent haematopoietic stem cells are activated by IFN-gamma in response to chronic infection. Nature. 2010;465(7299):793-7.

108. Okada S, Nakauchi H, Nagayoshi K, Nishikawa S, Miura Y, Suda T. In vivo and in vitro stem cell function of c-kit- and Sca-1-positive murine hematopoietic cells. Blood. 1992;80(12):3044-50.

109. Birbrair A, Frenette PS. Niche heterogeneity in the bone marrow. Ann N Y Acad Sci. 2016;1370(1):82-96.

110. Kiel MJ, Iwashita T, Yilmaz OH, Morrison SJ. Spatial differences in hematopoiesis but not in stem cells indicate a lack of regional patterning in definitive hematopoietic stem cells. Dev Biol. 2005;283(1):29-39.

111. Schofield R. The relationship between the spleen colony-forming cell and the haemopoietic stem cell. Blood Cells. 1978;4(1-2):7-25.

112. Dexter TM, Allen TD, Lajtha LG. Conditions controlling the proliferation of haemopoietic stem cells in vitro. J Cell Physiol. 1977;91(3):335-44.

113. Lord BI, Testa NG, Hendry JH. The relative spatial distributions of CFUs and CFUc in the normal mouse femur. Blood. 1975;46(1):65-72.

114. Calvi LM, Adams GB, Weibrecht KW, Weber JM, Olson DP, Knight MC, et al. Osteoblastic cells regulate the haematopoietic stem cell niche. Nature. 2003;425(6960):841-6.

115. Park D, Spencer JA, Koh BI, Kobayashi T, Fujisaki J, Clemens TL, et al. Endogenous bone marrow MSCs are dynamic, fate-restricted participants in bone maintenance and regeneration. Cell Stem Cell. 2012;10(3):259-72.

116. Ding L, Morrison SJ. Haematopoietic stem cells and early lymphoid progenitors occupy distinct bone marrow niches. Nature. 2013;495(7440):231-5.

117. Gao X, Xu C, Asada N, Frenette PS. The hematopoietic stem cell niche: from embryo to adult. Development. 2018;145(2).

118. Kiel MJ, Yilmaz OH, Iwashita T, Yilmaz OH, Terhorst C, Morrison SJ. SLAM family receptors distinguish hematopoietic stem and progenitor cells and reveal endothelial niches for stem cells. Cell. 2005;121(7):1109-21.

119. Crane GM, Jeffery E, Morrison SJ. Adult haematopoietic stem cell niches. Nat Rev Immunol. 2017;17(9):573-90.

120. Greenbaum A, Hsu YM, Day RB, Schuettpelz LG, Christopher MJ, Borgerding JN, et al. CXCL12 in early mesenchymal progenitors is required for haematopoietic stem-cell maintenance. Nature. 2013;495(7440):227-30.

121. Himburg HA, Termini CM, Schlussel L, Kan J, Li M, Zhao L, et al. Distinct Bone Marrow Sources of Pleiotrophin Control Hematopoietic Stem Cell Maintenance and Regeneration. Cell Stem Cell. 2018;23(3):370-81 e5.

122. Butler JM, Nolan DJ, Vertes EL, Varnum-Finney B, Kobayashi H, Hooper AT, et al. Endothelial cells are essential for the self-renewal and repopulation of Notch-dependent hematopoietic stem cells. Cell Stem Cell. 2010;6(3):251-64.

123. Himburg HA, Muramoto GG, Daher P, Meadows SK, Russell JL, Doan P, et al. Pleiotrophin regulates the expansion and regeneration of hematopoietic stem cells. Nat Med. 2010;16(4):475-82.

124. Winkler IG, Barbier V, Nowlan B, Jacobsen RN, Forristal CE, Patton JT, et al. Vascular niche E-selectin regulates hematopoietic stem cell dormancy, self renewal and chemoresistance. Nat Med. 2012;18(11):1651-7.

125. Nombela-Arrieta C, Pivarnik G, Winkel B, Canty KJ, Harley B, Mahoney JE, et al. Quantitative imaging of haematopoietic stem and progenitor cell localization and hypoxic status in the bone marrow microenvironment. Nat Cell Biol. 2013;15(5):533-43.

126. Singh A, Veeriah V, Xi P, Labella R, Chen J, Romeo SG, et al. Angiocrine signals regulate quiescence and therapy resistance in bone metastasis. JCI Insight. 2019;4(13).

127. Sacchetti B, Funari A, Michienzi S, Di Cesare S, Piersanti S, Saggio I, et al. Self-renewing osteoprogenitors in bone marrow sinusoids can organize a hematopoietic microenvironment. Cell. 2007;131(2):324-36.

128. Katayama Y, Battista M, Kao WM, Hidalgo A, Peired AJ, Thomas SA, et al. Signals from the sympathetic nervous system regulate hematopoietic stem cell egress from bone marrow. Cell. 2006;124(2):407-21.

129. Lucas D, Battista M, Shi PA, Isola L, Frenette PS. Mobilized hematopoietic stem cell yield depends on species-specific circadian timing. Cell Stem Cell. 2008;3(4):364-6.

130. Mendez-Ferrer S, Lucas D, Battista M, Frenette PS. Haematopoietic stem cell release is regulated by circadian oscillations. Nature. 2008;452(7186):442-7.

131. Lucas D, Scheiermann C, Chow A, Kunisaki Y, Bruns I, Barrick C, et al. Chemotherapy-induced bone marrow nerve injury impairs hematopoietic regeneration. Nat Med. 2013;19(6):695-703.

132. Yamazaki S, Ema H, Karlsson G, Yamaguchi T, Miyoshi H, Shioda S, et al. Nonmyelinating Schwann cells maintain hematopoietic stem cell hibernation in the bone marrow niche. Cell. 2011;147(5):1146-58.

133. Nilsson SK, Johnston HM, Coverdale JA. Spatial localization of transplanted hemopoietic stem cells: inferences for the localization of stem cell niches. Blood. 2001;97(8):2293-9.

134. Visnjic D, Kalajzic Z, Rowe DW, Katavic V, Lorenzo J, Aguila HL. Hematopoiesis is severely altered in mice with an induced osteoblast deficiency. Blood. 2004;103(9):3258-64.

135. Nilsson SK, Johnston HM, Whitty GA, Williams B, Webb RJ, Denhardt DT, et al. Osteopontin, a key component of the hematopoietic stem cell niche and regulator of primitive hematopoietic progenitor cells. Blood. 2005;106(4):1232-9.

136. Stier S, Ko Y, Forkert R, Lutz C, Neuhaus T, Grunewald E, et al. Osteopontin is a hematopoietic stem cell niche component that negatively regulates stem cell pool size. J Exp Med. 2005;201(11):1781-91.

137. Qian H, Buza-Vidas N, Hyland CD, Jensen CT, Antonchuk J, Mansson R, et al. Critical role of thrombopoietin in maintaining adult quiescent hematopoietic stem cells. Cell Stem Cell. 2007;1(6):671-84.

138. Yoshihara H, Arai F, Hosokawa K, Hagiwara T, Takubo K, Nakamura Y, et al. Thrombopoietin/MPL signaling regulates hematopoietic stem cell quiescence and interaction with the osteoblastic niche. Cell Stem Cell. 2007;1(6):685-97.

139. Zhu J, Garrett R, Jung Y, Zhang Y, Kim N, Wang J, et al. Osteoblasts support B-lymphocyte commitment and differentiation from hematopoietic stem cells. Blood. 2007;109(9):3706-12.

140. Tavassoli M, Aoki M. Localization of megakaryocytes in the bone marrow. Blood Cells. 1989;15(1):3-14.

141. Yamazaki S, Iwama A, Takayanagi S, Eto K, Ema H, Nakauchi H. TGF-beta as a candidate bone marrow niche signal to induce hematopoietic stem cell hibernation. Blood. 2009;113(6):1250-6.

142. Zhao M, Perry JM, Marshall H, Venkatraman A, Qian P, He XC, et al. Megakaryocytes maintain homeostatic quiescence and promote post-injury regeneration of hematopoietic stem cells. Nat Med. 2014;20(11):1321-6.

143. Bruns I, Lucas D, Pinho S, Ahmed J, Lambert MP, Kunisaki Y, et al. Megakaryocytes regulate hematopoietic stem cell quiescence through CXCL4 secretion. Nat Med. 2014;20(11):1315-20.

144. Zhao M, Ross JT, Itkin T, Perry JM, Venkatraman A, Haug JS, et al. FGF signaling facilitates postinjury recovery of mouse hematopoietic system. Blood. 2012;120(9):1831-42.

145. Chow A, Lucas D, Hidalgo A, Mendez-Ferrer S, Hashimoto D, Scheiermann C, et al. Bone marrow CD169+ macrophages promote the retention of hematopoietic stem and progenitor cells in the mesenchymal stem cell niche. J Exp Med. 2011;208(2):261-71.

146. Winkler IG, Sims NA, Pettit AR, Barbier V, Nowlan B, Helwani F, et al. Bone marrow macrophages maintain hematopoietic stem cell (HSC) niches and their depletion mobilizes HSCs. Blood. 2010;116(23):4815-28.

147. Hur J, Choi JI, Lee H, Nham P, Kim TW, Chae CW, et al. CD82/KAI1 Maintains the Dormancy of Long-Term Hematopoietic Stem Cells through Interaction with DARC-Expressing Macrophages. Cell Stem Cell. 2016;18(4):508-21.

148. Ludin A, Itkin T, Gur-Cohen S, Mildner A, Shezen E, Golan K, et al. Monocytes-macrophages that express alpha-smooth muscle actin preserve primitive hematopoietic cells in the bone marrow. Nat Immunol. 2012;13(11):1072-82.

149. Adams GB, Chabner KT, Alley IR, Olson DP, Szczepiorkowski ZM, Poznansky MC, et al. Stem cell engraftment at the endosteal niche is specified by the calcium-sensing receptor. Nature. 2006;439(7076):599-603.

150. Kollet O, Dar A, Shivtiel S, Kalinkovich A, Lapid K, Sztainberg Y, et al. Osteoclasts degrade endosteal components and promote mobilization of hematopoietic progenitor cells. Nat Med. 2006;12(6):657-64.

151. Mansour A, Abou-Ezzi G, Sitnicka E, Jacobsen SE, Wakkach A, Blin-Wakkach C. Osteoclasts promote the formation of hematopoietic stem cell niches in the bone marrow. J Exp Med. 2012;209(3):537-49.

152. Gandy KL, Domen J, Aguila H, Weissman IL. CD8+TCR+ and CD8+TCR- cells in whole bone marrow facilitate the engraftment of hematopoietic stem cells across allogeneic barriers. Immunity. 1999;11(5):579-90.

153. Kaufman CL, Colson YL, Wren SM, Watkins S, Simmons RL, Ildstad ST. Phenotypic characterization of a novel bone marrow-derived cell that facilitates engraftment of allogeneic bone marrow stem cells. Blood. 1994;84(8):2436-46.

154. Fujisaki J, Wu J, Carlson AL, Silberstein L, Putheti P, Larocca R, et al. In vivo imaging of Treg cells providing immune privilege to the haematopoietic stem-cell niche. Nature. 2011;474(7350):216-9.

155. Hirata Y, Furuhashi K, Ishii H, Li HW, Pinho S, Ding L, et al. CD150(high) Bone Marrow Tregs Maintain Hematopoietic Stem Cell Quiescence and Immune Privilege via Adenosine. Cell Stem Cell. 2018;22(3):445-53 e5.

156. Xie Y, Yin T, Wiegraebe W, He XC, Miller D, Stark D, et al. Detection of functional haematopoietic stem cell niche using real-time imaging. Nature. 2009;457(7225):97-101.

157. Lo Celso C, Fleming HE, Wu JW, Zhao CX, Miake-Lye S, Fujisaki J, et al. Live-animal tracking of individual haematopoietic stem/progenitor cells in their niche. Nature. 2009;457(7225):92-6.

158. Duarte D, Hawkins ED, Akinduro O, Ang H, De Filippo K, Kong IY, et al. Inhibition of Endosteal Vascular Niche Remodeling Rescues Hematopoietic Stem Cell Loss in AML. Cell Stem Cell. 2018;22(1):64-77 e6.

159. Acar M, Kocherlakota KS, Murphy MM, Peyer JG, Oguro H, Inra CN, et al. Deep imaging of bone marrow shows non-dividing stem cells are mainly perisinusoidal. Nature. 2015;526(7571):126-30.

160. Pinho S, Marchand T, Yang E, Wei Q, Nerlov C, Frenette PS. Lineage-Biased Hematopoietic Stem Cells Are Regulated by Distinct Niches. Dev Cell. 2018;44(5):634-41 e4.

161. Casanova-Acebes M, Pitaval C, Weiss LA, Nombela-Arrieta C, Chevre R, N AG, et al. Rhythmic modulation of the hematopoietic niche through neutrophil clearance. Cell. 2013;153(5):1025-35.

162. Arber DA, Orazi A, Hasserjian R, Thiele J, Borowitz MJ, Le Beau MM, et al. The 2016 revision to the World Health Organization classification of myeloid neoplasms and acute leukemia. Blood. 2016;127(20):2391-405.

163. Ferlay J, Colombet M, Soerjomataram I, Dyba T, Randi G, Bettio M, et al. Cancer incidence and mortality patterns in Europe: Estimates for 40 countries and 25 major cancers in 2018. Eur J Cancer. 2018;103:356-87.

164. Osgood ER, M. Mathews, T. . Aplastic anemia treated with daily transfusions and intravenous marrow; case report. Ann Intern Med. 1939;13.

165. Henig I, Zuckerman T. Hematopoietic stem cell transplantation-50 years of evolution and future perspectives. Rambam Maimonides Med J. 2014;5(4):e0028.

166. Pasquini MW, Z. Current use and outcome of hematopoietic stem cell transplantation: CIBMTR Summary Slides, 2018 [Available from: https://www.cibmtr.org/ReferenceCenter/SlidesReports/SummarySlides/_layouts/15/WopiFrame.aspx?sourcedoc=/ReferenceCenter/SlidesReports/SummarySlides/Documents/2018%20Summary%20Slides%20-%20final%20-%20for%20web%20posting.pptx&action=default.

167. Ramasamy SK, Kusumbe AP, Itkin T, Gur-Cohen S, Lapidot T, Adams RH. Regulation of Hematopoiesis and Osteogenesis by Blood Vessel-Derived Signals. Annu Rev Cell Dev Biol. 2016;32:649-75.

168. Mazo IB, von Andrian UH. Adhesion and homing of blood-borne cells in bone marrow microvessels. J Leukoc Biol. 1999;66(1):25-32.

169. Itkin T, Gomez-Salinero JM, Rafii S. Open the gates: vascular neurocrine signaling mobilizes hematopoietic stem and progenitor cells. J Clin Invest. 2017;127(12):4231-4.

170. Pusic I, Jiang SY, Landua S, Uy GL, Rettig MP, Cashen AF, et al. Impact of mobilization and remobilization strategies on achieving sufficient stem cell yields for autologous transplantation. Biol Blood Marrow Transplant. 2008;14(9):1045-56.

171. Jillella AP, Ustun C. What is the optimum number of CD34+ peripheral blood stem cells for an autologous transplant? Stem Cells Dev. 2004;13(6):598-606.

172. Christopher MJ, Rao M, Liu F, Woloszynek JR, Link DC. Expression of the G-CSF receptor in monocytic cells is sufficient to mediate hematopoietic progenitor mobilization by G-CSF in mice. J Exp Med. 2011;208(2):251-60.

173. Demetri GD, Griffin JD. Granulocyte colony-stimulating factor and its receptor. Blood. 1991;78(11):2791-808.

174. Lapidot T, Petit I. Current understanding of stem cell mobilization: the roles of chemokines, proteolytic enzymes, adhesion molecules, cytokines, and stromal cells. Exp Hematol. 2002;30(9):973-81.

175. Lapid K, Glait-Santar C, Gur-Cohen S, Canaani J, Kollet O, Lapidot T. Egress and Mobilization of Hematopoietic Stem and Progenitor Cells: A Dynamic Multi-facet Process. StemBook. Cambridge (MA)2008.

176. Petit I, Szyper-Kravitz M, Nagler A, Lahav M, Peled A, Habler L, et al. G-CSF induces stem cell mobilization by decreasing bone marrow SDF-1 and up-regulating CXCR4. Nat Immunol. 2002;3(7):687-94.

177. Spiegel A, Shivtiel S, Kalinkovich A, Ludin A, Netzer N, Goichberg P, et al. Catecholaminergic neurotransmitters regulate migration and repopulation of immature human CD34+ cells through Wnt signaling. Nat Immunol. 2007;8(10):1123-31.

178. Heissig B, Hattori K, Dias S, Friedrich M, Ferris B, Hackett NR, et al. Recruitment of stem and progenitor cells from the bone marrow niche requires MMP-9 mediated release of kit-ligand. Cell. 2002;109(5):625-37.

179. Vagima Y, Avigdor A, Goichberg P, Shivtiel S, Tesio M, Kalinkovich A, et al. MT1-MMP and RECK are involved in human CD34+ progenitor cell retention, egress, and mobilization. J Clin Invest. 2009;119(3):492-503.

180. Christopherson KW, 2nd, Uralil SE, Porecha NK, Zabriskie RC, Kidd SM, Ramin SM. G-CSF- and GM-CSF-induced upregulation of CD26 peptidase downregulates the functional chemotactic response of CD34+CD38- human cord blood hematopoietic cells. Exp Hematol. 2006;34(8):1060-8.

181. Christopherson KW, 2nd, Cooper S, Broxmeyer HE. Cell surface peptidase CD26/DPPIV mediates G-CSF mobilization of mouse progenitor cells. Blood. 2003;101(12):4680-6.

182. Christopherson KW, Cooper S, Hangoc G, Broxmeyer HE. CD26 is essential for normal G-CSF-induced progenitor cell mobilization as determined by CD26-/- mice. Exp Hematol. 2003;31(11):1126-34.

183. Broxmeyer HE, Hoggatt J, O'Leary HA, Mantel C, Chitteti BR, Cooper S, et al. Dipeptidylpeptidase 4 negatively regulates colony-stimulating factor activity and stress hematopoiesis. Nat Med. 2012;18(12):1786-96.

184. Hashimoto N, Ikuma K, Konno Y, Hirose M, Tadokoro H, Hasegawa H, et al. DPP-4 inhibition protects human umbilical vein endothelial cells from hypoxia-induced vascular barrier impairment. J Pharmacol Sci. 2017;135(1):29-36.

185. Donzella GA, Schols D, Lin SW, Este JA, Nagashima KA, Maddon PJ, et al. AMD3100, a small molecule inhibitor of HIV-1 entry via the CXCR4 co-receptor. Nat Med. 1998;4(1):72-7.

186. European Medecines Agency: Mozobil (plerixafor) 20 mg/ml solution for injection: EU summary of product characteristics [http://www.ema.europa.eu/docs/en_GB/document_library/EPAR_-_Product_Information/human/001030/WC500030686.pdf].

187. Iyer CV, Evans RJ, Lou Q, Lin D, Wang J, Kohn W, et al. Rapid and recurrent neutrophil mobilization regulated by T134, a CXCR4 peptide antagonist. Exp Hematol. 2008;36(9):1098-109.

188. Abraham M, Biyder K, Begin M, Wald H, Weiss ID, Galun E, et al. Enhanced unique pattern of hematopoietic cell mobilization induced by the CXCR4 antagonist 4F-benzoyl-TN14003. Stem Cells. 2007;25(9):2158-66.

189. Pelus LM, Bian H, Fukuda S, Wong D, Merzouk A, Salari H. The CXCR4 agonist peptide, CTCE-0021, rapidly mobilizes polymorphonuclear neutrophils and hematopoietic progenitor cells into peripheral blood and synergizes with granulocyte colony-stimulating factor. Exp Hematol. 2005;33(3):295-307.

190. Zhong R, Law P, Wong D, Merzouk A, Salari H, Ball ED. Small peptide analogs to stromal derived factor-1 enhance chemotactic migration of human and mouse hematopoietic cells. Exp Hematol. 2004;32(5):470-5.

191. Craddock CF, Nakamoto B, Andrews RG, Priestley GV, Papayannopoulou T. Antibodies to VLA4 integrin mobilize long-term repopulating cells and augment cytokine-induced mobilization in primates and mice. Blood. 1997;90(12):4779-88.

192. Papayannopoulou T, Priestley GV, Nakamoto B, Zafiropoulos V, Scott LM. Molecular pathways in bone marrow homing: dominant role of alpha(4)beta(1) over beta(2)-integrins and selectins. Blood. 2001;98(8):2403-11.

193. Papayannopoulou T, Priestley GV, Nakamoto B. Anti-VLA4/VCAM-1-induced mobilization requires cooperative signaling through the kit/mkit ligand pathway. Blood. 1998;91(7):2231-9.

194. Kikuta T, Shimazaki C, Ashihara E, Sudo Y, Hirai H, Sumikuma T, et al. Mobilization of hematopoietic primitive and committed progenitor cells into blood in mice by anti-vascular adhesion molecule-1 antibody alone or in combination with granulocyte colony-stimulating factor. Exp Hematol. 2000;28(3):311-7.

195. Devine SM, Brown RA, Mathews V, Trinkaus K, Khoury H, Adkins D, et al. Reduced risk of acute GVHD following mobilization of HLA-identical sibling donors with GM-CSF alone. Bone Marrow Transplant. 2005;36(6):531-8.

196. Vasu C, Dogan RN, Holterman MJ, Prabhakar BS. Selective induction of dendritic cells using granulocyte macrophage-colony stimulating factor, but not fms-like tyrosine kinase receptor 3-ligand, activates thyroglobulin-specific CD4+/CD25+ T cells and suppresses experimental autoimmune thyroiditis. J Immunol. 2003;170(11):5511-22.

197. Parajuli P, Mosley RL, Pisarev V, Chavez J, Ulrich A, Varney M, et al. Flt3 ligand and granulocyte-macrophage colony-stimulating factor preferentially expand and stimulate different dendritic and T-cell subsets. Exp Hematol. 2001;29(10):1185-93.

198. Itkin T, Gur-Cohen S, Spencer JA, Schajnovitz A, Ramasamy SK, Kusumbe AP, et al.Distinct bone marrow blood vessels differentially regulate haematopoiesis. Nature. 2016;538(7624):274.

199. Dar A, Goichberg P, Shinder V, Kalinkovich A, Kollet O, Netzer N, et al. Chemokine receptor CXCR4-dependent internalization and resecretion of functional chemokine SDF-1 by bone marrow endothelial and stromal cells. Nat Immunol. 2005;6(10):1038-46.

200. Dar A, Schajnovitz A, Lapid K, Kalinkovich A, Itkin T, Ludin A, et al. Rapid mobilization of hematopoietic progenitors by AMD3100 and catecholamines is mediated by CXCR4-dependent SDF-1 release from bone marrow stromal cells. Leukemia. 2011;25(8):1286-96.

201. Morrison SJ, Scadden DT. The bone marrow niche for haematopoietic stem cells. Nature. 2014;505(7483):327-34.

202. Mendelson A, Frenette PS. Hematopoietic stem cell niche maintenance during homeostasis and regeneration. Nat Med. 2014;20(8):833-46.

203. Ikushima YM, Arai F, Nakamura Y, Hosokawa K, Kubota Y, Hirashima M, et al. Enhanced Angpt1/Tie2 signaling affects the differentiation and long-term repopulation ability of hematopoietic stem cells. Biochem Biophys Res Commun. 2013;430(1):20-5.

204. Qu X, Tompkins K, Batts LE, Puri M, Baldwin HS. Abnormal embryonic lymphatic vessel development in Tie1 hypomorphic mice. Development. 2010;137(8):1285-95.

205. Wang Y, Nakayama M, Pitulescu ME, Schmidt TS, Bochenek ML, Sakakibara A, et al. Ephrin-B2 controls VEGF-induced angiogenesis and lymphangiogenesis. Nature. 2010;465(7297):483-6.

206. Till JE, Mc CE. A direct measurement of the radiation sensitivity of normal mouse bone marrow cells. Radiat Res. 1961;14:213-22.

207. Mazo IB, Gutierrez-Ramos JC, Frenette PS, Hynes RO, Wagner DD, von Andrian UH. Hematopoietic progenitor cell rolling in bone marrow microvessels: parallel contributions by endothelial selectins and vascular cell adhesion molecule 1. J Exp Med. 1998;188(3):465-74.

208. Serefhanoglu S, Goker H, Buyukasik Y, Turgut M, Sayinalp N, Haznedaroglu IC, et al. Changes in vascular endothelial growth factor, angiopoietins, and Tie-2 levels with G-CSF stimulation in healthy donors. Ann Hematol. 2009;88(7):667-71.

209. Yang JZ, Sun LX. Decreased soluble TGF-beta1, Tie-2, and angiopoietins serum levels in bone marrow after treating healthy donors with granulocyte colony-stimulating factor. Transfus Apher Sci. 2012;47(1):39-42.

210. Szmigielska-Kaplon A, Krawczynska A, Czemerska M, Pluta A, Cebula-Obrzut B, Szmigielska K, et al. Angiopoietins in haematopoietic stem cell mobilisation in patients with haematological malignancies. Blood Transfus. 2015;13(1):102-8.

211. Imhof BA, Aurrand-Lions M. Angiogenesis and inflammation face off. Nat Med. 2006;12(2):171-2.

212. Scholz A, Lang V, Henschler R, Czabanka M, Vajkoczy P, Chavakis E, et al. Angiopoietin-2 promotes myeloid cell infiltration in a beta(2)-integrin-dependent manner. Blood. 2011;118(18):5050-9.

213. Thurston G, Rudge JS, Ioffe E, Zhou H, Ross L, Croll SD, et al. Angiopoietin-1 protects the adult vasculature against plasma leakage. Nat Med. 2000;6(4):460-3.

214. Baffert F, Le T, Thurston G, McDonald DM. Angiopoietin-1 decreases plasma leakage by reducing number and size of endothelial gaps in venules. Am J Physiol Heart Circ Physiol. 2006;290(1):H107-18.

215. Gavard J, Patel V, Gutkind JS. Angiopoietin-1 prevents VEGF-induced endothelial permeability by sequestering Src through mDia. Dev Cell. 2008;14(1):25-36.

216. Helfrich I, Edler L, Sucker A, Thomas M, Christian S, Schadendorf D, et al. Angiopoietin-2 levels are associated with disease progression in metastatic malignant melanoma. Clin Cancer Res. 2009;15(4):1384-92.

217. Park JH, Park KJ, Kim YS, Sheen SS, Lee KS, Lee HN, et al. Serum angiopoietin-2 as a clinical marker for lung cancer. Chest. 2007;132(1):200-6.

218. Kuboki S, Shimizu H, Mitsuhashi N, Kusashio K, Kimura F, Yoshidome H, et al. Angiopoietin-2 levels in the hepatic vein as a useful predictor of tumor invasiveness and prognosis in human hepatocellular carcinoma. J Gastroenterol Hepatol. 2008;23(7 Pt 2):e157-64.

219. Fuxe J, Lashnits E, O'Brien S, Baluk P, Tabruyn SP, Kuhnert F, et al. Angiopoietin/Tie2 signaling transforms capillaries into venules primed for leukocyte trafficking in airway inflammation. Am J Pathol. 2010;176(4):2009-18.

220. Dellinger M, Hunter R, Bernas M, Gale N, Yancopoulos G, Erickson R, et al. Defective remodeling and maturation of the lymphatic vasculature in Angiopoietin-2 deficient mice. Dev Biol. 2008;319(2):309-20.

221. Pitera JE, Woolf AS, Gale NW, Yancopoulos GD, Yuan HT. Dysmorphogenesis of kidney cortical peritubular capillaries in angiopoietin-2-deficient mice. Am J Pathol. 2004;165(6):1895-906.

222. Eash KJ, Means JM, White DW, Link DC. CXCR4 is a key regulator of neutrophil release from the bone marrow under basal and stress granulopoiesis conditions. Blood. 2009;113(19):4711-9.

223. Cheng T, Rodrigues N, Shen H, Yang Y, Dombkowski D, Sykes M, et al. Hematopoietic stem cell quiescence maintained by p21cip1/waf1. Science. 2000;287(5459):1804-8.

224. Zheng W, Nurmi H, Appak S, Sabine A, Bovay E, Korhonen EA, et al. Angiopoietin 2 regulates the transformation and integrity of lymphatic endothelial cell junctions. Genes Dev. 2014;28(14):1592-603.

225. Li XM, Hu Z, Jorgenson ML, Wingard JR, Slayton WB. Bone marrow sinusoidal endothelial cells undergo nonapoptotic cell death and are replaced by proliferating sinusoidal cells in situ to maintain the vascular niche following lethal irradiation. Exp Hematol. 2008;36(9):1143-56.

226. Samlowski WE, Johnson HM, Hammond EH, Robertson BA, Daynes RA. Marrow ablative doses of gamma-irradiation and protracted changes in peripheral lymph node microvasculature of murine and human bone marrow transplant recipients. Lab Invest. 1987;56(1):85-95.

227. Penack O, Socie G, van den Brink MR. The importance of neovascularization and its inhibition for allogeneic hematopoietic stem cell transplantation. Blood. 2011;117(16):4181-9.

228. Ziegler T, Horstkotte J, Schwab C, Pfetsch V, Weinmann K, Dietzel S, et al. Angiopoietin 2 mediates microvascular and hemodynamic alterations in sepsis. J Clin Invest. 2013.

229. La Porta S, Roth L, Singhal M, Mogler C, Spegg C, Schieb B, et al. Endothelial Tie1-mediated angiogenesis and vascular abnormalization promote tumor progression and metastasis. J Clin Invest. 2018;128(2):834-45.

230. Garcia J, Sandi MJ, Cordelier P, Binetruy B, Pouyssegur J, Iovanna JL, et al. Tie1 deficiency induces endothelial-mesenchymal transition. EMBO Rep. 2012;13(5):431-9.

231. Li L, McBride DW, Doycheva D, Dixon BJ, Krafft PR, Zhang JH, et al. G-CSF attenuates neuroinflammation and stabilizes the blood-brain barrier via the PI3K/Akt/GSK-3beta signaling pathway following neonatal hypoxia-ischemia in rats. Exp Neurol. 2015;272:135-44.

232. Powell TM, Paul JD, Hill JM, Thompson M, Benjamin M, Rodrigo M, et al. Granulocyte colony-stimulating factor mobilizes functional endothelial progenitor cells in patients with coronary artery disease. Arterioscler Thromb Vasc Biol. 2005;25(2):296-301.

233. Yen LF, Wei VC, Kuo EY, Lai TW. Distinct patterns of cerebral extravasation by Evans blue and sodium fluorescein in rats. PLoS One. 2013;8(7):e68595.

234. Shariatmadar S, Sharma S, Cabana R, Powell S, Ruiz P, Krishan A. Electronic volume of CD34 positive cells from peripheral blood apheresis samples. Cytometry B Clin Cytom. 2008;74(3):182-8.

235. Chen H, Tong X, Lang L, Jacobson O, Yung BC, Yang X, et al. Quantification of Tumor Vascular Permeability and Blood Volume by Positron Emission Tomography. Theranostics. 2017;7(9):2363-76.

236. Benest AV, Kruse K, Savant S, Thomas M, Laib AM, Loos EK, et al. Angiopoietin-2 is critical for cytokine-induced vascular leakage. PLoS One. 2013;8(8):e70459.

237. He XC, Li Z, Sugimura R, Ross J, Zhao M, Li L. Homing and migration assays of hematopoietic stem/progenitor cells. Methods Mol Biol. 2014;1185:279-84.

238. Bixel MG, Kusumbe AP, Ramasamy SK, Sivaraj KK, Butz S, Vestweber D, et al. Flow Dynamics and HSPC Homing in Bone Marrow Microvessels. Cell Rep. 2017;18(7):1804-16.

239. D'Amico G, Korhonen EA, Anisimov A, Zarkada G, Holopainen T, Hagerling R, et al. Tie1 deletion inhibits tumor growth and improves angiopoietin antagonist therapy. J Clin Invest. 2014;124(2):824-34.

240. Takakura N, Huang XL, Naruse T, Hamaguchi I, Dumont DJ, Yancopoulos GD, et al. Critical role of the TIE2 endothelial cell receptor in the development of definitive hematopoiesis. Immunity. 1998;9(5):677-86.

241. Busch K, Klapproth K, Barile M, Flossdorf M, Holland-Letz T, Schlenner SM, et al. Fundamental properties of unperturbed haematopoiesis from stem cells in vivo. Nature. 2015;518(7540):542-6.

242. Nakamura-Ishizu A, Suda T. Hematopoietic stem cell niche: an interplay among a repertoire of multiple functional niches. Biochim Biophys Acta. 2013;1830(2):2404-9.

243. Krause DS, Scadden DT, Preffer FI. The hematopoietic stem cell niche--home for friend and foe? Cytometry B Clin Cytom. 2013;84(1):7-20.

244. Kwarteng EO, Heinonen KM. Competitive Transplants to Evaluate Hematopoietic Stem Cell Fitness. J Vis Exp. 2016(114).

245. Puri MC, Rossant J, Alitalo K, Bernstein A, Partanen J. The receptor tyrosine kinase TIE is required for integrity and survival of vascular endothelial cells. EMBO J. 1995;14(23):5884-91.

246. Livak KJ, Schmittgen TD. Analysis of relative gene expression data using real-time quantitative PCR and the 2(-Delta Delta C(T)) Method. Methods. 2001;25(4):402-8.